

# Regional Biophysics Conference (RBC2016)

## BOOK OF ABSTRACTS



25-28 August 2016, Trieste (Italy)

<http://rbc2016.sibpa.it>

**SIBPA**  
Società Italiana di Biofisica e Applicata  
dal 1962

**ibf**  
CNR - Istituto di Biofisica



UNIVERSITÀ  
DEGLI STUDI DI TRIESTE

DIPARTIMENTO DI  
SCIENZE DELLA VITA



Biophysics in Europe

**cost**  
EUROPEAN COOPERATION  
IN SCIENCE AND TECHNOLOGY

**ALFATEST**  
strumentazione scientifica

**LaB SAH**  
LaBoratory of  
Sequence & Structure  
Analysis for Health



EDINBURGH  
INSTRUMENTS



**AMO**  
TEMPER  
technologies

**European  
Biophysics Journal**  
with Biophysics Letters

**HORIBA**  
Scientific



**ARBRE MOBIEU**  
BETWEEN ATOM AND CELL

**HAMAMATSU**  
PHOTON IS OUR BUSINESS

**IMMAGINA**  
· BioTECHNOLOGY ·

© copyright RBC2016, Trieste 2016.

Proprietà letteraria riservata.

I diritti di traduzione, memorizzazione elettronica,  
di riproduzione e di adattamento totale e parziale  
di questapubblicazione, con qualsiasi mezzo  
(compresi i microfilm, le fotocopie e altro)  
sono riservati per tutti i paesi.

ISBN 978-88-8303-757-3 (print)

ISBN 978-88-8303-758-0 (online)

EUT Edizioni Università di Trieste

via Weiss 21, 34128 Trieste

<http://eut.units.it>

<https://www.facebook.com/EUTEdizioniUniversitaTrieste>

# RBC2016

## Regional Biophysics Conference

25-28 August 2016, Trieste, Italy

RTM Living Trieste - Ex Ospedale Militare, via Fabio Severo 40, Trieste

### Scientific Committee

Thomas Stockner (Austria)

Nenad Pavin (Croatia)

László Mátyus (Hungary)

Pavle Andjus (Serbia)

Ján Jakuš (Slovakia)

Ales Iglič (Slovenia)

Carlo Musio (Italy)

Roland Malli (Austria)

Vesna Svetlicic (Croatia)

László Zimányi (Hungary)

Miroslav Živić (Serbia)

Daniel Jancura (Slovakia)

Primoz Ziherl (Slovenia)

Massimo Vassalli (Italy)

### Organizing Committee:

Alex Tossi (Univ. Trieste)

Mauro Dalla Serra (CNR-IBF & FBK)

Renato Gennaro (Univ. Trieste)

Cristina Potrich (FBK & CNR-IBF)

### Secretariat:

Elena Gerola (CNR-IBF)

Agata Mannino (Univ. Trieste)

Tiziana Martinelli (CNR & FBK)

Monica Benincasa (Univ. Trieste)

### Webmaster:

Gian-Piero Borello (CNR-IBF)

Marco Millio (CNR-IBF)



# Program

## Thursday, 25 August

12.00 – 14.00 *Registration and light lunch at the Congress Venue*

14.00 – 14.30 *Welcome addresses*

### **Session 1** *Molecular and Cell Biophysics*

**Chairs: László Mátyus, Renato Gennaro**

14.30 – 15.00 **PL1 Kovačić Damir** (University of Split, HR)

*A new auditory neuro-electronic interface: spiral ganglion neurons cultured on advanced micro-electrode array*

15.00 – 15.25 **IL1.1 Panyi György** (University of Debrecen, H)

*Shaker-IR  $K^+$  channel gating in heavy water: role of structural water molecules in inactivation*

15.25 – 15.50 **IL1.2 Zahradníková Alexandra** (Slovak Academy of Sciences, SK)

*Calcium wave generation in cardiac myocytes*

15.50 – 16.05 **SO1.1 Mesarec Luka** (University of Ljubljana, SLO)

*On the role of external force of actin filaments in the formation of tubular protrusions of closed membrane shapes with anisotropic membrane components*

16.05 – 16.40 *Coffee Break*

16.40 – 16.55 **SO1.4 Frečer Vladimír** (Comenius University in Bratislava & ICARST, SK)

*Computational Design of Histone Deacetylase Inhibitors as Antitumor Agents*

16.55 – 17.10 **SO1.5 Božič Bojan** (University of Ljubljana, SLO)

*The cellular effects induced by the pore-forming agent nystatin*

19.00 – 23.30

*Congress Dinner*

## Friday, 26 August

### **Session 2** *Supramolecular Assemblies and Aggregation*

**Chairs: Valeria Militello, Srđan Antić**

09.00 – 09.30 **PL2 Hianik Tibor** (Comenius University Bratislava, SK)

*DNA-aptamers structure, physical properties and applications*

09.30 – 09.55 **IL2.1 Librizzi Fabio** (CNR-Istitute of Biophysics, I)

*Amyloid formation and its inhibition by chaperones and chaperon-like molecules: the effect on different nucleation mechanisms*

09.55 – 10.20 **IL2.2 Sedlák Erik** (Safarik University, SK)

*Role of cardiolipin for stability of cytochrome c oxidase*

10.20 – 10.35 **SO2.1 Kozelka Jiri** (Masaryk Univ., Brno CZ & Univ. Paris Descartes, Paris, F)

*Lone-pair- $\pi$  interactions in nucleic acids and proteins: physical origin and significance*

10.35 – 10.50 **SO2.2 Tkalec Uroš** (Univ. Ljubljana & Univ. Maribor & Jožef Stefan Inst. Ljubljana, SLO)

*Manipulating liquid crystal flows in microfluidic environment*

10.50 – 11.05 **SO2.3 Podlipec Rok** (Jožef Stefan Institute, Ljubljana, SLO)

*Role of Calcium in localization of a blood clot in an ex vivo injured blood vessel*

11.05 – 11.30

*Coffee Break*

- Session 3A**     **Synthetic Biology and Integrative Biophysics and Complex Systems**  
**Chairs: Aleksandar Krmpot, Vladimir Frecer**
- 11.30 – 12.00 **PL3 Podgornik Rudolf** (Jožef Stefan Institute & University of Ljubljana, SLO)  
*Electrostatics goes viral*
- 12.00 – 12.15 **SO3.1 Dobovišek Andrej** (University of Maribor, SLO)  
*Entropy production in enzyme reactions*
- 12.15 – 12.30 **SO3.2 Dolanski Babić Sanja** (University of Zagreb, HR)  
*The effect of magnesium ions on the structure of thin DNA films: an infrared spectroscopy study*
- 12.30 – 14.30 *Light Lunch*
- Session 3B**     **Synthetic Biology and Integrative Biophysics and Complex Systems.**  
**Chairs: Aleksandar Krmpot, Vladimir Frecer**
- 14.30 – 14.55 **IL3.1 Fajmut Ales** (University of Maribor, SLO)  
*Systems pharmacology model for the assessment of bronchoconstriction rate due to non-steroidal anti-inflammatory drugs*
- 14.55 – 15.20 **IL3.2 Tomić Sanja** (Ruđer Bošković Institute, HR)  
*Understanding substrate recognition and function of human dipeptidyl peptidase III*
- 15.20 – 15.35 **SO3.3 Svetina Saša** (University of Ljubljana & Jožef Stefan Institute, Ljubljana, SLO)  
*Investigating cell functioning by theoretical analysis of cell-to-cell variability*
- Session 4**     **Nanoclustering of membranes and membrane proteins**  
**Chairs: Eva Sevcsik, Pavle Andjus**
- 15.35 – 16.00 **PL4 Eggeling Christian** (University of Oxford, UK)  
*Studying membrane bioactivity with advanced (super-resolution) optical microscopy*
- 16.00 – 16.25 **IL4.1 Sevcsik Eva** (TUWIEN, A)  
*Combining protein micropatterning and single molecule microscopy to decipher plasma membrane organization*
- 16.25 – 16.50 **IL4.2 Fameli Nicola** (Medical University of Graz, A)  
*ER nanojunctions and ER Ca<sup>2+</sup> refilling in vascular endothelial cells: experiments and models*
- 16.50 – 17.20 *Coffee Break*
- 17.20 – 17.45 **IL4.3 Posocco Paola** (University of Trieste, I)  
*Insights on the morphology and biological activity of gold nanoparticles protected by self-assembling mixtures of ligands*
- 17.45 – 18.00 **SO4.1 Nagy Peter** (University of Debrecen, H)  
*Changes in the biophysical properties of the plasma membrane in Gaucher disease, a lysosomal storage disorder*
- 18.00 – 18.15 **SO4.2 Brameshuber Mario** (Institute of Applied Physics, TU Wien, A)  
*Direct imaging of nanoplatforms in the live cell plasma membrane*
- 18.15 – 18.30 **SO4.3 Zoranić Larisa** (University of Split, HR)  
*Connecting the mechanism of action with lipid composition: Molecular dynamic study of the antimicrobial peptide maculatin 1.1*
- 18.30 – 20.00 *Poster Session*

**Saturday, 27 August**

**Session 5      *Biophysical Medicine and Neuroscience***

**Chairs: Bozidar Casar, Sanja Tomić**

- 09.00 – 09.30 **PL5 Antić Srđan** (UConn Health Center, USA)  
*Biophysical Properties of Dendrites of Cortical Pyramidal Neurons - Simultaneous Sodium and Calcium Imaging*
- 09.30 – 09.55 **IL5.1 Milošević Nebojša** (University of Belgrade, SRB)  
*Fractal and lacunarity analysis in neuroscience: application in 2D image of the brain neurons*
- 09.55 – 10.20 **IL5.2 Gualdani Roberta** (University of Florence, I)  
*Molecular mechanisms and pharmacological implications of a new family of TRP antagonists*
- 10.20 – 10.35 **SO5.1 Thi-huong Nguyen** (University of Greifswald, D)  
*Rupture Forces among Human Blood Platelets at different Degrees of Activation*
- 10.35 – 10.50 **SO5.2 Pavićević Aleksandra** (University of Belgrade, SRB)  
*In vivo EPR measurements of the pharmacokinetics of nitroxides: The role of modeling in the assessment of the redox status*
- 10.50 – 11.30 *Coffee Break*
- 11.30 – 11.45 **SO5.3 Andjus Pavle** (University of Belgrade, SRB)  
*Intracellular pathophysiological changes of astrocytes from a rat model of amyotrophic lateral sclerosis*
- 11.45 – 12.00 **SO5.4 Žerovnik Eva** (Jožef Stefan Institute, Ljubljana, SLO)  
*Alternative functions of stefin B: a role in cell's response to mis-folded proteins and oxidative stress*
- 12.00 – 12.30 **IL5.3 Diaspro Alberto** (IIT, Genova, I)  
*Converging and correlative approaches towards optical nanoscopy*
- 12.30 – 14.30 *Light Lunch and RBC advisory board meeting\**

**Session 6      *Material Science and Nanobiophysics***

**Chairs: Zoran Arsov, Roberta Gualdani**

- 14.30 – 15.00 **PL6 Viappiani Cristiano** (University of Parma, I)  
*Imaging protein-based nanostructured photosensitizers with subdiffraction resolution*
- 15.00 – 15.25 **IL6.1 Horváth Róbert** (Institute of Technical Physics and Materials Science, H)  
*Novel label-free optical biosensors for cell dynamics on biomimetic coatings*
- 15.25 – 15.50 **IL6.2 Štrancar Janez** (Jožef Stefan Institute, SLO)  
*Interaction of materials with model and cell membranes studied by Fluorescence Microscopy and Microspectroscopy*
- 15.50 – 16.05 **SO6.1 Potrich Cristina** (LaBSSAH, Fond. Bruno Kessler, Trento & CNR-IBF, Trento, I)  
*Bio-functional surfaces for microRNAs purification and analysis*
- 16.05 – 16.20 **SO6.2 Zavadlav Julija** (National Institute of Chemistry, Ljubljana, SLO)  
*Adaptive resolution simulations of biomolecular systems*
- 16.20 – 17.00 *Coffee Break*

- 17.00 – 17.15 **SO6.3 Parisse Pietro** (INSTM-ST Unit, Trieste & Elettra – Sincrotrone Trieste S.C.p.A., I)  
*Atomic Force Microscopy analysis of extracellular vesicles*
- 17.15 – 17.30 **SO6.4 Eroglu Emrah** (Medical University of Graz, A)  
*Development of novel FP-based probes for live-cell imaging of nitric oxide dynamics*
- 17.30 – 18.00 **IL6.3 Donati Ivan** (University of Trieste, I)  
*A polysaccharide based approach to mimic the extracellular matrix in biomaterials*

18.00 – 20.00

*Poster Session*

## **Sunday, 28 August**

**Session 7** *Emerging Methods in Biophysics: Live Imaging, Nanoscopy et al.*  
**Chairs: Peter Zavodszky, Gregor Anderluh**

- 09.00 – 09.30 **PL7 Ormos Pál** (Hungarian Academy of Sciences, H) *Light microrobotics in biology*
- 09.30 – 09.55 **IL7.1 Krmpot Aleksandar** (University of Belgrade, SRB) *Mapping of hemoglobin residuals in erythrocyte ghosts using two photon excited fluorescence microscopy*
- 09.55 – 10.20 **IL7.2 Vuletić Tomislav** (Institute of Physics, HR) *Polyelectrolyte composite: hyaluronic acid mixture with DNA*

10.20 – 11.00

*Coffee Break*

- 11.00 – 11.15 **SO7.1 Lukacs Andras** (Medical School, Pécs, H)  
*Functional dynamics of an unusual photolyase revealed by transient absorption*
- 11.15 – 11.30 **SO7.2 Urbančič Iztok** (Jožef Stefan Institute, Ljubljana, SLO)  
*Bleach-rate imaging – fluorescence microspectroscopy at hand*
- 11.30 – 11.45 **SO7.3 Szabo-Meleg Edina** (University of Pécs, H)  
*Intercellular highways - membrane nanotube networks between B lymphocytes: fundamental growth determinants and transport functions*
- 11.45 – 12.00 **SO7.4 Arsov Zoran** (Jožef Stefan Institute, Ljubljana, SLO)  
*Development of smart fluorescent probes to reveal internalization and accumulation in cells through aggregation-induced spectral shift*
- 12.00 – 12.15 **SO7.5 Galajda Peter** (BRC Hungarian Academy of Sciences, Szeged, H)  
*Swimming Motility of Bacteria in Microfabricated Environments*
- 12.15 – 12.45 **IL7.3 Gilbert Robert** (University of Oxford, UK)  
*Biophysics networks in Europe: the "Association of Resources for Biophysical Research in Europe (ARBRE)" and the COST Action "Between Atom and Cell: Integrating Molecular Biophysics Approaches for Biology and Healthcare (MOBIEU)"*

12.45 – 14.30

*Closing remarks and Light Lunch*

\*During lunch in a separated room, members of the RBC advisory board will have their normal meeting

# Abstracts

## Lectures (L)

### **PL1 A new auditory neuro-electronic interface: spiral ganglion neurons cultured on advanced micro-electrode array**

D. Kovačić

Speech and Hearing Research Lab, School of Medicine & Faculty of Science, University of Split (HR)  
e-mail: kovacic@znanost.org

One of the strategies to improve the cochlear implant technology is to increase the selectivity of the electrical stimulation of the auditory nerve. We are proposing a novel neuro-electronic interface based on micro-nail-shaped electrode array embedded on silicon-based integrated circuits. Herein we test the in vitro interaction of these substrates with rat spiral ganglion neurons (SGN) [1]. Silicon substrates with micro-nails of different dimensions and spacing were fabricated using standard CMOS-based post-processing [2]. SGN were extracted from P5 rat pups and cultured in vitro on poly-L-ornithine coated silicon substrates in Neurobasal-A with B27 and GDNF. Glass coverslips were used as controls. Cell cultures were fixed and stained with Tuj1 (neurons) and DAPI (cell nuclei). Tuj1+ SGNs grew successfully on micro-electrode arrays, as on control surfaces ( $139 \pm 43$  and  $181 \pm 53$  neurons respectively). The micro-nails allowed excellent neurite outgrowth and induced intimate interactions between cell and silicon. After 7 days in vitro, 21% of SGN on micro-electrode arrays showed neurites longer than  $100 \mu\text{m}$ , similarly as SGN on control surfaces (29%). Nail shaped electrodes also promoted axonal guidance, as proved previously with other types of neurons [3] Neurites were oriented preferentially along  $30^\circ$ ,  $90^\circ$  or  $60^\circ$  in nail structures with spacing between  $1\mu\text{m}$  and  $2.4\mu\text{m}$ , following the underlying geometry of the silicon surface. Micro-nails support in vitro SGN growth and interaction with neurite outgrowth. Moreover, the neuronal outgrowth followed geometrical features of the surface, indicating these engineered surfaces could be used for directed neuronal growth and differentiation. Altogether, these results indicate micro-electrode arrays are a promising technology for future auditory neuro-electronic interfaces.

#### **References:**

[1] Mattotti M, Micholt L, Braeken D, Kovačić D (2015) Characterization of spiral ganglion neurons cultured on silicon micro-pillar substrates for new auditory neuro-electronic interfaces. *J Neural Eng* 12:026001. [2] Braeken D, Huys R, Loo J, Bartic C, Borghs G, Callewaert G, Eberle W (2010) Localized electrical stimulation of in vitro neurons using an array of sub-cellular sized electrodes. *Biosens Bioelectron*:5–8. [3] Micholt L, Gärtner A, Prodanov D, Braeken D, Dotti CG, Bartic C (2013) Substrate Topography Determines Neuronal Polarization and Growth In Vitro. *PLoS One* 8:1–14.

### IL1.1 Shaker-IR K<sup>+</sup> channel gating in heavy water: role of structural water molecules in inactivation

T.G. Szanto<sup>1</sup>, Sz.M. Gaal<sup>1</sup>, Z. Varga<sup>1,2</sup>, G. Panyi<sup>1,2</sup>

<sup>1</sup>Department of Biophysics and Cell Biology, University of Debrecen, Debrecen, Hungary

<sup>2</sup>MTA-DE-NAP B Ion Channel Structure-Function Research Group, University of Debrecen, Debrecen, Hungary

e-mail: panyi@med.unideb.hu

It has been reported earlier that the slow (C-type) inactivated conformation in eukaryotic K<sub>v</sub> channels is stabilized by a multipoint hydrogen-bond network behind the selectivity filter. Furthermore, the selectivity filter is sterically locked in the inactive conformation by buried water molecules and the binding of these 'hidden' molecules influence the inactivation process. We found that applying a heavy water (deuterium oxide, D<sub>2</sub>O)-based extracellular solution dramatically slowed the entry into the inactivated state which might indicate the role of the „structural water” molecules in the conformational stability of the selectivity filter. Alternatively, these observations can be explained by an increase in the viscosity or an altered residency time/exit rate of K<sup>+</sup> from the selectivity filter in a D<sub>2</sub>O-based extracellular solution. We mimicked the increased viscosity by adding glycerol to the extracellular solution and determined the inactivation kinetics in Shaker-IR channels having the following mutations and allowing slow inactivation at various rates: T449A and T449A/I470A. The channels were transiently expressed in tsA\_201 cells and ionic current experiments were recorded from either inside-out or outside-out patches. We found that application of 5% glycerol had negligible effect on the rate of inactivation kinetics. The exit rate of K<sup>+</sup> ions was studied by changing the K<sup>+</sup> gradient to allow the inactivation time constants to be determined for both outward and inward currents. Our results showed that exposure of the patches to extracellular D<sub>2</sub>O did not change the  $\tau_{\text{outward}}/\tau_{\text{inward}}$  ratio as compared to control (H<sub>2</sub>O on both sides). Therefore, our macroscopic current measurements support the hypothesis that structural water molecules may have specific effects on the inactivation kinetics by accessing to the region behind the selectivity filter, as proposed by molecular modelling data.

## IL1.2 Calcium wave generation in cardiac myocytes

A. Zahradníková

Institute of Molecular Physiology and Genetics, Slovak Academy of Sciences, Bratislava (SK)  
e-mail: alexandra.zahradnikova@savba.sk

Diastolic calcium concentration in the cytosol of cardiac myocytes fluctuates due to spontaneous calcium release events through clusters of ryanodine receptors (RyRs). This process is fundamental for proper function of cardiac muscle. In failing heart and in arrhythmias caused by RyR mutations, spontaneous calcium release events proliferate into potentially arrhythmogenic calcium waves. We used a stochastic model of RyR gating together with a deterministic model of cytosolic calcium handling to analyze how the formation of calcium release events, that is, calcium sparks and calcium waves, relates to RyR gating and to organization of RyRs in calcium release sites. Importantly, increased frequency of calcium spark formation per se does not affect propensity to calcium wave formation. Propagation of calcium sparks into calcium waves is most strongly affected by the balance between binding of the activating  $\text{Ca}^{2+}$  ions and the non-activating  $\text{Mg}^{2+}$  ions to the RyR activation sites, by the strength of allosteric interaction between  $\text{Ca}^{2+}$  binding and RyR opening, and by the rate of  $\text{Mg}^{2+}$  unbinding from RyR activation sites. These factors regulate the propensity of calcium release events to organize into self-propagating calcium waves by modulating the sensitivity of  $\text{Ca}^{2+}$  spark activation to cytosolic calcium concentration and/or the number of activated RyRs per release site.

Our model provides mechanistic explanation for the phenomenon of store overload-induced calcium release (SOICR). Increased luminal calcium sensitivity leads to SOICR by increasing the allosteric effect of cytosolic calcium, as previously observed. However, increased cytosolic calcium sensitivity of the RyR activation site has a similar effect, since it affects both calcium sensitivity of spark frequency and the average number of open RyRs in sparks to the same extent as increased allosteric effect of cytosolic calcium. Thus, a decreased threshold for "store-overload induced calcium release" can be observed without a change in the effect of luminal calcium on the ryanodine receptor. Therefore, it is questionable whether it is possible to distinguish whether the primary cause of ryanodine receptor dysregulation is modulation of luminal or of cytosolic calcium binding.

*Supported by European Union Contracts No. LSHM-CT-2005-018802/CONTICA and LSHM-CT-2005-018833/EUGeneHeart, by the grants APVV-0721-10, APVV-15-0302, VEGA 2/0148/14, and by the ESF program FuncDyn.*

## **PL2 DNA-aptamers structure, physical properties and applications**

T. Hianik<sup>1</sup>, A. Poturnayova<sup>1,2</sup>, M. Snejdarkova<sup>2</sup>, L. Babelova<sup>2</sup>, M. Burikova<sup>2</sup>, J. Bizik<sup>3</sup>, M. Leitner<sup>4</sup>, A. Ebner<sup>5</sup>

<sup>1</sup>Department of Nuclear Physics and Biophysics, FMFI UK, Mlynska dolina F1, 842 48 Bratislava, Slovakia

<sup>2</sup>Institute of Animal Biochemistry and Genetics, Slovak Academy of Sciences, 900 28 Ivanka pri Dunaji, Slovakia

<sup>3</sup>Biomedical Center of the Slovak Academy of Science, Dubravska cesta 9, 845 05 Bratislava, Slovakia

<sup>4</sup>Center for Advanced Bioanalysis GmbH, Gruberstrasse 40, 4020 Linz, Austria

<sup>5</sup>Institute of Biophysics, Johannes Kepler University Linz, Gruberstrasse 40, 4020 Linz, Austria  
e-mail: tiber.hianik@fmph.uniba.sk

Aptamers are single stranded DNA or RNA molecules that are specially selected by SELEX method (Systematic Evolution of Ligands by EXponential enrichment) [1] toward various targets, such as proteins, drugs, biomarkers, viruses, bacteria or whole cells. In a solution aptamers fold into 3D structure containing binding site for the target. The affinity of aptamers to their targets is in the micromolar to the subnanomolar range and can therefore be comparable and in certain cases even better than, those of antibodies for the same targets. In contrast with antibodies, aptamers are selected in vitro. In comparison with antibodies they are more stable and flexible. Once the aptamer sequence is developed this can be reproduced with high accuracy. In addition, aptamers can be chemically modified by various labels, that allowing them to be immobilized at various surfaces at which can serve as receptors in biosensors [2]. The chemical modification also increases the aptamer stability. Electroactive, optical labels, quantum dots and nanoparticles can also be conjugated with aptamers, which allowing signal amplification using electrochemical, optical and piezoelectric methods [3]. Aptamers can be connected to the AFM tips, which allowing measurement of the forces between aptamer and its target at the solid support or at the surface of the cell [4]. In addition aptamers can be used as a probe for imaging the specific molecules at the surfaces and thus allowing to analyse their lateral distribution. In this contribution we will make introduction into the structure and physical properties of DNA aptamers and will show several applications of aptamers as a receptors in targeted drug delivery and in diagnosis of the cancer by means of detection of cancer markers at the surface of the cells using thickness shear mode acoustic method (TSM) and single molecule force spectroscopy (SMFS).

### **Acknowledgments**

This work was supported by Agency for Promotion Research and Development (Projects No. APVV-14-0267 and SK-AT-2015-0004) and by OEAD.

### **References**

[1] C. Tuerk, L. Gold, *Science* 249 (1990) 505–510. [2] T. Hianik, J. Wang, *Electroanalysis* 21 (2009) 1223–1235. [3] A. Miodek et al., *Anal. Chem.* 85 (2013) 7704–7712. [4] I. Neundlinger et al., *Biophys. J.* 101 (2011) 1781–1787.

## **IL2.1 Amyloid formation and its inhibition by chaperones and chaperon-like molecules: the effect on different nucleation mechanisms**

F. Librizzi, R. Carrotta, S. Vilasi, M.R. Mangione, D. Bulone and P.L. San Biagio

National Research Council, Institute of Biophysics, Via Ugo La Malfa 153, 90146 Palermo, Italy  
e-mail: fabio.librizzi@pa.ibf.cnr.it

The full understanding of the mechanisms underlying protein amyloid formation and deposition is still one of the most challenging research topics in biophysical chemistry. The main interest arises from the involvement of these processes in the etiology of a number of disorders, including Parkinson's and Alzheimer's disease, all characterized by the abnormal deposition within tissues of amyloid aggregates. Even if the detailed mechanisms responsible for amyloid toxicity are still poorly understood, it is now generally accepted that the most toxic species are small oligomers, which forms at the beginning of the aggregation process and/or can be released by mature fibrils. Regardless of the toxicity mechanisms, it is clearly of great importance to find methods able to inhibit or to influence amyloid formation. We report here different studies demonstrating the inhibiting effects on amyloid aggregation of chaperones and chaperon-like molecules, namely Hsp60 and  $\alpha$ -casein. The results will show that the mechanisms of action of the inhibitors can be different, depending both on the nature of the inhibiting molecule and on the detailed nucleation pathways underlying the aggregation process.

## IL2.2 Role of cardiolipin for stability of cytochrome c oxidase

E. Sedlák

Centre for Interdisciplinary Biosciences, Faculty of Science, P.J. Šafárik University in Košice, Jesenná 5, 04001 Košice, Slovakia

e-mail: erik.sedlak@upjs.sk

Bovine cytochrome c oxidase (CcO) (ferrocytochrome c:O<sub>2</sub> oxidoreductase, EC 1.9.3.1) is the terminal enzyme (complex IV) of the inner mitochondrial electron transport chain, catalyzing electron transfer from reduced cytochrome c to molecular oxygen. The complex is composed of 13 nonidentical protein subunits and two redox centers, one containing a copper atom and two heme A moieties; the other two copper atoms. The multisubunit enzyme, an integral membrane complex, spans the inner mitochondrial membrane and is in contact with an annulus of membrane phospholipids. CcO crystallizes as a dimer, which is generally seen as the functional unit within the inner membrane [1]. CcO isolated from the mitochondrial membrane is a protein–phospholipid complex solubilized by detergent. The purified, detergent-solubilized complex typically contains 15–20 phospholipids, 13 of which have been resolved within the three-dimensional crystal structure [2]. The 13 PLs are bound primarily at the interface between adjacent subunits, suggesting that they may function as a stabilizing factor in the quaternary structure. Most of these phospholipids can be removed without altering the functional activity of CcO or the structural stability of the detergent-solubilized complex. However, three or four cardiolipins (CLs) are tightly bound to each monomer and have an especially important functional and structural role [3,4].

To avoid structural artefacts due to harsh way of removal of tightly-bound CLs by detergents, we developed gentle method of delipidation of CcO based on enzymatic hydrolysis of CL by phospholipase A<sub>2</sub>. This method enabled us to show that CL is not only essential for full electron transport activity, but also has an important structural role in stabilizing the association of subunits VIa and VIb within the remainder of the bovine heart enzyme [3]. Moreover, we showed the role of tightly-bound CL as stabilizing factor (i) in the quaternary structure of CcO against chemical and thermal denaturation [5,6] and (ii) in its homodimeric structure.

We propose that this conclusion regarding stabilization role of tightly-bound CL for stability of CcO may be applicable to other multisubunit membrane proteins.

### Acknowledgement

This work was supported by the research grants from the Slovak grant agency VEGA no. 2/0062/14 and 1/0423/16 and the grant from CELIM (316310) funded by 7FP EU Programs REGPOT.

### References

[1] Tsukihara T, Aoyama H, et al. (1996) The whole structure of the 13-subunit oxidized cytochrome c oxidase at 2.8 Å. *Science* 272, 1136-1144. [2] Shinzawa-Itoh K, Aoyama H, et al. (2007) Structures and physiological roles of 13 integral lipids of bovine heart cytochrome c oxidase. *EMBO J.* 26, 1713–1725. [3] Sedlák E, Robinson NC (1999) Phospholipase A<sub>2</sub> digestion of cardiolipin bound to bovine cytochrome c oxidase alters both activity and quaternary structure. *Biochemistry* 38, 14966-14972. Planas-Iglesias J, Dwarakanath H, et al. (2015) Cardiolipin Interactions with Proteins. *Biophys. J.* 109, 1282-1294. [4] Sedlák E, Panda M, et al. (2006) Photolabeling of cardiolipin binding subunits within bovine heart cytochrome c oxidase. *Biochemistry* 45, 746-754. [5] Sedlák E, Varhač R, et al. (2014) The kinetic stability of cytochrome C oxidase: effect of bound phospholipid and dimerization. *Biophys J.* 107, 2941-2999. [6] Sedlák E, Robinson NC (2015) Destabilization of the Quaternary Structure of Bovine Heart Cytochrome c Oxidase upon Removal of Tightly Bound Cardiolipin. *Biochemistry* 54, 5569-5577.

### **PL3 Electrostatics goes viral**

R. Podgornik

Jožef Stefan Institute and University of Ljubljana, Ljubljana, Slovenia  
e-mail: rudolf.podgornik@ijs.si

I will present several models of the effects of electrostatic interactions on viruses. Starting from a discussion of charge distribution and the pertaining charge regulation description, I will explore in detail several examples of the role of charge-charge interactions for capsid stability as well as the interactions between the capsid proteins and the compactified genetic cargo. I will particularly concentrate on the effects of base sequence on electrostatic interactions between RNA and viral capsid.

### **IL3.1 Systems pharmacology model for the assessment of bronchoconstriction rate due to non-steroidal anti-inflammatory drugs**

A. Fajmut

University of Maribor, Faculty of Natural Sciences and Mathematics, Koroška cesta 160, Maribor, Slovenia

University of Maribor, Faculty of Health Sciences, Žitna ulica 15, Maribor, Slovenia

e-mail: ales.fajmut@um.si

App. 1% of population is intolerant to non-steroidal anti-inflammatory drugs (NSAIDs). Intolerance is manifested by either urticaria, conjunctivitis, rhino-sinusitis, bronchoconstriction, nasal polyposis or their combinations. There is increasing evidence that NSAID-triggered hypersensitivity partly originates from the imbalance of eicosanoids, the metabolites of arachidonic acid (AA), secreted by activated leukocytes. This imbalance, in concert with hyperresponsiveness and inflammation, results in bronchial hyper-reactivity – a characteristic symptom of asthma. Metabolism of arachidonic acid (AA) is generally divided into the cyclooxygenase and the lipoxygenase pathway revealing prostanoids and leukotrienes as metabolites, respectively. NSAIDs inhibit two enzymes of the cyclooxygenase pathway (COX-1 and COX-2) resulting in the reduction of prostanoids production. As a consequence, this might result in a higher cysteinyl leukotrienes production. Low prostanoid levels and high cysteinyl leukotrienes levels are typical characteristics of aspirin induced asthma at the metabolomic level. On the proteomic level, the differences in the expression of important enzymes in the AA metabolic pathway, are detected. Research on the tissue and organ level is oriented in determining the asthmatics' bronchial hyperreactivity and hypersensitivity towards the type and the dose of different NSAIDs. This is carried out with provocation tests, whereby forced expiratory volume in first second (FEV1) is measured at gradually increasing doses of NSAID.

With our systems pharmacology model that couples pharmacokinetic model of oral or intravenous (IV) NSAID dosing with the metabolism of AA in activated eosinophils we predict the resulting effect of eicosanoids on the airway smooth muscle reactivity in terms of the time-evolution of FEV1 of a virtual patient in response to the particular dose and type of NSAID. The model is first tested and calibrated for the subgroups of non-asthmatics as well as tolerant and intolerant asthmatic populations. Then, the model is fitted to the time-dependencies of the FEV1 measured within the provocation tests of individual extremely hypersensitive patients, and the key parameters, which determine their extreme hypersensitivity to NSAIDs are emphasized. These are: the expressions of the enzymes, controlling the production rate of cysteinyl leukotrienes and prostaglandin E2 within the metabolism of AA; parameters, determining the hypersensitivity in the stress-agonist relationship of the airway smooth muscles; and the total number of activated eosinophils, infiltrated into the airways. Calculations concerning different subgroups of aspirin intolerant asthmatics are carried out in the basal state (i.e. without drug) and after gradual dosing of different NSAIDs. The limiting doses (causing a 20% fall in FEV1) of each of the NSAIDs (aspirin, indomethacin, ibuprofen, naproxen and celecoxib etc.) and paracetamol are determined. All model simulations are carried out in two different model states, no-inflammation and inflammation. In this way we predict and simulate, how an individual patient or a patient group with a distinguishing pattern in eicosanoid production as well as with characteristic differences in the expression of the key enzymes within the AA metabolic pathway would respond to different NSAIDs in cases of treated or untreated asthma.

## IL3.2 Understanding substrate recognition and function of human dipeptidyl peptidase III

S. Tomić

Ruđer Bošković Institute, Zagreb, HR  
e-mail: Sanja.Tomic@irb.hr

Dipeptidyl peptidase III (DPP III, EC 3.4.14.4) is a monozinc metalloexopeptidase that hydrolyzes dipeptides from the N-terminus of its substrates consisting of three or more amino acids. Widely distributed in mammalian tissue, DPP III has been considered to participate in intracellular protein catabolism but it is also indicated in pain modulation<sup>1</sup> as well as in the stress response mechanism in mammals.<sup>2</sup> DPP III contributes to the activation of transcription factor Nrf2, a constituent of the Nrf2-Keap1 signaling pathway, the main defense mechanism against many environmental toxic agents and carcinogens in cells.<sup>3</sup>

Until now several 3D structures of human DPP III (h.DPP III) have been determined, ligand free and in complexes with natural peptides (PDB\_codes 3FVY, 5E33, and 3T6B, 3T6J, 5E3A, 5E2Q, 5EHH and 5E3C, respectively). H.DPP III structure consists of two domains, the catalytic one bearing the metal ion and the larger, "satellite" domain with a deep cleft in between. The presence of the interdomain cleft, together with promiscuous substrate specificity,<sup>1</sup> suggested that h.DPP III could experience significant internal motions. In order to rationalize the experimental data and to better understand its catalytic function we performed exhaustive in silico study of h.DPP III.<sup>4-9</sup> Using molecular dynamics (MD) simulation techniques we investigated the conformational landscape of h.DPP III as well as the influence of ligand binding on the protein structure and dynamics.<sup>4-7</sup> We found that h.DPP III can adopt a number of different forms in solution<sup>6,7</sup> wherein the most compact form was determined as the most stable. The substrate to be hydrolyzed binds preferably into a semi-closed conformation in a way to interact with both domains, influences the mutual orientation of domains and shifts the conformational equilibrium towards more compact protein form. In agreement with the experimental data we found that DPP III prefers ligands that adopt  $\beta$ -strand form and binds to the five-stranded  $\beta$ -core of the enzyme in an antiparallel fashion.

Using QM/MM calculations we determined the Zn<sup>2+</sup> coordination in different h.DPP III conformations, and showed that the most compact enzyme form is the catalytically active one.<sup>8</sup> Based on this result we were able to determine the reaction mechanism of the peptide bond hydrolysis in the enzyme active site.

Recently we have also studied h.DPP III binding to Keap1. In accord with the experimental data we showed that h.DPP III binds to the kelch domain via the flexible loop containing an "ETGE" motif.<sup>9</sup>

### References

1. Baršun M., Jajčanin N., Vukelić B., Špoljarić J. and Abramić M., *Biol. Chem.* 388 (2007) 343-348.
2. Liu Y., Kern J., Walker J.R., Johnson J.A., Schultz P.G., Luesch H., *Proc. Natl. Acad. Sci. USA* 104 (2007) 5205-5210.
3. Hast B.E., Goldfarb D., Mulvaney K.M., Hast M.A., Siesser P.F., Yan F., Hayes D.N. and Major M.B., *Cancer Res.* 73 (2013) 2199-2210.
4. Tomić A., Abramić M., Špoljarić J., Agić D., Smith D.M., Tomić S., *J. Mol. Recognit.* 24 (2011) 804-814.
5. Špoljarić J., Tomić A., Vukelić B., Salopek-Sondi B., Agić D., Tomić S. and Abramić M., *Croatica Chemica Acta* 84 (2011) 259-268.
6. Tomić A., Gonzalez M., Tomić S., *J. Chem. Information Model.* 52 (2012); 1583-1594.
7. Tomić A., Berynskyy M., Wade C. R., Tomić S., *Mol. BioSyst.* (2015) 11 3068-3080.
8. Tomić A., Tomić S., *Dalton transactions.* 43 (2014) 15503-155149.
9. Gundić M., Tomić A., Wade C.R., Tomić S., submitted for publication

## **PL4 Studying membrane bioactivity with advanced (super-resolution) optical microscopy**

C. Eggeling

University of Oxford, UK

e-mail: christian.eggeling@rdm.ox.ac.uk

Molecular interactions are key in cellular signalling. They are often ruled or rendered by the mobility of the involved molecules. We present different tools that are able to determine such mobility and potentially extract interaction dynamics. Specifically, the direct and non-invasive observation of the interactions in the living cell is often impeded by principle limitations of conventional far-field optical microscopes, specifically with respect to limited spatio-temporal resolution. We depict how novel details of molecular membrane dynamics can be obtained by using advanced microscopy approaches such as the combination of super-resolution STED microscopy with fluorescence correlation spectroscopy (STED-FCS), of fast beam-scanning with FCS (scanning (STED-)FCS), of fluorescence recovery after photobleaching (FRAP), or of single-particle tracking. Their performance on investigating different diffusion modes of plasma membrane proteins and lipids in the living cell are compared, and we highlight how these modes give novel details of membrane bioactivity such as in immune cells. It is often optimal to gather complementary information from all techniques.

#### **IL4.1 Combining protein micropatterning and single molecule microscopy to decipher plasma membrane organization**

G. Fülöp, A. Koffler, M. Brameshuber, G. Schütz, [E. Sevcsik](#)

Institute of Applied Physics, TU Wien, Vienna, Austria

e-mail: [sevcsik@iap.tuwien.ac.at](mailto:sevcsik@iap.tuwien.ac.at)

The plasma membrane displays a tremendous complexity of proteins and lipids necessary for cell function but it is unclear how proteins sense and influence their lipid environment, and vice versa. Sterol-rich nanoscopic lipid “raft” phases were proposed to mediate protein interactions but have not yet been directly observed. In a recent study, we have combined a protein micropatterning approach with single-molecule tracking to measure the local membrane environment of immobilized GPI-anchored proteins, which are considered to be archetypical raft residents [1]. We found no indication for the existence of nanoscopic ordered domains associated with these proteins. Essentially, the immobilized proteins behaved as inert obstacles to the diffusion of other membrane constituents indicating that phase partitioning is not a fundamental element of protein organization in the live cell plasma membrane. We have used a similar experimental approach to probe the membrane environment of other membrane proteins, such as palmitoylated transmembrane proteins.

#### **References**

[1] Eva Sevcsik, Mario Brameshuber, Martin Fölser, Julian Weghuber, Alf Honigmann, Gerhard J. Schütz (2015) “GPI-anchored proteins do not reside in ordered domains in the live cell plasma membrane” *Nat. Commun.* 6 6969.

#### IL4.2 ER nanojunctions and ER Ca<sup>2+</sup> refilling in vascular endothelial cells: experiments and models

C. M. L. Di Giuro<sup>1</sup>, K. Groschner<sup>1</sup>, R. Malli<sup>2</sup>, N. Shrestha<sup>1</sup>, C. van Breemen<sup>3</sup>, N. Fameli<sup>1</sup>

<sup>1</sup> Institute of Biophysics, Medical University of Graz, Graz, Austria

<sup>2</sup> Institute of Molecular Biology and Biochemistry, Medical University of Graz, Graz, Austria

<sup>3</sup> Department of Anesthesiology, Pharmacology and Therapeutics, The University of British Columbia; Child & Family Research Institute Vancouver, B. C., Canada

e-mail: nicola.fameli@medunigraz.at

The ER is notoriously involved in a multitude of cellular processes and better understanding of basic ER Ca<sup>2+</sup> content regulation appears important, not least potentially to elucidate links between ER stress and related diseases, since current knowledge of the fundamental ER stress mechanisms points to Ca<sup>2+</sup> transport deterioration to/from ER itself.

We employed fluorescent microscopy (Fura-2) to study the role of Na<sup>+</sup>/Ca<sup>2+</sup> exchangers (NCX), store-operated Ca<sup>2+</sup> entry (SOCE) and the involvement of plasma membrane (PM)-endoplasmic reticulum (ER) junctions in the refilling of ER Ca<sup>2+</sup> in vascular endothelial cells (EA.hy926). Part of the motivation stems from previous findings showing that in vascular smooth muscle the NCX play a critical role in refilling the sarcoplasmic reticulum with extracellular Ca<sup>2+</sup>.

To characterize this mechanism, we inhibited a host of transporters (NCX, Orai, transient receptor potential canonical channels (TRPC), ATPases) involved in the Ca<sup>2+</sup> communication between the extracellular space and the ER and found that following histamine (100 μM)-stimulated ER Ca<sup>2+</sup> release, blockade of NCX Ca<sup>2+</sup>-influx mode (by 10 μM KB-R7943) in WT cells diminished the ER refilling capacity by about 40%, while in Orai1-transfected cells ER refilling decreased by about 60%. Conversely, inhibiting the high-ouabain-affinity Na<sup>+</sup>/K<sup>+</sup>ATPases (10 nM ouabain), enhanced the ER Ca<sup>2+</sup> content by about 20%, thereby supporting the hypothesis that this process of privileged ER refilling is assisted by PM-ER junctions. The latter were observed in the cell ultrastructure and their main parameters of membrane-membrane separation and lateral extension were measured as (9 ± 5) nm and (109 ± 56) nm, respectively.

These results shed further light on the mechanism and function of a previously hypothesized subplasmalemmal Ca<sup>2+</sup> control unit during the refilling of the ER.

### IL4.3 Insights on the morphology and biological activity of gold nanoparticles protected by self-assembling mixtures of ligands

M. Guida,<sup>1</sup> M. Sologan,<sup>2</sup> D. Marson,<sup>3</sup> S. Boccardo,<sup>3</sup> S. Pricl,<sup>3</sup> L. Pasquato,<sup>2</sup> A. Tossi,<sup>1</sup> S. Pacor<sup>1</sup> and P. Posocco<sup>3\*</sup>

<sup>1</sup>Department of Life Sciences, University of Trieste, 34127, Trieste, Italy

<sup>2</sup>Department of Chemical and Pharmaceutical Sciences, University of Trieste, 34127 Trieste, Italy

<sup>3</sup>Molecular Simulation Engineering Laboratory (MOSE), Department of Engineering and Architecture, University of Trieste, 34127 Trieste, Italy

\*e-mail: paola.posocco@dia.units.it

The promise held by nanomaterials for diagnostic/therapeutic applications has greatly excited the entire scientific community.<sup>1</sup> Unfortunately, many hurdles including toxicity, immunogenicity, and decreased efficacy heavily hampered the use of nanoparticles (NPs) in bio-nanomedicine. Thus, a full understanding of NP ability to negotiate biological barriers will undoubtedly lead to an improved knowledge of their basic biology, enhanced control over their potential adverse effects, and ultimately the development of enriched classes of diagnostic/therapeutic agents.

Gold NPs (AuNPs) are ideal candidates to elucidate fundamental properties of biological interactions at the nano- and molecular-scale, particularly when protected with self-assembled monolayers (SAMs). When mixed SAMs of unlike molecules are used to coat AuNPs, nanoscale domains spontaneously form in the particle ligand shell. The formation of these 3D-patterns (typically patched, striped and Janus domains) provides AuNPs with surface dependent properties which, in turn, are expected to determine NP biological outcome.<sup>2</sup>

In this contribution we describe the first evidences of our investigation of the self-organization of mixtures of immiscible amphiphilic PEG-terminated fluorinated and hydrogenated ligands on the surface of AuNPs.<sup>3</sup> Studies of the morphology of these mixed monolayers were carried out experimentally by electron spin resonance (ESR) measurements; concomitantly, an *in silico* approach based on multiscale molecular simulations in explicit water was used to predict the microphase segregation morphology of the ligands on the metal surface at molecular level. Then, again combining theory and surface plasmon resonance (SPR) experiments on model membranes as well as *in vitro* experiments, we investigated the role of ligand arrangement and composition on the interaction with lipid bilayer and on cellular toxicity and uptake of these monolayer protected NPs.

The Italian Ministry of University Research (MIUR) through the Scientific Independence of Young Researchers (SIR) project "Structure and FunctiOn at the Nanoparticle bioInterfAce" (grant RBSI14PBC6) supports these activities.

1. (a) Doane, T. L.; Burda, C. *Chem. Soc.Rev.* **2012**, *41*, 2885; (b) Dreaden, E. C.; Alkilany, A. M.; Huang, X.; Murphy, C. J.; El-Sayed, M. A. *Chem. Soc.Rev.* **2012**, *41*, 2740.
2. (a) Kim, S. T.; Saha, K.; Kim, C.; Rotello, V. M. *Acc. Chem. Res.* **2013**, *46*, 681; (b) Verma, A.; Uzun, O.; Hu, Y.; Hu, Y.; Han, H. S.; Watson, N.; Chen, S.; Irvine, D. J.; Stellacci, F. *Nature Mat.* **2008**, *7*, 588.
3. Posocco, P.; Gentilini, C.; Bidoggia, S.; Pace, A.; Franchi, P.; Lucarini, M.; Fermeglia, M.; Pricl, S.; Pasquato, L. *ACS Nano* **2012**, *6*, 7243.

## PL5 Biophysical Properties of Dendrites of Cortical Pyramidal Neurons - Simultaneous Sodium and Calcium Imaging

S. D. Antic<sup>1,3</sup>, K. Miyazaki<sup>2,3</sup>, W. N. Ross<sup>2,3</sup>

<sup>1</sup>UConn Health, Farmington, CT, USA

<sup>2</sup>New York Med. Col., Valhalla, NY, USA

<sup>3</sup>Marine Biological Laboratory, Woods Hole, MA, USA.

e-mail: antic@uchc.edu

Strong synaptic inputs generate glutamate-mediated plateau potentials in basal dendrites of cortical pyramidal neurons (Milojkovic *et al.*, 2004). Plateau potentials propagate into the soma, sometimes causing relatively large amplitude (~20 mV) sustained (~200 ms) somatic depolarizations, often accompanied by bursts of action potentials. Such dendritic plateau potentials are regenerative in nature and dependent on mixtures of activated conductances (AMPA, NMDA, Na<sup>+</sup> channels, voltage-gated Ca<sup>2+</sup> channels (VGCC) and K<sup>+</sup> channels) in a process dubbed “spike-chain mechanism” (Schiller *et al.*, 2000). Because activation of one conductance can influence activation of other conductances through voltage and/or resulting ion fluxes (e.g. [Ca<sup>2+</sup>]<sub>i</sub>), it is difficult to determine the precise relative contribution and order of spikes in the dendritic spike-chain event based solely on the actions of selective channel antagonists on the spike waveform. One way to determine more information about the relevant dendritic currents is to observe concentration changes resulting from fluxes of ions to which receptors and channels are permeable. For example the influx of Na<sup>+</sup> reports activity of dendritic AMPA, NMDA and Na<sup>+</sup> channels, while the influx of Ca<sup>2+</sup> reports activity of NMDA and VGCCs. In the present study we simultaneously monitored dendritic Na<sup>+</sup> and Ca<sup>2+</sup> influxes during subthreshold and suprathreshold glutamate-mediated potentials. Simultaneous Na-Ca imaging (Miyazaki & Ross, 2015) was used to detect concentration changes in L5 pyramidal neurons in brain slices cut from (male and female) rat medial prefrontal cortex. [Na<sup>+</sup>]<sub>i</sub> changes were detected with a Na-sensitive dye, SBFI; [Ca<sup>2+</sup>]<sub>i</sub> changes were detected with one of the following Ca-sensitive dyes: OGB-5N or OGB-1 or Bis-fura-2. Focal glutamate microiontophoresis was used to trigger plateau potentials. Fluorescence signals were recorded with a fast camera. We observed Ca<sup>2+</sup> transients from multiple locations along dendrites. The largest responses were at the input site and were blocked by NMDA receptor antagonist, APV. Application of VGCC antagonists, reduced the Ca<sup>2+</sup> signal beyond the input site. Na<sup>+</sup> transients were detected at the input site only. They persisted in the presence of TTX showing that they were receptor mediated. In many experiments most of the Na<sup>+</sup> signal remained after the addition of APV suggesting a strong AMPA receptor component in these responses.

### Abbreviations:

NMDA - N-methyl-D-aspartate; AMPA - α-amino-3-hydroxy-5-methyl-4-isoxazolepropionic acid; SBFI - sodium-binding benzofuran isophthalate; OGB – Oregon Green Bapta; VGCC - voltage-gated calcium channels.

**Support:** NIH Grants MH109091 & NS085729, MBL Fellowship

### References:

Milojkovic BA, Radojicic MS, Goldman-Rakic PS & Antic SD (2004). Burst generation in rat pyramidal neurones by regenerative potentials elicited in a restricted part of the basilar dendritic tree. *J Physiol* **558**, 193-211.

Miyazaki K & Ross WN (2015). Simultaneous Sodium and Calcium Imaging from Dendrites and Axons. *eNeuro* **2**.

Schiller J, Major G, Koester HJ & Schiller Y (2000). NMDA spikes in basal dendrites of cortical pyramidal neurons. *Nature* **404**, 285-289.

## **IL5.1 Fractal and lacunarity analysis in neuroscience: application in 2D image of the brain neurons**

N.T. Milošević

Department of Biophysics, School of Medicine, University of Belgrade, Belgrade, Serbia  
e-mail: mtn@med.bg.ac.rs

This paper calls attention to the box-counting method, either to calculate fractal dimension of an object or to perform equivalent type of lacunarity analysis. Box-counting method is used following previous conclusions, that this is best technique to obtain fractal dimension among other fractal methods. This paper illustrates the box-count and corresponding lacunarity analysis on two dimensional neuronal images from the human dentate nucleus. Parameters of neuronal space-filling and shape, irregularity of dendrites and heterogeneity or rotational invariance of the image were analyzed in order to test whether they discriminate small sample of border neurons, taking into account their position within dentate nucleus. Mean values of four parameters were different between samples of outside and inside border neurons. Further statistical analysis investigates possibility of new classification scheme and gives better insight in the morphology of the human dentate neurons. The essence of applying box-counting analysis to neuronal morphology is the calculation of the box dimension and lacunarity. As for image of the neuron, apart from quantifying neuronal morphology, these parameters could be of relevance for intra- and/or inter-species comparisons of neuronal populations.

## **IL5.2 Molecular mechanisms and pharmacological implications of a new family of TRP antagonists**

R. Galdani

Department of Chemistry "Ugo Schiff", University of Florence, via della Lastruccia, 3 50019 Sesto F.no (FI), Italy  
e-mail: rgaldani@unifi.it

Transient receptor potential (TRP) channels are a large family of non-selective cation channels. Several TRP channel family members, including TRP channel subfamily V member 1 (TRPV1), TRP channel subfamily A member 1 (TRPA1) and TRP channel melastatin 8 (TRPM8), are expressed in primary sensory neurons of the trigeminal, vagal and dorsal root ganglia, and are deputed to detect a great deal of external stimuli, including pressure, temperature, and chemicals. In recent years, many efforts have been dedicated to the discovery of better and safer analgesics. However, the medical need for this type of drugs remains substantially unmet. In particular, compounds capable of targeting both inflammatory and neuropathic pain are lacking. To this purpose, a small molecule compound library was synthesized and screened by patch-clamp recordings on primary neurons and cell cultures expressing the human or the mouse isoforms of TRPA1 channel. Among all compounds analyzed, a new class of water soluble derivatives of lipoic acid was described [1]; these compounds rapidly and significantly inhibited TRPA1 inward and outward currents by a mechanism requiring the synergic combination of calcium-mediated binding and disulphide-bridge-forming of the lipoic acid moiety. In addition to a high binding constant vs. TRPA1 channel, these molecules showed: i) a remarkable safe profile; ii) an intriguing behaviour vs. TRPV1 channel; iii) the ability to significantly revert both oxaliplatin-induced neuropathic pain and mechanical facial inflammatory allodynia in rats [2]. Noteworthy, testing our compounds we shed light on the unprecedented involvement of both TRPA1 and TRPV1 channels in orofacial pain.

### **References**

- [1] C. Nativi, R. Galdani et al. (2013) Scientific Rep. 3, 2005, 1-10.
- [2] R. Galdani et al. (2015) ACS Chem. Neurosci., 6(3), 380-5.

### IL5.3 Converging and correlative approaches towards optical nanoscopy

A. Diaspro

Nanoscopy, Nanophysics, Istituto Italiano di Tecnologia, Genoa, 16163, Italy;  
Department of Physics, University of Genoa, Via Dodecaneso 33, 16146, Genoa, Italy;  
Nikon Imaging Center, Istituto Italiano di Tecnologia, Via Morego 30, 16163, Genoa, Italy  
e-mail: alberto.diaspro@iit.it

The sentence “Microscopy has become nanoscopy”, as reported in the Nobel Prize 2014 statement, updates the phrase “microscopium nominare libuit” that introduced optical microscopy referred to the Galileo Galilei’s optical microscope. So far, optical nanoscopy refers to those methods that in the last 25 years (circa) have been developed to crumble the diffraction limit by two far-field principles that lead to fluorescence-based microscopy with a spatial resolution that is further the Abbe’s limit. These methods have been referred as “super-resolved ensemble fluorophore microscopy” and as “super-resolved single fluorophore microscopy” also known as targeted and stochastic read out methods, respectively [1]. We will discuss converging and correlative techniques linked to optical nanoscopy, a sort of new roadmap for developments [2-3]. The main focus is related to on imaging techniques that permit direct measurements of the live-cell molecular dynamics at the nanometer scale including the study of thick biological samples. An important list of converging technologies is currently under development, for example: recent advances in camera technology and real-time image processing coupled with data analysis have led to substantially improved time resolution, Reversible Saturable Optical Fluorescence Transitions (RESOLFT) nanoscopy and the utilization of temporal information for decoding spatial information, as in the cases of gated-STED and SPLIT approaches, allowed super resolution at reduced beam intensities, the advent of new fluorescent molecules are providing better quantitative abilities, original image deconvolution approaches for noise removal, in vivo imaging, new lenses and beam shapers. Today, we have a tunable microscope in terms of spatial and temporal resolution allowing different contrast mechanisms. Do we have set of appropriate questions for exploiting such an instrument? Moreover, correlative approaches coupling optical super resolved methods with electron and scanning probe microscopes are providing interesting developments that will be outlined, too [4, 5].

#### References

- [1] Diaspro, A. 2014. Circumventing the diffraction limit. *Il Nuovo Saggiatore* 30: 45–51.
- [2] Hell, S.W. et al. 2015. The 2015 super-resolution microscopy roadmap. *J.Phys.D Appl.Phys.* in press: 1–36.
- [3] Diaspro A. and van Zandvoort M.A.M.J. (eds) 2016. *Super-resolution Imaging in Biomedicine*. CRC press
- [4] Chacko, J.V., F.C. Zancchi, and A. Diaspro. 2013. Probing cytoskeletal structures by coupling optical superresolution and AFM techniques for a correlative approach. *Cytoskeleton (Hoboken)*. 70: 729–740.
- [5] Monserrate, A., S. Casado, and C. Flors. 2013. Correlative Atomic Force Microscopy and Localization-Based Super-Resolution Microscopy: Revealing Labelling and Image Reconstruction Artefacts. *ChemPhysChem*. 15: 647–650.

## PL6 Imaging protein-based nanostructured photosensitizers with subdiffraction resolution

P. Delcanale<sup>1</sup>, C. Montali<sup>1</sup>, S. Abbruzzetti<sup>2</sup>, S. Bruno<sup>3</sup>, M. Tognolini<sup>3</sup>, C. Giorgio<sup>3</sup>, F. Pennacchietti<sup>4</sup>, M. Oneto<sup>4</sup>, P. Bianchini<sup>4</sup>, A. Diaspro<sup>4</sup>, P. Foggi<sup>5</sup>, C. Viappiani<sup>1</sup>

<sup>1</sup> Dipartimento di Fisica e Scienze della Terra, Università di Parma, 43124 Parma, Italy

<sup>2</sup> Dipartimento di Bioscienze, Università di Parma, 43124 Parma, Italy

<sup>3</sup> Dipartimento di Farmacia, Università di Parma, 43124 Parma, Italy

<sup>4</sup> Fondazione Istituto Italiano di Tecnologia, 16163 Genova, Italy

<sup>5</sup> Dipartimento di Chimica, Università di Perugia, 06123 Perugia, Italy

e-mail: cristiano.viappiani@unipr.it

Localizing a photosensitizer is a valuable information in the evaluation of the efficacy of its photodynamic action against the target cells, since the photoinduced reactive singlet oxygen is a short lived species which can exert its phototoxic action on a very restricted range, close to the site of generation.

We report on the use of the self-assembled complex between the naturally occurring photosensitizer hypericin (Hyp) and apomyoglobin (apoMb) [1] as a fluorescent photosensitizer which is fully functional for photodynamic inactivation of bacteria and tumor cells. Other protein scaffolds proved to be excellent carriers for Hyp. [2]

We show that the excited state properties of the naturally occurring photosensitizer hypericin can be exploited to perform Stimulated Emission Depletion (STED) microscopy on cells incubated with the complex between hypericin and apomyoglobin, a self-assembled nanostructure that confers very good bioavailability to the photosensitizer. The present study establishes the potential of Hyp as a probe for superresolution microscopy. [3]

Antibacterial treatments based on photosensitized production of reactive oxygen species is a promising approach to address local microbial infections. Given the small size of bacterial cells, identification of the sites of binding of the photosensitizing molecules is a difficult issue to address with conventional microscopy. Hypericin fluorescence is mostly localized at the bacterial wall, and accumulates at the polar regions of the cell and at sites of cell wall growth. While these features are shared by Gram-negative and Gram-positive bacteria, only the latter are effectively photoinactivated by light exposure.

Superresolution images can be collected also on cultured tumor cells. At the employed concentrations, ApoMb-Hyp rapidly accumulated on the plasma membrane. Upon illumination, extensive damage is induced, which leads to membrane blebbing and permeation, resulting in necrotic cell death.

### References:

[1] J. Comas-Barceló, B. Rodríguez-Amigo, S. Abbruzzetti, P. Rey-Puech, M. Agut, S. Nonell, C. Viappiani *RSC Advances* **2013**, *3*, 17874.

[2] B. Rodríguez-Amigo, P. Delcanale, G. Rotger, J. Juárez-Jiménez, S. Abbruzzetti, A. Summer, M. Agut, F.J. Luque, S. Nonell, C. Viappiani *J. Dairy Sci.* **2015**, *98*, 89.

[3] P. Delcanale, F. Pennacchietti, G. Maestrini, B. Rodríguez-Amigo, P. Bianchini, A. Diaspro, A. Iagatti, B. Patrizi, P. Foggi, M. Agut, S. Nonell, S. Abbruzzetti, C. Viappiani *Scientific Reports* **2015**, *5*, 15564.

## **IL6.1 Novel label-free optical biosensors for cell dynamics on biomimetic coatings**

R. Horváth

Nanobiosensorics Group, MTA EK MFA, Budapest (H)  
e-mail: horvathr@mfa.kfki.hu

The present talk highlights the outstanding potentials of planar optical waveguide based sensors in biophysics and cell biology. Novel waveguide configurations allow to monitoring refractive index variations inside the evanescent fields of the waveguide modes with excellent sensitivity, dynamic range, temporal and spatial resolution. Adsorbing biomolecules and living cells adhering on the waveguide surface increase the refractive index inside the evanescent field and perturb the excited optical modes. By monitoring the effective refractive indices or the intensities of the modes, biological and biophysical processes can be in situ followed in a completely label-free manner. Novel optical waveguide based sensor configurations, such as, grating coupled interferometry, resonant waveguide grating, and resonant waveguide grating with intensity-based readout will be highlighted with key application examples relevant to recording the kinetics of cell-surface interactions and dynamic changes in the distribution of cell mass due to external stimuli. The combination of the biosensors with recently developed technologies for single cell manipulation and analysis will be presented, too.

### References

1. R Ungai-Salánki, T Gerecsei, P Fürjes, N Orgovan, N Sandor, E Holczer, R Horvath, B Szabó Automated single cell isolation from suspension with computer vision SCIENTIFIC REPORTS 6: Paper 20375. 9 p. (2016)
2. Y Nazirizadeh, V Behrends, A Proosz, N Orgovan, R Horvath, AM Ferrie, Y Fang, C Selhuber-Unkel, M Gerken Intensity interrogation near cutoff resonance for label-free cellular profiling SCIENTIFIC REPORTS 6: Paper 24685. 6 p. (2016)
3. N Orgovan, B Peter, S Bosze, JJ Ramsden, B Szabo, R Horvath Dependence of cancer cell adhesion kinetics on integrin ligand surface density measured by a high-throughput label-free resonant waveguide grating biosensor SCIENTIFIC REPORTS 4: Paper 4034. 8 p. (2014)

This work was supported by the Momentum (Lendület) Program of the Hungarian Academy of Sciences and by the ERC\_HU Program of the National Research, Development and Innovation Office.

## **IL6.2 Interaction of materials with model and cell membranes studied by Fluorescence Microscopy and Microspectroscopy**

Z. Arsov, I. Urbančič, M. Garvas, R. Podlipec, B. Kokot, T. Koklič, J. Štrancar

Laboratory of Biophysics, Solid State Physics Department, "Jožef Stefan" Institute, Jamova cesta 39, SI-1000 Ljubljana, Slovenia  
e-mail: janez.strancar@ijs.si

Fluorescence microscopy success relies on the superior contrast between the observed biologically relevant objects and their environment. The contrast is gained because re-emitted light appears at larger wavelengths than the excitation light thus enabling the removal of the latter. Analogously, the sensitivity can be further enhanced, for example to molecular events, even without breaking the diffraction limit, if the emitted fluorescence (light) is spectrally analysed all-over the field-of-view. This can boost efficient detection of molecular conformations or identification and discrimination of bacteria against the polymer background. Nevertheless, one of the most powerful application identified so far is nanoparticle tracking in complex biological systems and studying the interactions between nanomaterial and the living cells. Such an application relies on the fact the spectral analysis reveal the information about the local molecular environment (e.g. modified-polarity-based spectral shift) or proximity (e.g. FRET-based identification molecular contact) which both appear at the nanometre scale. The later has been employed to detect the lipid wrapping around TiO<sub>2</sub> nanotubes and the accompanying model membrane disintegration. In addition to spectral detection, also micromanipulation of the samples can provide additional information about the interaction between the membranes and the materials. In our case, the optical tweezer has been employed to identify the power of adhesion between cells and polymer materials which nicely correlate with the cell on-growth and can thus be used to characterize the so-called biocompatibility of the polymer materials.

### **IL6.3: A polysaccharide based approach to mimic the extracellular matrix in biomaterials**

E. Marsich, A. Travan, M. Borgogna, S. Paoletti, I. Donati

Department of Life Sciences, University of Trieste, Via Licio Giorgieri 5, I-34127 Trieste, Italy.  
e-mail: [idonati@units.it](mailto:idonati@units.it)

The contemporary presence of proper biochemical and biophysical stimuli is the key aspect of the natural extracellular matrix which embeds the cells in a niche where cell recognition and mechano-transduction, with their cascade of cellular and molecular events, is a fundamental part of the healthy tissue development. For this reason, the tissue regeneration/engineering approach in biomedical applications strongly relies on the development of a synthetic ExtraCellular Matrix (ECM) which mimics the biochemistry and mechanics of the natural one. The architecture and chemical milieu provided by the synthetic matrix, as well as the possible hierarchical and anisotropic assembly, dictates the mechanical forces exerted on cells and their biological cross-talk with the surrounding environment.[1] In order to reproduce the structural complexity of the ECM, which can be described as a hybrid system with multiple structural and interdigitated functional components at different scale lengths,[2] we must look at concepts such as macromolecular features, compatibility and effect of charge density and interactions with ions. Among the different class of polymers, polysaccharides possess unique properties. They compose the natural highly hydrated structure embedding cells in the ECM enabling both biological recognition and proper viscoelastic responses to stress. In the field of biomaterials, polysaccharides have been largely used as coating materials for implants, for cell encapsulation purposes and for preparation of scaffolds and nanocomposites.[3] In addition, polysaccharides are characterized by a very high versatility which makes them ideal candidates for chemical modifications with bioactive molecules such as peptides and saccharides involved in cell adhesion.

#### **References:**

1. Griffith L.G., Swartz M.A. , Nat. Rev. Mol. Cell Bio. 2006, 7, 211.
2. Birk D.E., Yurchenco P.D., Mecham R.P., 1994, in Extracellular Matrix Assembly and Structure, Academic Press, San Diego
3. Travan A., Pelillo C., Donati I., Marsich E., Benincasa M., et al. Biomacromolecules 2009, 10, 1429

## **PL7 Light microrobotics in biology**

P. Ormos

Institute of Biophysics, Biological Research Centre of the Hungarian Academy of Sciences,  
Temesvári krt 62. H-6726 Szeged (H)  
e-mail: ormos.pal@brc.mta.hu

In the basic scheme of optical micromanipulation a focussed Gaussian light beam traps a spherical object defining its position. Since typically objects of micrometer size are grabbed by pN forces, the method is extremely useful in the study of biological objects. The possibilities can be vastly extended if the trapping light is structured and the object has an appropriate non-trivial shape. Key components of the procedure are the fabrication of complex shaped microparticles and the generation of structured trapping light field.

Two-photon excitation induced photopolymerization is the procedure to produce particles with shapes of arbitrary complexity, and holographic beam shaping is achieved by the use of Spatial Light Modulators (SLM). By the combination of these technologies complex manipulation schemes can be realized, creating a new field of light robotics. I will show characteristic examples to illustrate the possibilities.

The grabbed objects can be rotated, creating an optical wrench, enabling the measurement of the torsional properties of biological micromolecules. With the help of the light actuated microtools one can determine local mechanical properties of biological objects, local fluorescence or Raman excitation with submicrometer resolution can be achieved using plasmonic excitation. The indirect optical manipulation of live cells with the help of the microtools enables the separation of the trapping light from the trapped object, thus preventing light damage of the cells, so that a prolonged investigation becomes possible.

Optically manipulated microparticles also offer excellent model systems to study special properties of biological motion at the micrometer scale. Two examples will be discussed: Hydrodynamic synchronization and quasi-autonomous moving robots driven by light.

### IL7.1 Mapping of hemoglobin residuals in erythrocyte ghosts using two photon excited fluorescence microscopy

K. Bukara<sup>1,2</sup>, S. Jovanić<sup>3</sup>, I. Drvenica<sup>1</sup>, A. Stančić<sup>4</sup>, V. Ilić<sup>4</sup>, M. D. Rabasović<sup>3</sup>, D. V. Pantelić<sup>3</sup>, B. M. Jelenković<sup>3</sup>, B. Bugarski<sup>1</sup>, A. J. Krmpot<sup>3</sup>

<sup>1</sup> Department of Chemical Engineering, Faculty of Technology and Metallurgy, University of Belgrade, Karnegijeva 4, 11 000 Belgrade, Serbia

<sup>2</sup> Department Pharmaceutics, University of Antwerp, Universiteitsplein 1, 2610 Antwerp, Belgium

<sup>3</sup> Institute of Physics Belgrade, University of Belgrade, Pregrevica 118, 11 080 Belgrade, Serbia

<sup>4</sup> Institute for Medical Research, University of Belgrade, Dr Subotića br 4, 11 129 Belgrade, Serbia

e-mail: krmpot@ipb.ac.rs

Nonlinear laser scanning microscopy (NLSM) with its three modalities, two photon excited fluorescence (TPEF), second and third harmonic generation (SHG/THG) is advanced optical technique mostly used in biomedicine for label free and in vivo imaging [1]. Hemoglobin, the main intracellular component of erythrocytes, emits strong Soret fluorescence peaked at 438 nm upon two-photon excitation in red and near infrared region (600-750 nm) [2]. Human and animal erythrocyte membranes (i. e. ghosts) as model membranes in proteomics and lipidomics, they found application in modern studies for prolonged and controlled drug delivery [3-6]. During preparation of erythrocyte ghosts a certain amount of hemoglobin remains bound to membranes in the resulting erythrocyte ghosts [5]. This so called residual hemoglobin significantly affects subsequent encapsulation process and encapsulated drug releasing profile [7]. The amount of residual hemoglobin in ghosts' suspension is quantified by spectrophotometric, cyanmethemoglobin method. However, this method does not provide information on spatial distribution and localization of residual hemoglobin. Based on findings reported by Zheng and co-workers [2] we have utilized TPEF microscopy to map the spatial distribution of residual hemoglobin. The home made experimental set up for NLSM utilizes the train of the femtosecond pulses from Ti:Sapphire laser (Coherent, Mira 900-F) at 730nm. The repetition rate is 76MHz, and pulse duration is 160fs. Porcine slaughterhouse blood and human outdated blood were used as a starting biological material. Porcine and human erythrocyte ghosts were prepared by gradual hypotonic hemolysis [5]. First we have used TPEF microscopy and endogenous fluorescence of hemoglobin to image the intact erythrocytes at single cell level and to study their morphology. Two types of erythrocytes, human and porcine, characterized with discocyte and echynocyte morphology, respectively, were examined. We have shown that the distribution of hemoglobin in intact erythrocytes follows the cells' shape with pronounced abundance in the proximity of cell membrane. The TPEF images have also revealed that despite an extensive washing out procedure after gradual hypotonic hemolysis process, residual haemoglobin localized on intracellular side of the ghost membranes. The TPEF estimated hemoglobin distribution in intact erythrocytes and residual hemoglobin distribution in erythrocyte ghosts could be of importance in biotechnological processes but also in diagnosis of different pathological conditions.

#### References

[1] Masters, B. R. & So, P. T. C. (2008) Handbook of Biomedical Nonlinear Optical Microscopy. Oxford University Press. [2] W. Zheng, D. Li, Y. Zeng, Y. Luo, and J. Y. Qu, Biomed Opt Express 2, 71-79 (2010). [3] V. Leuzzi, L. Rossi, C. Gabucci, F. Nardecchia, and M. Magnani, J. Inherit. Metab. Dis., 1-12 (2016). [4] V. Borgeaux, J. M. Lanao, B. E. Bax, and Y. Godfrin, Drug Des. Dev. Ther. 10, 665-676 (2016). [5] I. Kostić, V. Ilić, V. Đorđević, K. Bukara, S. Mojsilović, V. Nedović, D. Bugarski, Đ. Veljović, D. Mišić, and B. Bugarski, Colloids Surf B 122, 250-259 (2014). [6] R. Deak, J. Mihaly, I. C. Sziguarto, A. Wacha, G. Lelkes, and A. Bota, Colloids and Surf. B 135, 225-234 (2015). [7] Kostić IT. Preserved erythrocyte membranes produced from slaughterhouse blood as systems for prolonged delivery of active substances. Doctoral Dissertation, Faculty of Technology and Metallurgy, University of Belgrade, 2015.

## IL7.2 Polyelectrolyte composite: hyaluronic acid mixture with DNA

I. Delač Marion<sup>1</sup>, D. Grgičin<sup>1</sup>, K. Salamon<sup>1</sup>, S. Bernstorff<sup>2</sup> and T. Vuletić<sup>1</sup>

<sup>1</sup>Institut za fiziku, Bijenička 46, 10000 Zagreb, Croatia;

<sup>2</sup>Elettra-Sincrotrone Trieste, 34102 Basovizza, Italy

e-mail: tvuletic@ifs.hr

We studied salt-free mixtures of DNA and hyaluronic acid (HA) across a broad range of concentration ratios  $c_{HA}/c_{DNA}=0.05-50$  ( $c=5-200$  g/L) [1]. By polarizing microscopy we established that DNA and HA form clearly separated thread-like domains defined and oriented by solution shear. We applied small angle x-ray scattering (SAXS) and observed a polyelectrolyte (PE) correlation peak at  $q^*$  wave vector, ascribed to DNA subphase and thus reporting on its effective concentration  $c^*_{DNA}$ , via deGennes scaling  $q^*\sim c^{1/2}$  [2]. From  $c^*_{DNA}$  it was possible to infer the  $c^*_{HA}$  of HA subphase. We found a ratio  $\Gamma = c^*_{HA}/c^*_{DNA}\approx 0.85$  across the studied range. As there is the osmotic pressure,  $\Pi$  equilibrium between DNA and HA subphases, the constant  $\Gamma$  indicates that  $\Pi\sim c^{9/8}$  scaling commonly found for DNA and other highly charged PEs is valid also for HA which does not feature counterion condensation. Therefore we propose that this deviation from the conventional osmotic pressure scaling  $\Pi\sim c$  can not originate from the concentration dependence of counterion condensation, which is a common interpretation in the literature. Further, without condensation, for HA all counterions contribute to  $\Pi$ , so the HA osmotic coefficient  $\phi_{HA}$  can be a measure of  $\phi_{DNA}$ . We found the latter to be 0.28. Thus, we corroborate the work by Raspaud et al. [3] who found that the concentration of counterions controlling the osmotic pressure is double the Manning-condensation theory defined value for DNA or PSS.

[1] Delač Marion I, Grgičin D., Salamon K., Bernstorff S., Vuletić T., (2015) *Polyelectrolyte Composite: Hyaluronic Acid Mixture with DNA*, *Macromolecules* 48, 2686

[2] Salamon K, Aumiler D, Pabst G, Vuletić T (2013) *Probing the Mesh Formed by the Semirigid Polyelectrolytes*, *Macromolecules* 46, 1107-1118

[3] Raspaud E, da Conceição M, Livolant F (2000) *Do Free DNA Counterions Control the Osmotic Pressure?*, *Phys. Rev. Lett.* 84, 2533-2536.

### **IL7.3 Biophysics networks in Europe: the "Association of Resources for Biophysical Research in Europe (ARBRE)" and the COST Action "Between Atom and Cell: Integrating Molecular Biophysics Approaches for Biology and Healthcare (MOBIEU)"**

R. Gilbert

University of Oxford, UK  
e-mail: gilbert@strubi.ox.ac.uk

The Association of Resources for Biophysical Research in Europe (ARBRE, <https://www.structuralbiology.eu/networks/association-resources-biophysical-research-europe>) is an open pan-European network which aims to bring together academic and industrial research infrastructures, core facilities and resource labs that provide access to biophysical instrumentation and expertise for the molecular-scale characterization of biological systems. The network aims to generate a community focused on broadening expertise and inspiring novel methodological development. It addresses all scientists and technicians who utilize biophysical instrumentation to characterize the intrinsic properties of biological macromolecules and the assemblies in which they are involved.

Molecular-scale biophysics is a dynamic and ever-expanding interdisciplinary field that aims to study biological macromolecules and assemblies as a whole, at an intermediate level between atomic-resolution structural descriptions and cellular-level observations ("Between Atom and Cell"), with significant applications in biomedicine and drug discovery. The MOBIEU Action ([http://www.cost.eu/COST\\_Actions/ca/CA15126](http://www.cost.eu/COST_Actions/ca/CA15126)) aims to seed a large-scale pan-European interdisciplinary synergistic clustering, allowing to ally and synergize the power of spectroscopic, hydrodynamic, real-time microfluidic, thermodynamic and single-molecule approaches.

This novel open network, that has been originated from ARBRE, will create an optimal environment for the development of innovative integrative biophysical approaches, at the level of data acquisition, analysis and modeling, as well as for the design of unprecedented and ambitious combinations of methodologies, to decipher more efficiently crucial biological phenomena and to overcome significant biomedical challenges.

MOBIEU will also broadly disseminate knowledge, notably through the organization of a strong program of workshops and Training Schools, and the setting up of a STSM scheme, aimed in priority to Early Career Investigators and technical scientists.

In parallel, it will place a special emphasis on the construction of a new distributed molecular-scale biophysics European infrastructure, aiming to facilitate the transnational access to instrumentation and expertise for a wide user community, in particular from Inclusiveness Target Countries.

Finally, MOBIEU will provide a platform for scientists to establish early contacts with instrument developers (at the level of concept or prototype), allowing to set-up win-win partnerships that will allow to define and develop together future instrumentation that genuinely meets the needs of the broad biomedical and life sciences communities.

## Selected Orals (S)

### **SO1.1 On the role of external force of actin filaments in the formation of tubular protrusions of closed membrane shapes with anisotropic membrane components**

L. Mesarec<sup>1</sup>, S. Kralj<sup>2,3</sup>, W. Gózdź<sup>4</sup>, V. Kralj-Iglič<sup>1,5</sup> and A. Iglič<sup>1</sup>

<sup>1</sup>Laboratory of Biophysics, Faculty of Electrical Engineering, University of Ljubljana, Tržaška 25, SI-1000 Ljubljana, Slovenia

<sup>2</sup>Department of Physics, Faculty of Natural Sciences and Mathematics, University of Maribor, Koroška cesta 160, SI-2000 Maribor, Slovenia

<sup>3</sup>Jožef Stefan Institute, P.O. Box 3000, SI-1000 Ljubljana, Slovenia

<sup>4</sup>Institute of Physical Chemistry, Polish Academy of Sciences, Kasprzaka 44/52, 01-224 Warsaw

<sup>5</sup>Laboratory of Clinical Biophysics, Faculty of Health Sciences, University of Ljubljana, Zdravstvena 5, SI-1000 Ljubljana, Slovenia

e-mail: mesarec.luka@gmail.com

Biological membranes are in general composed of different nanodomains and there is no reason to assume that these domains are all isotropic. Membrane tubular protrusions were experimentally observed and theoretically predicted, even without the application of external force, when the anisotropic membrane properties were taken into account. It was shown that the self-assembled aggregates formed by anisotropic membrane components could induce or facilitate the growth of long plasma membrane protrusions. Tubular protrusions can also be generated or stabilised by the pushing force of actin filaments. Our theoretical study focuses on the role of anisotropic constituents in the membrane tubular structures generated or stabilised by actin filaments. The influence of the cell/vesicle reduced volume on the width and length of tubular protrusion was investigated numerically. We also studied the effect of the entropy of mixing of membrane components on the shape of membrane protrusions. It is indicated that the entropy of mixing prevents the total separation of anisotropic and isotropic membrane components. We calculated the equilibrium vesicle shapes with different lengths of the actin rod-like structure inside the vesicle. It is shown that the growth of actin cytoskeleton inside the vesicle can induce the partial separation of different membrane components, which means that the effect of the entropy of mixing is in this case significantly reduced.

## SO1.4 Computational Design of Histone Deacetylase Inhibitors as Antitumor Agents

J. Kollár<sup>1,2</sup>, P. Polonec<sup>3</sup>, Z. Tučeková<sup>4</sup>, S. Miertus<sup>4,5</sup> and V. Frečer<sup>3,5\*</sup>

<sup>1</sup>Department of Nuclear Physics and Biophysics, Faculty of Mathematics, Physics and Informatics, Comenius University in Bratislava, Mlynska Dolina, SK-84248 Bratislava, Slovakia

<sup>2</sup>Department of Pharmaceutical Analysis and Nuclear Pharmacy, Faculty of Pharmacy, Comenius University in Bratislava, Odbojarov 10, SK-832 32 Bratislava, Slovakia

<sup>3</sup>Department of Physical Chemistry of Drugs, Faculty of Pharmacy, Comenius University in Bratislava, Odbojarov 10, SK-83232 Bratislava, Slovakia

<sup>4</sup>Department of Biotechnologies, Faculty of Natural Sciences, University of Ss. Cyril and Methodius, Nam. J. Herdu 2, SK-91701 Trnava, Slovakia

<sup>5</sup>International Centre for Applied Research and Sustainable Technology (ICARST n.o.), Jamnickeho 19, SK-84104 Bratislava, Slovakia

e-mail: frecer@fpharm.uniba.sk

Currently, cancer is ranked among the most prevalent causes of death in the developed countries. In addition, available cancer therapy is not sufficiently efficient nor specific. Tumours often relapse and develop resistance to previously used therapeutics. Therefore, development of new anticancer drugs is of great importance. Histone deacetylase (HDAC) inhibitors represent a new class of anticancer therapy<sup>[1]</sup>. Different HDAC isoforms occurring in diverse multi-protein complexes are involved in regulation of gene expression by means of acetylation of lysine residues on the histone tails. Eleven human HDAC isoforms are known, each having a particular role in a specific type of cancer. Inhibition of different isoforms causes apoptosis in different tissues. Intriguingly, tumour cells are more responsive to treatment by HDAC inhibitors than normal cells.

In this contribution, we have focused on optimisation of HDAC4 inhibitors. HDAC4 is involved in renal carcinoma, breast cancers and acute promyelocytic leukaemia, in addition its inhibition slows down angiogenesis<sup>[2]</sup>. In a pursuit for developing improved HDAC4 inhibitors, we have computationally explored the chemical space around trisubstituted diarylcyclopropane-hydroxamic acids, molecules similar to those synthesized and tested by Bürli *et al.*<sup>[3]</sup>.

We have created three different quantitative structure-activity relationship models (QSAR) that correlated computed HDAC4 - inhibitor interaction energies with observed inhibitory activities ( $pIC_{50}^{exp}$ ) of a set of inhibitors prepared, synthesized and tested by Bürli *et al.*<sup>[3]</sup>. The first QSAR model was based on molecular docking and *in silico* screening of inhibitors in the crystal structure of HDAC4. The second model utilised interaction energies ( $E_{int}$ ) between the enzyme and inhibitor calculated by means of molecular mechanics (MM). The third and most robust model was based on hybrid quantum mechanical / molecular mechanical approach (QM/MM) to  $E_{int}$  calculation. Thereafter, a virtual combinational library of more than 26000 analogues of the diarylcyclopropanehydroxamic acids was generated with the goal to explore more deeply the chemical space around the active analogues. Then, Lipinsky rule of five and additional ADME-related properties were applied to filter out molecules with reduced drug-like character. The remaining analogues were docked into the crystal structure of HDAC4 and the best scoring molecules were further processed to predict their HDAC4 binding affinities using MM and QM/MM approaches. Finally, 10 of the most promising potential HDAC4 inhibitors based on our predictions were docked to crystal structures of deacetylases HDAC2, 6 and 8 to explore their isoform selectivity. Five compounds with predicted inhibitory activities in the low nanomolar concentration range were recommended for synthesis and testing as selective HDAC4 inhibitors.

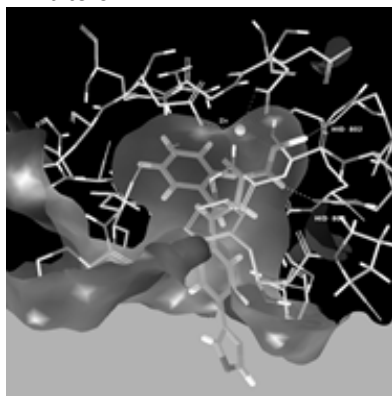


**Fig. 1.** Crystal structure of the active site of histone deacetylase 4 co-crystallized with trisubstituted diarylcyclopropanehydroxamic acid reference inhibitor with  $IC_{50}^{exp} = 0.02 \mu M$  [3].

### Acknowledgement

Partial financial support from the Slovak Research and Development Agency (APVV-14-0294), (APVV-14-0393) and Faculty of Pharmacy, Comenius University in Bratislava (FAF/35/2016) is gratefully acknowledged.

### References

[1] Kim H., Bae S.: *Am. J. Transl. Res.* **3**, 166-179 (2011). [2] Qian D., et al.: *Cancer Res.* **66**, 8814-8821 (2006). [3] Bürli R. et al.: *J. Med. Chem.* **56**, 9934-9954 (2013).

### **SO1.5 The cellular effects induced by the pore-forming agent nystatin**

**B. Božič<sup>1</sup>, Š. Zemljič Jokhadar<sup>1</sup>, L. Kristanc<sup>1</sup>, G. Gomišček<sup>1,2</sup>**

<sup>1</sup>Institute of Biophysics, Faculty of Medicine, University of Ljubljana, Ljubljana, Slovenia

<sup>2</sup>Faculty of Health Sciences, University of Ljubljana, Ljubljana, Slovenia

e-mail: bojan.bozic@mf.uni-lj.si

The responses of Chinese hamster ovary epithelial cells, caused by the pore-forming agent nystatin, were investigated using optical microscope. Different phenomena, i.e., the detachment of cells, the formation of blebs, the occurrence of “cell-vesicles” and cell ruptures, were observed. These phenomena were compared to those discovered in giant phospholipid vesicles. A theoretical model, based on the osmotic effects that occur due to the size-discriminating nystatin transmembrane pores in phospholipid vesicles, was extended with a term that considers the conservation of the electric charge density in order to describe the cell’s behavior. The time dependence of the concentrations of the most abundant ions in the cell was predicted and correlated with the increased cellular volume. The cell responses were explained primarily on the basis of the mechanical properties of the membrane.

## SO2.1 Lone-pair- $\pi$ interactions in nucleic acids and proteins: physical origin and significance

J. Novotný,<sup>1</sup> S. Bazzi,<sup>1,2,3</sup> R. Marek,<sup>1,3</sup> and J. Kozelka<sup>2,4</sup>

<sup>1</sup>CEITEC-Central European Institute of Technology, Masaryk University, Kamenice 5/44, CZ-625 00 Brno, Czech Republic

<sup>2</sup>Masaryk University, Faculty of Science, Department of Condensed Matter Physics, Kotlářská 2, 611 37 Brno, Czech Republic

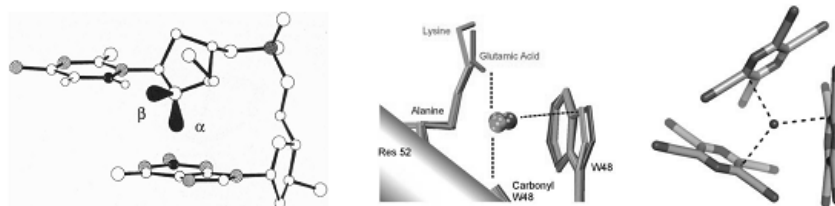
<sup>3</sup>National Center for Biomolecular Research, Faculty of Science, Masaryk University, Kamenice 5/44, CZ-625 00 Brno, Czech Republic

<sup>4</sup>Laboratoire de Chimie et Biochimie Pharmacologiques et Toxicologiques, UMR 8601 CNRS, Université Paris Descartes, 45, rue des Saints-Pères, 75270 Paris, France  
e-mail: kozelka.jiri@gmail.com

The lone-pair- $\pi$  interaction is a still relatively unexplored bonding between a lone-pair (lp) of electrons of an electronegative atom and a  $\pi$ -system. In 1995, Egli and Gessner identified in the d(CpG) steps of Z-DNA an interaction between an oxygen lp of the cytidine deoxyribose and the guanine base, which they classified as  $n \rightarrow \pi^*$  hyperconjugation and related to the stability of Z-DNA.<sup>1</sup> A similar type of interaction was suggested to occur in many protein crystal structures where water molecules were observed to contact a tryptophan or a histidine residue along the normal to the ring plane through the endocyclic N atom.<sup>2</sup>

A subclass of lp- $\pi$  interactions are anion- $\pi$  interactions, where the interacting lp is a part of an anionic residue. For instance, electron-deficient arenes such as 1,2,4,5-tetracyanobenzene (TCB) or tetracyanopiperazine (TCP) form with halide ions in solution and in solid phase complexes whose charge-transfer absorption bands are indicative of a weakly covalent interaction. Since the halides interact with the  $\pi$ -face of the arene in a similar manner as does water with tryptophan in proteins and deoxyribose with nucleobases in nucleic acids (see figure below), one may ask to which extent charge transfer, evidently operating in the halide-arene complexes, contributes to the binding of the lp- $\pi$  interactions in the biopolymers. Asking more generally: What are the energy components stabilizing lone-pair- $\pi$  interactions and how does their balance depend on the molecular properties of the interacting partners? Do force-field calculations portray such interactions properly?

The talk will attempt to provide the answer.



Left: lp- $\pi$  interaction stabilizing Z-DNA.<sup>1</sup> Middle: lp- $\pi$  interaction suggested to operate between a conserved water molecule and tryptophan W48 in the Engrailed homeodomain and its mutants.<sup>2</sup> Right: lp- $\pi$  interaction observed in the X-ray structure of the charge-transfer complex between Br<sup>-</sup> and TCP.<sup>3</sup>

<sup>(1)</sup> Egli, M.; Gessner, R. *Proc. Nat. Acad. Sci. USA* **1995**, *92*, 180-184.

<sup>(2)</sup> Stollar, E. J.; Gelpi, J. L.; Velankar, S.; Golovin, A.; Orozco, M.; Luisi, B. F. *Proteins* **2004**, *57*, 1-8.

<sup>(3)</sup> Rosokha, Y. S.; Lindeman, S. V.; Rosokha, S. V.; Kochi, J. K. *Angew. Chem. Int. Ed.* **2004**, *43*, 4650-4652.

## SO2.2 Manipulating liquid crystal flows in microfluidic environment

T. Emeršič<sup>1,2</sup> and U. Tkalec<sup>1,2,3\*</sup>

<sup>1</sup>Institute of Biophysics, Faculty of Medicine, University of Ljubljana, Ljubljana, Slovenia

<sup>2</sup>Faculty of Natural Sciences and Mathematics, University of Maribor, Maribor, Slovenia

<sup>3</sup>Condensed Matter Physics Department, Jožef Stefan Institute, Ljubljana, Slovenia

e-mail: uros.tkalec@mf.uni-lj.si

Liquid crystals are well-known anisotropic fluids that probe elasticity, fluidity, phase transitions and topology all at the same time [1, 2]. Their microscopic flow is characterized by complex interplay between hydrodynamics, viscosity and orientational order that is absent in conventional isotropic fluids [3, 4]. We explore the structure and dynamics of nematic mesophases in rectangular microchannels with perpendicular surface alignment of molecules under pressure-driven flows and optical manipulation with laser tweezers [5]. The microchannels with various aspect ratios are prepared by standard soft lithography methods, the nematic flows are observed under polarizing optical microscope and optical traps are set to manipulate and control the flowing material with embedded topological defects. We will show how the nematic reacts to thermally induced gradients in the molecular orientation field and discuss thermo-optical effects that can find use in sensing and lead to similar interpretations in collective motion of active biological matter.

### References

- [1] A. Sengupta, U. Tkalec, M. Ravnik, *et al.*, *Phys. Rev. Lett.* **110**, 048303 (2013).
- [2] A. Sengupta, S. Herminghaus, C. Bahr, *Liq. Cryst. Rev.* **2**, 73 (2014).
- [3] V. M. O. Batista, M. L. Blow, M. M. Telo da Gama, *Soft Matter* **11**, 4674 (2015).
- [4] R. Zhang, T. Roberts, I. S. Aranson, J. J. de Pablo, *J. Chem. Phys.* **144**, 084905 (2016).
- [5] T. Emeršič, U. Tkalec, *in preparation*.

### **SO2.3 Role of Calcium in localization of a blood clot in an *ex vivo* injured blood vessel**

R. Podlipec, Z. Arsov, J. Štrancar, T. Koklič

Laboratory of Biophysics, Solid State Physics Department, "Jožef Stefan" Institute, Jamova cesta 39, SI-1000 Ljubljana, Slovenia

e-mail: rok.podlipec@ijs.si

The role of calcium ( $\text{Ca}^{2+}$ ) in blood coagulation has been known for a long time, yet recent research indicates that it might have an important role in regulating localization of a blood clot in an injured blood vessel. The  $\text{Ca}^{2+}$  ion has an intermediate binding affinity for many proteins, which makes it an ideal on/off switch that plays a pivotal role in many essential cellular processes. Low concentration of plasma calcium and increased concentrations of phosphatidylserine containing membranes (PS-containing membranes) were found to be correlated with enhanced coagulation in different patients<sup>1</sup>. These observations have suggested a link between plasma  $\text{Ca}^{2+}$  and the availability of PS-containing membranes in regulating blood coagulation; however, the biochemical nature of this link has been identified only recently. Koklic et al. have shown that a drop in calcium concentration below physiological concentration of about 1.1 mM switches on activity of factor Xa (fXa)<sup>2</sup>, which is one of the key enzymes in initiating blood coagulation. This occurs in absence as well as in presence of its cofactor factor Va<sup>3</sup>. Based on these results Koklic et al. have formulated a hypothesis, which states that  $\text{Ca}^{2+}$  concentration gradient at the site of a wounded blood vessel endothelium is responsible for localization of the blood clot to the site of the injury<sup>3</sup>.

In this work we have explored how the  $\text{Ca}^{2+}$  gradient at the site of injured blood vessel localizes initiation of blood coagulation to the site of the wound, where local concentration of calcium drops and amount of PS-containing membranes is high. Blood coagulation was observed in the intact as well as in the isolated porcine retinal tissue. Vessel walls were ruptured using a nanosecond pulsed NIR laser diode source and local calcium concentration in relation with coagulation was measured on an inverted fluorescence microscope. As predicted by the hypothesis, we confirmed that blood coagulation is localized at the site of a ruptured blood vessel endothelium, where  $\text{Ca}^{2+}$  concentration drops below approximately 1.5 mM.

#### **References:**

1. Hansson, G. K. Inflammation, atherosclerosis, and coronary artery disease. *N. Engl. J. Med.* 352, 1685–1695 (2005).
2. Koklic, T., Majumder, R. & Lentz, B. R.  $\text{Ca}^{2+}$  switches the effect of PS-containing membranes on Factor Xa from activating to inhibiting: implications for initiation of blood coagulation. *Biochem. J.* 462, 591–601 (2014).
3. Koklic, T., Chattopadhyay, R., Majumder, R. & Lentz, B. R. Factor Xa dimerization competes with prothrombinase complex formation on platelet-like membrane surfaces. *Biochem. J.* 467, 37–46 (2015).

### SO3.1 Entropy production in enzyme reactions

A. Dobovišek<sup>1,2</sup>, A. Fajmut<sup>1,3</sup>, M. Brumen<sup>1,2,3,4</sup>

<sup>1</sup>University of Maribor, Faculty of Natural Sciences and Mathematics,  
Koroška cesta 160, 2000 Maribor, Slovenia

<sup>2</sup>University of Maribor, Faculty of Medicine, Taborska 8, 2000 Maribor, Slovenia

<sup>3</sup>University of Maribor, Faculty of Health Sciences, Žitna ulica 15, 2000 Maribor, Slovenia

<sup>4</sup>Jožef Stefan Institute, Jamova cesta 39, 1000 Ljubljana, Slovenia

e-mail: andrej.dobovisek@um.si

Enzymes in living cells operate in open reaction systems with incoming and outgoing fluxes of the reactants and energy. Such systems spontaneously tend towards a non-equilibrium steady state characterised with constant and positive entropy production. Since biological systems by nature operate far from equilibrium, equilibrium thermodynamics does not provide appropriate theoretical concepts for their description. Thus, the search for the principles that enable the description of functioning of biological systems in stable steady states, is of basic importance. One of such principles is the maximum entropy production principle, which states that non-equilibrium processes spontaneously tend towards stationary states in which they dissipate energy and produce entropy with maximal possible rate.

The results of recently developed model indicate that enzyme kinetics is indeed such that enzymes in stationary state within an open reaction system produce entropy with maximal possible rate. Regarding that, an optimization problem, which enables maximization of the entropy production in a reversible two state enzyme reaction with respect to the enzyme rate constants, is discussed. It is demonstrated that maximum in entropy production exists, if conservation of the enzyme's Gibbs free energy is considered as an optimization constraint. Maximization of the entropy production involves in addition to the maximization of the reaction entropy also the minimization of the enzyme catalytic cycle time. The procedure of maximization of the entropy production enables theoretical predictions of several important reaction parameters. These are: values of the enzyme rate constants, product yield of a reaction, maximal reaction flux, reaction entropy and enthalpy as well as the enzyme turnover number. Theoretical model is tested for the reactions taking place close to and far from equilibrium and the results of the model are compared with measured data for the enzyme Glucose Isomerase.

Our study points out that the enzyme's Gibbs free energy conservation is as a necessary constraint for the existence of well-defined maximum in the entropy production. Constant and maximal entropy production rate is achieved with maximal possible entropy difference achieved within the shortest possible time interval. The comparison of theoretical predictions with experimental data for the enzyme Glucose Isomerase indicates that enzymes in living cells indeed operate with maximal possible rate of entropy production.

### **S03.2 The effect of magnesium ions on the structure of thin DNA films: an infrared spectroscopy study**

S. Dolanski Babić<sup>1</sup>, K. Serec<sup>1</sup>, S. Tomić<sup>2</sup>, R. Podgornik<sup>3,4</sup>

<sup>1</sup> Department of Physics and Biophysics, School of Medicine, University of Zagreb, Croatia

<sup>2</sup> Institute of Physics, Zagreb, Croatia

<sup>3</sup> Department of Theoretical Physics, J.Stefan Institute, Ljubljana, Slovenia

<sup>4</sup> Department of Physics, Faculty of Mathematics and Physics, Ljubljana, Slovenia

e-mail: sanja.dolanski.babic@gmail.com

Utilizing Fourier transform infrared spectroscopy we have investigated the vibrational spectrum of thin dsDNA films with intrinsic sodium cations in order to track the structural changes upon addition of magnesium ions. In the range of low magnesium concentration ( $r = [\text{magnesium}]/[\text{phosphate}] < 0.5$ ), both the red shift and the intensity of asymmetric  $\text{PO}_2$  stretching band decrease, indicating an increase of magnesium–phosphate binding in the backbone region. Vibration characteristics of the A-conformation of the dsDNA vanish, whereas those characterizing the B-conformation become fully stabilized. In the crossover range with comparable Mg and intrinsic Na DNA ions ( $r \approx 1$ ) B-conformation remains stable. At high Mg contents ( $r > 10$ ), the vibrational spectra broaden and show a striking intensity rise, while the base stacking remains unaffected. We argue that at these extreme conditions, where condensed counterions neutralize 92-94% of DNA, DNA may undergo a structural transition into a more compact form.

Also, we are investigating the vibrational spectra of thin dsDNA films with intrinsic magnesium cations in order to track the structural changes upon addition of magnesium ions. The results will be compared with the spectra of thin dsDNA films with intrinsic sodium cations.

#### **References**

1. R. G. Bhattacharyya, K. K. Nayak, and A. N. Chakrabarty, *Inorg Chim a-Bioinor* 153, 79 (1988)
2. M. Langlais, H. A. Tajmirriahi, and R. Savoie, *Biopolymers* 30, 743 (1990)
3. J. Duguid, V. A. Bloomfield, J. Benevides, and G. J. Thomas, *Biophys J* 65, 1916 (1993)
4. R. Ahmad, H. Arakawa, and H. A. Tajmir-Riahi, *Biophys J* 84, 2460 (2003)
5. A. M. Polyanichko, V. V. Andrushchenko, E. V. Chikhirzhina, V. I. Vorob'ev, and H. Wieser, *Nucleic Acids Res* 32, 989 (2004)

### **SO3.3 Investigating cell functioning by theoretical analysis of cell-to-cell variability**

S. Svetina

Institute of Biophysics, Faculty of Medicine, University of Ljubljana, Slovenia  
Jožef Stefan Institute, Ljubljana, Slovenia  
e-mail: sasa.svetina@mf.uni-lj.si

Cell-to-cell variability in isogenic cell populations is analyzed by taking into consideration causal relations between the parameters that define the state of individual cells. A population of red blood cells is treated as an example to show that it is possible, from the relationships between standard deviations of distribution functions with respect to various cell parameters and their corresponding correlation coefficients, to unravel previously unidentified causal relations between these parameters. It is suggested that this approach can be employed in searching for the causal relations, which, in analogy with the process of self-reproduction of vesicles, could be required for the proper division of cells that grow and divide. On the basis of a vesicular origin of primordial life, it is concluded that the cell-to-cell variability could be a consequence of asymmetric vesicle divisions needed for the sustainability of early evolution.

#### **SO4.1 Changes in the biophysical properties of the plasma membrane in Gaucher disease, a lysosomal storage disorder**

G. Batta, L. Soltész, T. Kovács, P. Nagy

Department of Biophysics and Cell Biology, University of Debrecen, Egyetem square 1, 4032 Debrecen, Hungary  
e-mail: nagyp@med.unideb.hu

The plasma membrane is not only a border, but also an interface between the intracellular and extracellular space mediating transmembrane signaling. These events require the dynamical interaction between membrane proteins and lipids which is influenced by the lipid composition of the membrane. Lipid rafts, cholesterol- and sphingolipid-rich microdomains, have been shown to be involved in a multitude of processes including signaling and membrane trafficking. The composition of the membrane and the relative fraction of raft-specific lipids are known to be altered in a multitude of diseases in which they are assumed to contribute to the symptoms of the disease. Lysosomal storage diseases are a group of inherited metabolic disorders resulting from the absence of a certain lysosomal hydrolase. The most frequent lysosomal storage disease is Gaucher disease in which the enzyme glucocerebrosidase is mutated resulting in the accumulation of undigested sphingolipids (gangliosides) in the cell. Although the symptoms of the disease are assumed to result from the accumulation of undigested gangliosides in lysosomes, neither the amount of undigested gangliosides, nor the residual enzyme activity correlates with the severity of symptoms calling for alternative explanations. Since the involvement of the plasma membrane in Gaucher disease has not been investigated, we set out to clarify its role in this disorder.

Gaucher cells were generated by incubating macrophages derived from THP-1 monocytes in the presence of conduritol B epoxide, an inhibitor of glucocerebrosidase. We measured the lateral mobility and mobile fraction of fluorescently labeled membrane proteins and a lipid analogue by fluorescence recovery after photobleaching (FRAP). The results showed that the diffusion of TAMRA-labeled dipalmitoyl-phosphatidylethanolamine and that of non-raft membrane proteins is more restricted in Gaucher cells than in control samples. On the other hand, the mobility of glycosylphosphatidylinositol (GPI)-anchored GFP was not significantly affected in Gaucher cells. The fluorescence anisotropy of TMA-DPH and the generalized polarization of Laurdan were both higher in Gaucher cells than in control samples implying that the rotational freedom is inhibited and the order is increased in the plasma membrane of Gaucher cells. The rate of internalization of transferrin receptor was also lower in Gaucher cells.

In summary, our results imply that alteration in the dynamical properties of the plasma membrane may be involved in the development of the symptoms Gaucher disease.

## SO4.2 Direct imaging of nanoplatfoms in the live cell plasma membrane

M. Brameshuber

Institute of Applied Physics, TU Wien  
e-mail: brameshuber@iap.tuwien.ac.at

Based on single molecule fluorescence microscopy we developed techniques, which enable the detection of mobile nanometer sized platforms or molecular aggregates diffusing in the plasma membrane of living cells. By utilizing a single molecule FRAP-approach termed TOCCSL ('Thinning Out Clusters while Conserving the Stoichiometry of Labeling')<sup>1,2</sup> combined with quantitative brightness analysis, nanoplatfoms are detected by their property to confine fluorescent labels on a timescale of seconds. A special photobleaching protocol is used to reduce the surface density of labeled mobile platforms down to the level of well-isolated diffraction-limited spots, without altering the single spot brightness. The statistical distribution of probe molecules per platform is determined by single molecule brightness analysis. As platform marker we chose monomeric GFP linked via a GPI (glycosyl-phosphatidylinositol) anchor to the cell membrane. We found cholesterol-dependent homo-association of mGFP-GPI in the plasma membrane of living CHO cells, thereby demonstrating the existence of small, mobile, stable platforms hosting these probes<sup>3</sup>. Raising the temperature to 39°C resulted in a clear disintegration of nanoplatfoms. A further temperature increase completely inhibited nanoplatfom assembly.

The strong homo-association could also be released by addition of 1-palmitoyl-2-(5-oxovaleroyl)-sn-glycero-3-phosphocholine (POVPC) or 1-palmitoyl-2-glutaroyl-sn-glycero-3-phosphocholine (PGPC), two oxidized lipids typically present in oxidatively modified low density lipoprotein. We found a clear dose-response relationship of mGFP-GPI nanodomain disintegration upon addition of POVPC, correlating with the signal of an apoptosis marker. Applying similar concentrations of lyso-lipid did not dissolve nanodomains. To understand the mechanism behind nanodomain disintegration we inhibited the activation of acid sphingomyelinase (aSMase), which activates several apoptotic signaling pathways via ceramide generation. Inhibition of aSMase by NB-19 before addition of POVPC completely abolished the nanodomain-disintegration effect of oxidized phospholipids, thereby proofing a rather indirect effect of oxidized phospholipids on lipid nanodomains.

---

<sup>1</sup> Moertelmaier, Brameshuber et al., APL 2005, 87(26): 263905

<sup>2</sup> Brameshuber and Schütz, Methods Enzymol. 2012, 505: 159-86

<sup>3</sup> Brameshuber et al., JBC 2010, 285(53): 411765-71

<sup>4</sup> Brameshuber et al., BiophysJ 2016, 110(1): 205-13

### SO4.3 Connecting the mechanism of action with lipid composition: Molecular dynamic study of the antimicrobial peptide maculatin 1.1

L. Zoranić and Y. Sonavane

Faculty of Science, University of Split, R. Boskovicica 33, Split Croatia, larisaz@pmfst.hr

e-mail: larisa@pmfst.hr, Larisa.Zoranic@pmfst.hr

Antimicrobial peptides (AMPs) are the first line of defense against pathogens in all organisms. They primarily target cell membrane, not to the specific membrane protein receptors, and therefore can be possible solution to the increasing problem of bacterial resistance to antibiotics. Maculatin 1.1. is one of the well studied alpha helical antimicrobial peptide found in the skin of Australian tree-frog species [1]. Experimental biophysical studies suggest that maculatin may exhibit different types of mode of action, depending on the membrane systems [2]. The multi-scale simulations indicate formation of the disordered, membrane-spanning multiple-peptide complexes, which are permeable to water [3]. Recent experimental study showed that maculatin-lipid interaction is strongly dependent on the lipid chain length [4]. The simulation study of several AMPs, including maculatin, showed that each peptide has a strong preferences to bind to the regions of high membrane curvature [5].

In this study we investigate interaction of maculatin with membranes of the different lipid composition using the all-atom molecular dynamic simulations. Simulations were done using GROMACS package and the GROMOS54a7 force field [6]. Several aspects that can contribute to the selectivity of peptides were analyzed such as the influence of the size of the lipid chain and the local curvature of lipid-forming structures like micelles and pre-formed pores in the bilayer. Combining the simulation and experimental data from literature, we aim to understand possible connection between lipid composition and some of the proposed mechanisms of action of the antimicrobial peptides. The implication of this study should be considered when preparing and interpreting future AMP simulations.

[1] M.A. Apponyi et al. *Peptides* **2004**, 25, pp 1035–1054.

[2] D. I. Fernandez et al. , *BBA* **2009**, 1788, pp 1630-1638

[3] D. L. Parton et al., *J. Phys. Chem.* **2012**, 116 (29), pp 8485–8493

[4] M.-A. Sani et al. , *BBA* **2012**, 1818, pp 205-211

[5] R. Chen and A. E. Mark, *Eur. Biophys J.* **2011**, 40(4), pp 545-53.

[6] [www.gromacs.org/](http://www.gromacs.org/); D. Poger et al. *J. Compt. Chem.* **2010**, 31, pp 1117-1125; C. Oostenbrink et al. *J. Compt. Chem.* **2004**, 25, pp 1656-1676

### **SO5.1 Rupture Forces among Human Blood Platelets at different Degrees of Activation**

T-h. Nguyen<sup>1,2</sup>, R. Palankar<sup>1,2</sup>, V-C. Bui<sup>1,2</sup>, N. Medvedev<sup>1</sup>, M. Delcea<sup>1,2</sup> and A. Greinacher<sup>2</sup>

<sup>1</sup>Nanostructure Group, ZIK HIKE - Center for Innovation Competence, Humoral Immune Reactions in Cardiovascular Diseases, University of Greifswald, 17489 Greifswald, Germany.

<sup>2</sup>Institute for Immunology and Transfusion Medicine, University Medicine Greifswald, 17475 Greifswald, Germany

e-mail: nguyent@uni-greifswald.de

Little is known about mechanics underlying the interaction among platelets during activation and aggregation. Although the strength of a blood thrombus has likely major biological importance, no previous study has measured directly the adhesion forces of single platelet-platelet interaction at different activation states. Here, we filled this void first, by minimizing surface mediated platelet-activation and second, by generating a strong adhesion force between a single platelet and an AFM cantilever, preventing early platelet detachment. We applied our setup to measure rupture forces between two platelets using different platelet activation states, and blockade of platelet receptors. The rupture force was found to increase proportionally to the degree of platelet activation, but reduced with blockade of specific platelet receptors. Quantification of single platelet-platelet interaction provides major perspectives for testing and improving biocompatibility of new materials; quantifying the effect of drugs on platelet function; and assessing the mechanical characteristics of acquired/inherited platelet defects.

#### References

Nguyen, T. H. et al. Rupture Forces among Human Blood Platelets at different Degrees of Activation. Scientific Reports 6, doi: Artn 25402 10.1038/Srep25402 (2016).

## **SO5.2 In vivo EPR measurements of the pharmacokinetics of nitroxides: The role of modeling in the assessment of the redox status**

A. Pavićević<sup>1</sup>, S. Stamenković<sup>2</sup>, M. Jovanović<sup>2</sup>, G. Bačić<sup>1</sup>

<sup>1</sup>University of Belgrade – Faculty of Physical Chemistry, EPR Laboratory, Studentski trg 12-16, 11158 Belgrade, Serbia

<sup>2</sup>University of Belgrade – Faculty of Biology, Center for Laser Microscopy, Studentski trg 3, 11158 Belgrade, Serbia

e-mail: aleks.pavicevic@ffh.bg.ac.rs

**Introduction and Aim.** Oxidative stress has been implicated in a number of pathological conditions, but it can also be induced by external agents. Regardless of the origin, evaluation of the alterations in redox state is essential in understanding of the underlying mechanisms. One way to measure the redox status is to add nitroxides (a ‘stable’ free radicals, *EPR visible*) to the system and to follow their reduction by endogenous reactive species to an *EPR silent* hydroxylamines, i.e. to follow the decay of the EPR signal in various organs *in vivo*. We employed this approach in studying *in vivo* reduction kinetics in the rat model of amyotrophic lateral sclerosis (ALS) and in the model of radiation induced oxidative stress.

**Experimental.** Experiments were performed on Sprague-Dawley wild-type (WT) and transgenic rats carrying the mutant human SOD1<sup>G93A</sup> gene. Three spin probes Tempol, 3CP (3-carbamoyl proxyl), and 3CxP (3-carboxy proxyl) having different biodistribution and reducing susceptibility were i.v. injected and the EPR signal decay was followed in the head or liver using the Bruker Elexsys II EPR spectrometer operating at the L-band. The *in vivo* spin probe decay curves were fitted using a mathematical two-compartment model with several factors describing contributions of different processes to the overall decay.

**Results and Discussion.** The overall decay kinetics in affected rats in both models was faster than in the control rats indicating increased reducing ability in ALS or irradiated rats. One has to be careful when interpreting such data as changes in the redox status alone, since the signal decay rate depends on several other kinetic factors not directly connected with redox status. Indeed, the overall pharmacokinetics in all rats (affected and control) displayed a complex non single-exponential behavior indicating involvement of multiple compartments/processes. Such behavior has been observed in numerous previous studies and requires performing a multiparametric fit, yet majority of authors treated those as the pseudo-first order kinetics (see [1] for the recent review). Our analysis showed involvement of multiple factors to overall decay kinetics, e.g. faster reduction of nitroxides in ALS rats when compared to WT rats is a consequence of altered redox status but also a consequence of increased permeability of blood brain barrier. These conclusions, however, can't be reached with certainty solely on the basis of kinetic modeling and the goodness of the fit; it was necessary to verify selected model by performing independent measurements of certain processes (see abstract, same volume).

[1] G. Bačić, A. Pavićević, F. Peyrot, *Redox Biol.* 8 (2016) 226-242.

### **SO5.3 Intracellular pathophysiological changes of astrocytes from a rat model of amyotrophic lateral sclerosis**

S. Stamenković<sup>1</sup>, T. Dučić<sup>2</sup>, P.R. Andjus<sup>1</sup>

<sup>1</sup>Center for Laser Microscopy, Faculty of Biology, University of Belgrade, Serbia,

<sup>2</sup>CELLS - ALBA Synchrotron Light Source, Barcelona, Spain

e-mail: pandjus@bio.bg.ac.rs

Amyotrophic lateral sclerosis (ALS) is a progressive and fatal neurodegenerative disorder leading to the death of neurons in the motor pathways of the central nervous system (CNS). Around 20% of familial cases are caused by mutations in the Cu-Zn-superoxide dismutase (SOD1), that induce the susceptibility of the protein to form insoluble intracellular aggregations which are recruited to the mitochondrial intermembrane space, leading to mitochondrial dysfunction and increased production of reactive oxygen species (ROS). The disease is non-cell autonomous with astroglia showing signs of pathological (reactive) alterations in both ALS patients and animals models. Here we examined more closely the protein accumulations of SOD1 within astrocytes, as well as the subcellular markers of these cells, both contributing to the pathological role of these non-neuronal cells during the disease development and progression.

Investigations on cultured cortical astrocytes (from the transgenic hSOD1<sup>G93A</sup> ALS rat model) with ROS production indicators, MitoSox red and H<sub>2</sub>DCDFA, clearly showed an increased susceptibility of these cells to oxidative stress induced by hydrogen-peroxide. Confocal imaging with immunostaining of glial fibrillary acidic protein and SOD1 on astrocytes from the ALS CNS tissue showed a pronounced glial intracellular accumulation of SOD1. Concurrently, synchrotron based transmission soft X-ray full-field microscopy operating in the “water window” energy range (520 eV) revealed striking intracellular alterations in primary cortical ALS astrocytes including prominent enlargement of cellular vesicles, as well as the presence of numerous multivesicular formations and cytoplasmic aggregations. These results bring new important insights into the intracellular and functional changes of astrocytes in ALS, and emphasize their role as disease cellular markers.

#### **Acknowledgements:**

This work was supported by the Grant MESTD RS #41005, the BioStruct-X project 5977 and the ALBA in-house research grant “X-ray imaging of the protein aggregates induced by nanoparticles in vitro”.

#### **SO5.4 Alternative functions of stefin B: a role in cell's response to mis-folded proteins and oxidative stress**

E. Žerovnik

Department of Biochemistry, Molecular and Structural Biology  
Jožef Stefan Institute, Jamova 39, 1000 Ljubljana, Slovenia  
e-mail: eva.zerovnik@ijs.si

Stefin B gene mutation causes EPM1, also called Unverricht-Lundborg disease. It should not be dismissed that the progressive myoclonus epilepsy - EPM1 is caused primarily by lack of stefin B function (in stefin B gene abnormalities inherited cases) (Joensuu, Lehesjoki, & Kopra, 2008; Lalioti, et al., 1997; Lalioti, et al., 1998; Pennacchio, et al., 1998). Except for the more common dodecamer repeats expansion mutation, several missense mutants were observed. The missense EPM1 mutants G4R, Q71P, G50E and the fragment R68X aggregation in cells could add toxic function to pathology of the disease (Ceru, et al., 2010; Polajnar, Zavasnik-Bergant, Kopitar-Jerala, Tusek-Znidaric, & Zerovnik, 2014).

Cystatins are also players in Alzheimer's disease. Stefin B was found, together with stefin A, in amyloid plaques of AD and different origin, respectively (Bernstein, et al., 1994; Li, Ito, Kominami, & Hirano, 1993). As well cystatin C (which is extracellular) was reported as a constituent of amyloid plaques (Maruyama, Kametani, Ikeda, Ishihara, & Yanagisawa, 1992). We have shown that oligomers of stefin B react with A-beta (Skerget, et al., 2010) and may perform an amateur chaperone function, in distinction to stefin A (Taler-Vercic & Zerovnik, 2010). Cystatin C also is A-beta binding protein (Mi, et al., 2009; Mi, et al., 2007; Sastre, et al., 2004). Thus, cystatins are believed to be neuroprotective (Tizon, Ribe, Mi, Troy, & Levy, 2010). Cystatin C rescued lack of function of stefin B in transgenic mice (Kaur & Levy, 2012; Kaur, et al.). KO stefin B macrophages show increased sensitivity to cell death (Kopitar-Jerala, Schweiger, Myers, Turk, & Turk, 2005) and neurons isolated from KO mice model and EPM1 patients show increased oxidative stress (Lehtinen, et al., 2009). It is generally known that cystatins are cysteine protease (cathepsins) inhibitors. However, some of their alternative functions may be cathepsin independent. We recently have reported that stefin B rescues other proteins from forming scattered protein aggregates (Polajnar, Zavasnik-Bergant, Skerget, et al., 2014) and may influence autophagic flux, similarly as reported for cystatin C (Tizon, et al.).

I will discuss possible proposals for the alternative function of stefin B based on our in vitro and cell culture studies.

### **SO6.1 Bio-functional surfaces for microRNAs purification and analysis**

C. Potrich<sup>1,2</sup>, V. Vaghi<sup>1</sup>, L. Lunelli<sup>1,2</sup>, L. Pasquardini<sup>1</sup>, G.C. Santini<sup>1</sup>, M. Cocuzza<sup>3,4</sup>, C.F. Pirri<sup>3,5</sup>, C. Pederzoli<sup>1</sup>

<sup>1</sup>LaBSSAH, Fondazione Bruno Kessler, Trento, Italy; <sup>2</sup>CNR-IBF, Trento, Italy; <sup>3</sup>Chilab - Department of Applied Science and Technology, Politecnico di Torino, Torino, Italy; <sup>4</sup>CNR-IMEM, Parma, Italy  
<sup>5</sup>Center for Space Human Robotics@PoliTo, Istituto Italiano di Tecnologia, Torino, Italy  
e-mail: cpotrich@fbk.eu

The increasing demand for new technologies in health and personalized medicine requires the realization of low cost, flexible devices and new nanomaterials for analysis and diagnostics. A general requisite for the successful implementation of these tools is the development of suitable bio-functional materials and surfaces.

Several fields could benefit from bio-functional surfaces, for example in the oncological field there is an increasing interest in circulating microRNAs (miRNAs) as potential non-invasive cancer biomarkers. In this context, the surface properties of several materials were explored by modifying both the surface charge and morphology. An optimal surface for total miRNAs purification from biological samples (human plasma and sera, cell lysates and tissue homogenates) was successfully set up and implemented on a polymeric microdevice, where miRNAs purification and reverse transcription occur in the same chamber. Bio-functional surfaces for specific classes of miRNAs (AGO2-bound miRNAs, exosomes-loaded miRNAs) were also investigated with promising results, starting from the immunocapture of specific antigenic proteins.

## **SO6.2 Adaptive resolution simulations of biomolecular systems**

J. Zavadlav, S. Bevc and M. Praprotnik

Department of Molecular Modeling, National Institute of Chemistry, Hajdrihova 19, SI-1001 Ljubljana, Slovenia

e-mail: [julija@cmm.ki.si](mailto:julija@cmm.ki.si)

We present recent biophysical applications of the adaptive resolution scheme (AdResS), which allows solvent molecules to change their resolution back and forth between atomistic and coarse-grained representations according to their positions in the system. First, we discuss coupling of atomistic and coarse-grained models of salt solution using a 1-to-1 molecular mapping, i.e., one coarse-grained bead represents one water molecule, for development of a multiscale salt solution model. In order to make use of coarse-grained molecular models that are compatible with the MARTINI force field one has to resort to a supramolecular mapping, in particular to a 4-to-1 mapping, where four water molecules are represented with one coarse-grained bead. To this end, bundled atomistic water models are employed, i.e., the relative movement of water molecules that are mapped to the same coarse-grained bead is restricted employing harmonic springs. The supramolecular coupling has been recently also extended to polarizable coarse-grained water models with explicit charges. Since these coarse-grained models consist of several interaction sites, orientational degrees of freedom of the atomistic and coarse-grained representations are coupled via a harmonic energy penalty term. The latter aligns the dipole moments of both representations. The presented multiscale solvent models are ready to be used in biomolecular simulations as illustrated on a few examples, e.g., solvated protein and DNA molecules.

### **SO6.3 Atomic Force Microscopy analysis of extracellular vesicles**

P. Parisse<sup>1,2</sup>, E. Ambrosetti<sup>1,2,3</sup>, A.P. Beltrami<sup>4</sup>, D. Cesselli<sup>4</sup>, L. Casalis<sup>1,2</sup>

<sup>1</sup> INSTM-ST Unit, Trieste, Italy

<sup>2</sup> Elettra – Sincrotrone Trieste S.C.p.A., Trieste, Italy

<sup>3</sup> University of Trieste, Trieste, Italy

<sup>4</sup> Department of Medical and Biological Sciences, University of Udine, Udine, Italy

e-mail: [pietro.parisse@elettra.eu](mailto:pietro.parisse@elettra.eu)

Extracellular vesicles (EVs) are small vesicles ensuring transport of molecules between cells and throughout the body. EVs contain cell-type specific signatures and have been proposed as biomarkers in a variety of diseases. Their small size (<1 $\mu$ m) and biological and physical functions make them obvious candidates for therapeutic agents in immune therapy, vaccination, regenerative medicine, and drug delivery. However, due to the complexity and heterogeneity of EV origin and composition, the actual mechanism through which these vesicles exert their functions is still unknown and represents a great biomedical challenge. Moreover due to their dimensions, the count, size distribution determination and biophysical characterization of these particles are challenging and still subject to controversy.

Here we will report our study of isolated EV derived from tumour cell lines by means of Atomic Force Microscopy (AFM), in air and liquid conditions. We performed AFM imaging and stiffness measurements by force spectroscopy analysis on EVs immobilized on different substrates (mica, glass and antibody functionalized gold films). The results obtained allowed us to point out some peculiar characteristics of tumour EVs, posing the basis for the collection of an “ID card” (size distribution, morphology, mechanical properties, biomolecular load) of exosomes derived from specific subpopulations of cells.

#### **SO6.4 Development of novel FP-based probes for live-cell imaging of nitric oxide dynamics**

E. Eroglu<sup>1</sup>, B. Gottschalk<sup>1</sup>, S. Charoensin<sup>1</sup>, S. Blass<sup>1</sup>, H. Bischof<sup>1</sup>, R. Rost<sup>1</sup>, C.T. Madreiter-Sokolowski<sup>1</sup>, B. Pelzmann<sup>2</sup>, E. Bernhart<sup>1</sup>, W. Sattler<sup>1</sup>, S. Hallström<sup>3</sup>, T. Malinski<sup>4</sup>, M. Waldeck-Weiermair<sup>1</sup>, W.F. Graier<sup>1</sup> & R. Malli<sup>1</sup>

<sup>1</sup>Institute of Molecular Biology and Biochemistry, Center of Molecular Medicine, Medical University of Graz, Harrachgasse 21/III, 8010 Graz, Austria

<sup>2</sup>Institute of Biophysics, Center of Physiological Medicine, Medical University of Graz, Harrachgasse 21/IV, 8010 Graz, Austria

<sup>3</sup>Institute of Physiological Chemistry, Center of Physiological Medicine, Medical University of Graz, Harrachgasse 21/II, 8010 Graz, Austria

<sup>4</sup>Nanomedical Research Laboratory, Department of Chemistry and Biochemistry, Ohio University, 350 West State Street, Athens, Ohio 45701, USA

e-mail: emrah.eroglu@medunigraz.at

Nitric oxide (NO•) is a free radical with a wide range of biological effects, but practically impossible to visualize in single cells. Here we report the development of novel multicolored fluorescent quenching-based NO• probes consisting of a bacterial-derived NO• binding domain conjugated with distinct fluorescent proteins. These probes provide a selective, specific and real-time read-out of cellular NO• dynamics and, hence, open a new era of NO• bio-imaging.

## **SO7.1 Functional dynamics of an unusual photolyase revealed by transient absorption spectroscopy**

L. Grama<sup>1</sup>, R. Kapronczai<sup>1</sup>, P. Müller<sup>2</sup>, K. Brettel<sup>2</sup>, M.H. Vos<sup>3</sup>, A. Lukacs<sup>1</sup>

<sup>1</sup> Department of Biophysics, Medical School, Szigeti Str. 12, H-7624 Pécs, Hungary

<sup>2</sup> Institute for Integrative Biology of the Cell (I2BC), CEA CNRS, Univ Paris-Sud, University Paris-Saclay

91198 Gif-sur-Yvette cedex (France)

<sup>3</sup> Laboratoire d'Optique et Biologie, Ecole Polytechnique, France

e-mail: andras.lukacs@aok.pte.hu

Cryptochromes comprise a large family of flavoproteins found in many organisms, having very distinct functions. Even though originally their function was rather cryptic (hence the name) during the last fifteen years many of them were identified: they are setting the biological clock in insects and plants, they are involved in photomorphogenesis, and even in magnetoreception of migratory birds. Cryptochromes are closely related to photolyases which have very similar structure but different function. Photolyases are light-driven DNA-repair enzymes which are able to repair UV-induced DNA lesions, cyclobutane pyrimidine dimers or pyrimidine-pyrimidone adducts (6-4 photoproduct).

Even though the fundamental electron transfer mechanism in cryptochrome and photolyase is quite similar, the photocycles of these proteins differ: after purification in photolyase FAD is in its neutral radical state and it is reduced to fully reduced state by photoinduced electron transfer. In cryptochrome FAD is in oxidized state and photoexcitation will induce the formation of the anionic flavin radical. A likely explanation for this behavior is that in photolyases the amino acid residue facing the N5 atom of the isoalloxazine ring, that strongly influences the protonation capabilities of the FAD, is an asparagine compared to the cryptochromes where one can find an aspartic acid.

In order to test this assumption we did a site directed mutagenesis and made the N378D mutant. The replacement of the asparagine to an aspartic acid altered the redox state of the flavin and turned FAD in its oxidized state.

We performed transient absorption measurements to elucidate the photochemistry of this mutant. Our measurements revealed that by the mutation of the asparagine by an aspartic acid, *E. coli* photolyase gained a cryptochrome like photocycle.

## **SO7.2 Bleach-rate imaging – fluorescence microspectroscopy at hand**

I. Urbančič, T. Koklič, Z. Arsov, J. Štrancar

Laboratory of Biophysics, Solid State Physics Department, “Jožef Stefan” Institute, Jamova cesta 39, SI-1000 Ljubljana, Slovenia

e-mail: iztok.urbancic@ijs.si

The excited electron of a fluorescent molecule can react with neighbouring molecules, possibly resulting in a permanent loss of the molecule's ability to fluoresce. Among microscopists and spectroscopists, the phrase *fluorescence photobleaching* has therefore almost exclusively had a negative connotation, as the phenomenon all too often precludes or hinders the desired measurements. The success of numerous fluorescence-based techniques has thus heavily relied on the development of probes that were photostable enough to survive illumination with increasingly powerful light sources. It has remained almost completely ignored, though, that the rate of photobleaching is intrinsically related to the lifetime of fluorescence – a (micro)spectroscopic modality that has regularly been exploited for monitoring molecular interactions, which requires elaborate and high-cost instrumentation.

We will show that the so-called bleach-rate spectroscopy and imaging, which can in principle be performed with any fluorescence spectrometer or microscope, respectively, can indeed be employed to monitor local molecular properties. Namely, the rate of photobleaching can reveal biomembrane composition and fluidity of giant unilamellar vesicles labelled with a photosensitive NBD-based membrane probe. In live cells, aggregation of fluorescent compounds can be tracked through the bleaching rate, and its response to metabolic activity or oxidative stress is under investigation. To enhance sensitivity and specificity of the method even further, the deduced bleaching rates can be combined with any other environment-sensitive information, e.g. spectral lineshape, into a rich multimodal technique.

Based on specific interactions between the fluorophores and surrounding molecular species, targeted experiments and assays can be designed. The latter will be demonstrated by identification of bacteria on nanomaterial-coated industrial surfaces stained on-site with a single rhodamine-based probe. As the probe adsorbs to both bacteria and (clustered) nanoparticles, they cannot be distinguished by conventional fluorescence microscopy. However, the interaction of the excited electron with the surface of semiconductor nanoparticles dramatically increases the bleaching rate of the probe, as well as shifts the spectrum for several tens of nanometres, allowing unambiguous discrimination of the two environments – even when spatially overlapping. Considering modest instrumentation requirements, the last example shows a potential for further practical field applications.

### **SO7.3 Intercellular highways - membrane nanotube networks between B lymphocytes: fundamental growth determinants and transport functions**

E. Szabo-Meleg<sup>1,2</sup>, A. Osteikoetxea-Molnar<sup>3</sup>, E.A. Toth<sup>3</sup>, T. Madarasz<sup>1</sup>, J. Matko<sup>3</sup> and M. Nyitrai<sup>1,2</sup>

<sup>1</sup>University of Pécs, Medical Faculty, Department of Biophysics, Szigeti street 12, Pécs, Hungary, H-7624

<sup>2</sup>University of Pécs, Szentágotthai Research Centre, Ifjúság street 20, Pécs, Hungary, H-7624

<sup>3</sup>Eötvös Loránd University, Department of Immunology, Pázmány Péter promenade 1/c, Budapest, Hungary, H-1117

e-mail: edina.meleg@aok.pte.hu

Direct cell-cell communication is crucial for multicellular organisms to crosstalk and to pass information from one cell to another. Until recently direct cell-cell communication was only described via gap junctions and synaptic signaling. They were assumed to be the only way of passing information between eukaryotic cells. Tunneling membrane nanotubes (TNTs) were identified in 2004 as a new form of intercellular communication and matter transport. Membrane nanotubes are thin and long membrane protrusions that physically connect two cells. These tubes were found to be intercellular highways for calcium ions, different cell organelles (e.g. mitochondria), lipid molecules, various proteins, prions, vesicles, DNA and RNA molecules. They have role in the effective propagation of bacteria and viruses (HIV) among cells. Such structures have already been reported for many cell types including HEK, NRK and T cells, macrophages, NK cells or dendritic cells. In the immune system antibody-producing B lymphocytes are key cellular components of the adaptive humoral immune response where TNTs may play important roles. However, in contrast to T lymphocytes and macrophages, TNTs between B cells are still largely unexplored and poorly characterized. Therefore laser scanning confocal and superresolution SIM microscopy were used to determine basic control mechanisms of nanotube growth as well as the transport properties of B cell TNTs.

Based on our findings only mature B lymphocytes form spontaneously extensive TNT networks under conditions resembling the physiological environment. Length- and width-distribution of B cell NTs showed large diversity. TNTs contain not only F-actin – based on our results the essential element in NT-growth and the skeleton of B cell NTs –, but in contrast to T cells, their majority also contain microtubules, which were found, however, not essential for TNT formation. Bidirectional transport of membranous vesicles was observed inside TNTs. Our data suggest that NTs mediate transport of mitochondria among B cells. Intercellular exchange of immunoregulatory molecules through TNTs was also demonstrated which may represent unexplored pathways of intercellular communication and immunoregulation.

Despite the continuously accumulating knowledge about membrane nanotubes, several fundamental questions about the molecular and genetic mechanisms controlling their growth as well as their *in vivo* functional significance remained open.

This work was partially supported by grant K109480 sponsored by the Hungarian National Science Fund (OTKA).

#### **S07.4 Development of smart fluorescent probes to reveal internalization and accumulation in cells through aggregation-induced spectral shift**

Z. Arsov, I. Urbančič, J. Štrancar

Laboratory of Biophysics, Department of Condensed Matter Physics, Jozef Stefan Institute, Jamova cesta 39, SI-1000 Ljubljana, Slovenia  
e-mail: zoran.arsov@ijs.si

A desirable property of fluorescent probes is that they can be activatable, i.e. that they become fluorescent [1] or change a particular spectral property only at the intended target. With such smart probes the background signal is minimized and thus target to background ratios can be improved.

There are a number of mechanisms for generating activatable probes that probe molecular vicinity or molecular confinement, but all require some kind of efficient intensity reduction or spectral change. Widely used is homo- or hetero-Förster resonance energy transfer (FRET). As an alternative, contact-based mechanisms are also possible. In the case of rhodamine derivatives, for example, aggregate formation leads to non-fluorescent ground state complexes or spectral shifts [2].

To demonstrate a possible application of spatially confined aggregation-induced effects, we present a fluorescence microspectroscopy (FMS) study of internalization of a smart probe by antigen-presenting dendritic cells (DCs). The antigen presentation is initiated by receptor internalization to endosomes and lysosomes. The interior of these organelles is acidic compared to mainly neutral pH of cytosol. Therefore, to study the internalization mechanism, a rhodamine-based fluorescent probe that combines the receptor ligand and a pH-sensitive dye has been designed and synthesized. Control experiments confirmed aggregation at relatively high probe contents through concentration dependence of excitation spectra shape and emission spectra shift. Thus, two particular properties of the probe could be exploited: activation in a low-pH environment and an aggregation-induced spectral shift. The latter is small, so only high spectral sensitivity of FMS [3] enabled detection of accumulation of the probe in the low-pH compartments of DCs. Microscopic localization of aggregation through the spectral shape change confirmed presumable probe targeting to endosomes and lysosomes [4].

#### *References*

- [1] M. Ogawa, N. Kosaka, P. L. Choyke, H. Kobayashi, *ACS Chem. Biol.* 4, 535–546 (2009)
- [2] T. P. Burghardt, J. E. Lyke, K. Ajtai, *Biophys. Chem.* 59, 119–131 (1996)
- [3] Z. Arsov, I. Urbančič, M. Garvas, D. Biglino, A. Ljubetič, T. Koklič, J. Štrancar, *Biomed. Opt. Express* 2, 2083–2095 (2011)
- [4] Z. Arsov, U. Švajger, J. Mravljak, S. Pajk, A. Kotar, I. Urbančič, J. Štrancar, M. Anderluh, *ChemBioChem* 16, 2660–2667 (2015)

### **SO7.5 Swimming Motility of Bacteria in Microfabricated Environments**

O. Sipos<sup>1</sup>, K. Nagy<sup>1</sup>, R. DiLeonardo<sup>2</sup>, [P. Galajda](#)<sup>1</sup>

<sup>1</sup>Institute of Biophysics, Biological research Centre of the Hungarian Academy of Sciences, Szeged, Hungary

<sup>2</sup>Dipartimento di Fisica, Università La Sapienza, Rome, Italy

e-mail: [galajda.peter@brc.mta.hu](mailto:galajda.peter@brc.mta.hu)

Swimming motility plays an important role in the life of bacteria: they can find favorable habitats and avoid harmful environments. In nature physical boundaries and constrictions are common in bacterial habitats. We have studied the swimming motility of bacteria in microfabricated structures mimicking various physical aspects of these habitats. We have found that hydrodynamic interaction of swimming cells may trap them near solid surfaces. We studied this trapping effect in detail and showed its importance in biofilm formation. Furthermore we observed that solid walls direct the swimming motion of nearby cells, and sometimes this affect the motion of the whole population. We have demonstrated that physical interactions between the cells and their surrounding may determine the structure and development of microbial populations.

## Poster (P)

### **P1 Biological effects of electric field on histopathological study, electrical properties and kidney function of albino rats**

S.E. Abo-Neima<sup>1</sup>, H.A. Motaweh<sup>1</sup>, H. Tourk<sup>1</sup> and M.F.Ragab<sup>2</sup>

<sup>1</sup>Department of physics, Faculty of Science, Damanhour University, Egypt

<sup>2</sup>Department of physics, Faculty of Science, Omar El-Moktar University, ElgoubaLebya  
e-mail: sahar\_amr2002@yahoo.com

The present study was to investigate the effects of electric field (EF) of strength 50Hz-3KV/m on the histopathology, dielectric properties and kidney function tests in albino rats. Fifty male albino rats were equally divided into three groups namely A, B and C. Animals of group A used as control group which didn't receive any treatment. Animals of group B was divided into two subgroups namely B<sub>1</sub> and B<sub>2</sub> which were discretely exposed to 50Hz, 3KV/m electric field for a period of 15 day (8 hours/day, 5day/week). Group B<sub>2</sub> were left to survive and housed at normal environmental conditions similar to control group A for a period of 15 day post exposed. Animals of group C are divided into two subgroups namely C<sub>1</sub> and C<sub>2</sub> were discretely exposed to the EF for a period of 30 day (8 hours/day, 5day/week). Group C<sub>2</sub> were left to survive and housed at normal environmental conditions similar to control group A for a period of 15 day post exposed. At the end of this period, fresh samples of kidney and blood were collected from all groups were measured immediately for experimental investigations. The dielectric constant ( $\epsilon$ ), electrical conductivity ( $\sigma$ ) was measured in frequency range 42Hz-5MHz to investigate any changes in kidney structure through studding histopathological examination. Also, the kidney function was studied through analysis of urea and creatinine after exposure to EF these biochemical parameters have been evaluated in the blood serum of rats. The results show high significant changes in the value of  $\epsilon$  and  $\sigma$  of kidney tissues for all groups exposed to EF as compared with control group. The exposure of rats to EF can induce significant increase in the levels of kidney profile creatinine and urea, these variations were recovered during two week after stopping exposure but they did not return to its original control values before exposure. On microscopic level; kidney histological section showing abnormal configuration of renal tubules RT, congested blood vessel and degenerated renal tubules arrow, necrosis N , glomerular shrinkage GS, and increase in space between glomerulus and Bowman's capsule .

**Keywords-** electric field, histopathology, kidney function, dielectric constant, conductivity.

## **P2 2-Aminoethoxydiphenyl Borate (2-ABP) Instantly Impairs Mitochondrial Bioenergetics and Causes Cellular ATP Depletion**

M.R. Depaoli<sup>1</sup>, C. Rossmann<sup>2</sup>, C.T. Madreiter-Sokolowski<sup>1</sup>, H. Imamura<sup>3</sup>, S. Hallström<sup>2</sup>, M. Waldeck-Weiermair<sup>1</sup>, W. F. Graier<sup>1</sup> & R. Malli<sup>1</sup>

<sup>1</sup>Institute of Molecular Biology and Biochemistry, Center of Molecular Medicine, Medical University of Graz, Harrachgasse 21/III, 8010 Graz, Austria.

<sup>2</sup>Institute of Physiological Chemistry, Center of Physiological Medicine, Medical University of Graz, Harrachgasse 21/II, 8010 Graz, Austria.

<sup>3</sup>Graduate School of Biostudies, Kyoto University, Japan, The Hakubi Center for Advanced Research, Kyoto University, Japan  
e-mail: m.depaoli@medunigraz.at

The compound 2-aminoethoxydiphenyl borate (2-APB) is frequently used in calcium research thanks to its function as inositol 1,4,5-trisphosphate receptor (IP<sub>3</sub>R) antagonist. However, 2-APB has further targets such as the sarco/endoplasmic reticulum Ca<sup>2+</sup>-ATPase (SERCA) as well as transient receptor potential (TRP) and K<sup>+</sup> channels, pointing to the existence of diverse 2-APB binding domains within different proteins. Accordingly, 2-APB is used as an unspecific Ca<sup>2+</sup> modulator, although the entire spectrum of its biological effects is far from being understood comprehensively. We now provide evidence that 2-APB instantly affects mitochondria and considerably alters the energy metabolism of mammalian cells. In different cell types 2-APB strongly reduces mitochondrial respiration and the mitochondrial membrane potential. In line with these effects, 2-APB treatment results in almost complete depletion of cellular ATP levels within several minutes. Furthermore, in vitro studies indicate that 2-APB interferes with the delta subunit of the mitochondrial ATP synthase. In summary, we demonstrate that mitochondria are a clear target of 2-APB, which sheds new light on the pharmacological actions of this promiscuous chemical compound.

### **P3 Role of mesenchymal and amoeboid cell migration in the formation of brain metastases**

C. Fazakas, J. Molnár, J. Haskó, Á. Nyúl-Tóth, A.G. Végh, G. Váró, I. Wilhelm, I.A. Krizbai

Institute of Biophysics, Biological Research Centre of the Hungarian Academy of Sciences, Szeged, Hungary

e-mail: fazakas.csilla@brc.mta.hu

Metastases of the Central Nervous System (CNS) originate mainly from lung cancer, breast cancer and melanoma. In breast cancer patients the incidence of brain metastases is relatively higher (30%), however, melanoma has elevated affinity to the brain. In order to enter the brain parenchyma, metastatic tumor cells have to extravasate through the microvascular endothelial cells of brain capillaries, which form the blood-brain barrier. During diapedesis through capillaries tumor cells are able to adopt two types of movements. The mesenchymal phenotype displays elongated cell morphology, large protrusions and involves Rac1 activity, and reduced Rho/ROCK signaling. In contrast, amoeboid migration depends on elevated Rho/ROCK signaling. Our goal was to describe which is the migration mode acquired by melanoma and breast cancer cells to infiltrate through the blood-brain barrier. To address this question, we used an in vitro blood-brain barrier model and a transmigration assay. ROCK inhibition in melanoma cells triggered the mesenchymal phenotype, with large lamellipodia, and elevated proteolytic activity. We observed that ROCK inhibition facilitated both the adhesion and transmigration of melanoma cells. Single cell force spectroscopy measurements revealed that ROCK inhibition elevates the adhesion force between melanoma and endothelial cells. Likewise, ROCK inhibition raised the number of transmigrated cells too. Nonetheless, in both tumor types inhibition of Rac1 (mesenchymal movement) resulted in significant decrease in the number of adherent and transmigrated cells. Yet, the presence of Rac1 inhibitor did not alter the adhesion forces between tumor cells and endothelial cells compared to control. Since Rac1 inhibition reduced the adhesion and transmigration of melanoma as well as breast cancer cells, we assume that the mesenchymal type of cell movement (characterized by: low ROCK activity, increased proteolysis and elongated morphology) is more important than the amoeboid type during extravasation through the brain endothelium.

#### **P4 Detection of Light Induced Singlet Oxygen Generated by Bacterial Reaction Centre**

K. Hajdu<sup>1</sup>, A. Kinka<sup>1</sup>, A.u. Rehman<sup>2</sup>, I. Vass<sup>2</sup>, L. Nagy<sup>1</sup>

<sup>1</sup>Institute of Medical Physics and Informatics, University of Szeged, Rerrich B. sq. 1. Szeged, 6720, Hungary

<sup>2</sup>Biological Research Center of the Hungarian Academy of Sciences, Institute of Plant Biology, Temesvári krt 62, Szeged, 6726, Hungary

e-mail: hajdu.kata@gmail.com

The primary events of photosynthesis take place in the photosynthetic reaction centre proteins (RCs), where the energy of light is converted into chemical potential. Under specific conditions the RC photochemistry can be oversaturated (excess light and/or blocking the photochemical processes) and reactive oxygen species (ROS, including, e.g., singlet oxygen ( $^1\text{O}_2$ ), superoxide anion ( $\text{O}^{2-}$ ), and hydroxyl radicals ( $\text{OH}\cdot$ )) are formed with large probability.<sup>1,2</sup>

There is a large interest in the singlet oxygen formation in many fields and aspects. In one hand, photodynamic ROS reactions are determinative in medical photodynamic therapy (cancer treatment with externally added photosensitizers). On the other hand, it would be preferable to reduce the formation of the ROS components in many cases because they decrease the efficiency of the photochemical energy conversion and damage the photosynthetic apparatus of plants because they react with the intracellular components resulting their degradation (the RC itself as well).

Different mechanisms are developed in nature in order to decrease the ROS concentration, including specific enzyme reactions (e.g. peroxidase, superoxide dismutase) and/or decaying the concentration of long lived excited species (e.g. energy transfer from chlorophyll triplets to carotenoids). In the present work we introduce our results on the formation of singlet oxygen under different measuring conditions, with the use of photosynthetic reaction centre purified from *Rhodobacter sphaeroides*. Carbon nanotubes (CNT) were also applied and CNT/RC hybrid bio-nanocomposites were prepared, as CNTs - in artificial systems - are also known to react with singlet oxygen.<sup>3</sup>

1. J.B. Arellano et al. "Formation and geminate quenching of singlet oxygen in purple bacterial reaction center", J. Photochem. Photobiol., 87, pp. 105-112, 2007.

2. A.F. Uchoa et al., "Singlet oxygen generation in the reaction centers of *Rhodobacter sphaeroides*", Eur Biophys J., 37, pp. 843-850, 2008.

3. M.A. Hamon et al., "Reacting soluble single-walled carbon nanotubes with singlet oxygen", Chemical Physics Letters, 447, pp. 1-4, 2007.

## **P5 7-deazapurines new targets for modification of DNA by osmium tetroxide complexes**

L. Havran, P. Vidláková, J. Špaček, and M. Fojta

Institute of Biophysics ASCR v.v.i., Královopolská 135, 612 65 Brno, Czech Republic  
e-mail: raven@ibp.cz

Intrinsic DNA electroactivity was utilized in a number of electroanalytical methods for detection of DNA interactions and damage [1]. For some applications including development of DNA hybridization sensors is a useful applied redox active tag to improve specificity of the analysis. One from utilized labels in this field are complexes of osmium tetroxide with nitrogen ligands (Os,L), which produce with DNA electroactive covalent adducts [2]. If 2,2'-bipyridine (bpy) is used as ligand, Os,bpy selectively react with thymine residues in single strand DNA. Forming adducts give at mercury and carbon electrodes set of voltammetric signals due to reduction/oxidation of Os atom in adduct. Moreover final reduction step at hanging mercury drop electrode (HMDE) is coupled to catalytic hydrogen evolution allowing determination of low concentrations of the osmium-labelled DNA or rare adducts in large excesses of unmodified DNA. For measurements at HMDE is necessary work with purified samples, but using of basal-plane pyrolytic graphite electrodes allowing direct analysis of reaction mixtures in combination with extraction of unbound Os,L from electrode surface by organic solvent [3].

7-deaza analogues of purine nucleobases containing same structural motive (C=C double bond) reactive to Os,L as pyrimidine nucleobases. Therefore can be expected similar reactivity of these analogues to Os,L. In this contribution will be presented results acquired by electrochemical analysis of products Os,bpy modification reaction with different types of DNA samples (oligonucleotides, PCR products) containing 7-deaza adenine or 7-deaza guanine.

### **References**

- [1] E.Paleček, M. Bartošík, Chemical Reviews 112 (2012) 3427.
- [2] M.Fojta, P.Kostečka, H.Pivoňková, P.Horáková, L. Havran, Curr. Anal. Chem. 7 (2011) 35.
- [3] M.Fojta, L.Havran, R.Kizek, S.Billova, Talanta, 56 (2002) 867.

### **Acknowledgments**

This work was supported by the GACR project no.15-08434S.

## **P6 Opsin photoreceptor proteins as optogenetic tools to control and manipulate cell physiology and behavior of neurosystems**

A. M. Jimenez-Garduño<sup>1</sup>, L. Liguori<sup>2</sup>, S. Caponi<sup>3</sup> and C. Musio<sup>1</sup>

<sup>1</sup>IBF-CNR Trento Unit & FBK LabSSAH, Trento, Italy; <sup>2</sup>IBS/Groupe Channels, Grenoble, France;

<sup>3</sup>IOM-CNR Perugia Unit, Perugia, Italy.

e-mail: jmenez@fbk.eu; carlo.musio@cnr.it

Opsin genes include microbial (Type I) and animal (Type II) opsins. Both superfamilies encode 7-TM helix structure able to bind a retinal chromophore, all-*trans* and 11-*cis* respectively for Type I and Type II, which photoisomerizes upon light stimulation. Type I opsins, e.g. bacteriorhodopsin (BR), sensory rhodopsins (SRs), are found in prokaryotes, algae and fungi where, acting as both photoreceptors and light-driven proton/ion pumps, they control phototaxis, energy storage, development, and retinal biosynthesis. Type II opsins (e.g., rod/cone opsins, melanopsin) are present only in higher eukaryotes: they encode G-protein-coupled receptors (GPCRs), and serve image- and non-image-forming vision (circadian vision). Channelrhodopsins, ChRs, belong to microbial opsins (e.g. BR, HR, SR I/II) found in prokaryotes, algae, and fungi where, they are photoreceptors which behave as light-driven proton/ion pump, and control phototaxis, energy storage, development, and retinal biosynthesis. ChRs, discovered in the green alga *Chlamydomonas* in early 2000, are directly light-gated ion channels: they possess intrinsic Na<sup>+</sup> and K<sup>+</sup> conductances and become permeable to cations upon blue light stimulation. Since ChR2 was found in 2005 to be expressed in mammalian neurons and, upon photostimulation, to precisely regulate light-driven depolarization, a ChR-based technology, named optogenetics, has been fastly developed to control and perturb cell physiology with a high spatio-temporal resolution. Targeted cell populations can heterologously express ChRs and upon blue-light stimulation they can be depolarized producing an excitation of the system. ChR proteins can be mutated and tailored with respect to absorption, substrate specificity, kinetics, and improved expression in host systems. Very recently also metazoan opsins, such as the non-visual opsin melanopsin of mammals and rhodopsin of the box-jellyfish *Carybdea*, have been demonstrated useful tools for the optogenetic control of G protein-coupled receptors (GPCRs) signaling. Opsin-like photopigments have been proven to be suitable optogenetic tools to activate motor functions, to regulate heart function, and to restore vision. The future challenge will be not only the design of new optogenetic tools but also their combination to achieve a multi-wavelength control and tuning of biological processes and networks. Our goals are to select novel ChRs wt and mutants and suitable cell model systems in order to deepen the biophysics of ChRs and their use as optogenetic tools to trigger, control and modify specific cellular and/or cross-stalk activities. We started to select suitable cell models and to transfect them with recombinant viruses to express ChRs. We used pGEMHE plasmids containing the genes of ChR-2 wt or its mutant in position 159 both fused to YFP, named respectively chop2-315YFP and ChR2(T159C) [gift from Georg Nagel, Würzburg Univ., D]. We obtained remarkable transfections in HeLa, an immortal cell line derived from tumoral human cervical cells, and in undifferentiated NSC-34 cells, a mouse motoneuron-like hybrid cell line. We positively checked the transfection efficiency and pattern with confocal microscopy by protocols used for GFP excitation at 488 nm. A detailed ion channel activity of the ChR-expressing cells, and its comparison in different cells by both the same ChRs wt and mutants, and a study of ChR-induced calcium dynamics by confocal microscopy using FRAP protocols will be faced. Finally, we are aimed to demonstrate that ChRs could be suitable optogenetic tools providing an endogenous non-invasive trigger of excitability in cellular nets interfacing memristive devices in bio-hybrid architectures.

*This research was developed in the framework of the MaDEleNA Project ("Grandi Progetti 2012" funded by PAT - Autonomous Province of Trento, Italy).*

## **P7 Control the metabolic activities of *E.coli* and *S. aureus* bacteria by Electric Field waves at Resonance Frequency in vitro study**

S.E. Abo-Neima<sup>1</sup>, Y.I. Khedr<sup>1</sup>, H.A. Motaweh<sup>1</sup>, M.M. Kotb<sup>2</sup> and A. Elhoseiny<sup>3</sup>

<sup>1</sup>Department of Physics, Faculty of Science, Damanhur University, Egypt

<sup>2</sup>Department of Medical Biophysics, Medical Research Institute, Alexandria University, Egypt.

<sup>3</sup>Master student at Department of physics, Faculty of Science, Damanhur University, Egypt.

e-mail: Sahar\_amr2002@yahoo.com

Weak electric currents generated using conductive electrodes have been used to increase the efficacy of antibiotics against bacterial biofilms, a phenomenon termed “the bioelectric effect” that formed metal ions and free radicals which can inhibit the growth of planktonic *Staphylococcus aureus* (*S. aureus*) and *Escherichia Coli* (*E. coli*) the effect is amplitude and frequency dependent, the aim of present study to define the parameters that are most effective against bacterial growth also to investigate the comparative study through inactivation of metabolic activities, growth rate, morphology, bacterial conductivity and antibiotic sensitivity between gram negative *E. coli* and gram positive *S. aureus* bacteria by extremely low frequency electric field. In this work, the frequency of electric impulses that interfere with the bioelectric signals generated during *E. coli* and *S. aureus* cellular division is investigated in order to compare cell viability, number of colony forming units (CFU) and growth rate (optical density at 600nm) bacterial conductivity, antibiotic susceptibility, molecular and morphological cellular structure by transmission TEM was determined. The results showed that a highly significant inhibition effect occurred when *S. aureus* and *E. coli* was exposed to resonance of 0.8, 0.5 Hz square amplitude modulated waves (QAMW) respectively for a single exposure (120min). Moreover, exposed cells became more sensitive to the tested antibiotics compared to control. Significant ultra-structural changes occurred as observed by Transmission Electron Microscope (TEM). Results of dielectric relaxation and TEM indicated molecular and morphological changes. It will be concluded that, the use of 0.8, 0.5 Hz QAMW in controlling the biological activity of *S. aureus* and *E. coli* respectively seems to be a new and promising medical activity.

**Keywords:** *S. aureus*, *E. coli*, electric field, modulated waves, TEM, antibiotic susceptibility, dielectric relaxation.

## **P8 Variability of calcium signalling during postnatal development in rat ventricular cardiomyocytes**

K. Macková, M. Hořka, A. Zahradníková Jr., I. Zahradník and A. Zahradníková

Institute of Molecular Physiology and Genetics, Slovak Academy of Sciences, Bratislava, Slovakia.  
e-mail: katarina.mackova@savba.sk

In the neonatal period, rapid growth of cardiomyocytes causes changes at the morphological and functional level. The tubular system (TS) develops which leads to formation of dyads, junctions where sarcolemmal L-type  $\text{Ca}^{2+}$  channels and ryanodine receptors of the sarcoplasmic reticulum are together involved in local  $\text{Ca}^{2+}$  control. The organization of E-C coupling in the developing heart is not fully understood yet. The aim of this work is to characterize growth phases of TS and to determine kinetic characteristics of L-type  $I_{\text{Ca}}$  in neonatal period.

Myocytes were isolated from the left cardiac ventricle of newborn and adult Wistar rat ( $n = 31$ , 1–20 days and 3 months) as previously described [1]. TS was labelled with the fluorescent lipophilic dye FM4-64 and imaged by confocal microscopy. The state of TS was evaluated by using the method of vertical sections [2] in the program *Graphic Cell Analyzer* [3]. L-type  $I_{\text{Ca}}$  were measured with whole-cell patch-clamp (80 ms depolarization from -50 to 0 mV) and described by a theoretical function [4] as a convolution of 3 processes: activation, slow current and voltage-inactivation, and calcium release-dependent inactivation.

The growth of cardiomyocytes was non-uniform: the average width of  $\sim 12 \mu\text{m}$  was not significantly changed during the first two weeks. In the longitudinal direction cardiomyocytes grew continually (1-3d:  $45.6 \mu\text{m}$ ; 19-20d:  $72.5 \mu\text{m}$ ; adult:  $105 \mu\text{m}$ ) by 10% per every 3 days. The stage of TS development was highly variable. TS was first observed on day 9 as short invaginations near peripheral sarcolemma, which became elongated on day 11 and in week 2 created a sparse and low-organized network. After day 16, TS was more regular and after day 19 it acquired the appearance of adult TS. Surface volume density of transversal tubules increased during the postnatal period (1-3d:  $0.06 \mu\text{m}^{-1}$ ; 19-20d:  $0.15 \mu\text{m}^{-1}$ ; adult:  $0.3 \mu\text{m}^{-1}$ ), whereas longitudinal tubules had a relatively stable surface density from day 14 on ( $0.08 \mu\text{m}^{-1}$ ). The density of  $I_{\text{Ca}}$  saturated on day 9 at a value of  $\sim 10 \text{ pA/pF}$ , comparable with that of adult myocytes. The rate of  $I_{\text{Ca}}$  inactivation did not change markedly after day 4. Calcium release-dependent inactivation appeared on day 4 ( $f_{\text{RDI}}=0.56$ ), when the t-tubules only started to form, and after day 14 it had a value comparable with that of adult myocytes ( $f_{\text{RDI}}=0.84$ ). This is apparent especially in the rate of calcium current decay, which on day 11 became as fast as in adult cardiac myocytes.

In conclusion, we observed high variability in growth of cells and development of tubular system that decreased at higher stage of development. Calcium release-dependent inactivation of calcium current precedes the development of t-tubular system by several days, indicating participation of the surface sarcolemma in dyadic E-C coupling in early postnatal period.

### **Acknowledgement**

Supported by APVV-15-0302 VEGA 2/0095/15 and VEGA 2/0147/14.

### **References**

- [1] A Zahradníková Jr., E Poláková, I Zahradník and A Zahradníková, *J Physiol* 578 (2007) 677-691.
- [2] AJ Baddeley, HJ Gundersen, LM Cruz-Orive, *J Microsc.* 142 (1986) 259-276.
- [3] J Parulek and I Zahradník, unpublished data
- [4] A Zahradníková, J Pavelková, Z Kubalová and I Zahradník, in *Calcium Signaling*, M. Morad and P. Kostyuk (Eds.), IOS press, Amsterdam (2001), pp. 42 – 51.

## **P9 Maleimido-proxyl as EPR spin probe for evaluation of conformational changes of albumin**

A. Pavićević, A. Popović-Bijelić, M. Mojović

University of Belgrade – Faculty of Physical Chemistry, EPR Laboratory, Studentski trg 12-16,  
11158 Belgrade, Serbia

e-mail: milos@ffh.bg.ac.rs

**Introduction and Aim.** Albumin is the most abundant plasma protein and as such has been subject of many studies using various techniques. One of the techniques which is able to track conformational changes and binding capacity of proteins is the approach employing spin labeling and electron paramagnetic resonance spectroscopy (EPR). So far, albumin has been investigated using number of different spin labels. Likewise, most of these studies were performed using spin labeled fatty acids (SLFAs), mainly 16-doxyl stearic acid (16-DS). Spin labeling of albumin with 16-DS has even been used for detection of cancer and various other diseases (sepsis, hepatitis, diabetes etc.) [1]. However, albumin can bind up to seven equivalents of fatty acids, and therefore when SLFAs are used for labeling, it is hard to determine which parts of the molecule exhibit conformational changes. In order to obtain information from the specific site, spin labels binding to free cystein residues can be used. In this work, the ability of such a probe, 3-maleimido proxyl (3-MP), to detect conformational changes was examined.

**Experimental.** Fatty acid free bovine serum albumin solution (BSA) was incubated with 10-fold excess of 3-MP for 24 h and the unbound probe was removed by extensive dialysis. In order to investigate effects of pH, the BSA solution was mixed with different buffers (pH ranging from 2.5 to 11.0). The effect of irreversible denaturation was studied by heating up the BSA solution up to 90°C. BSA solution was also incubated with several ligands (ibuprofen, bromazepam, fatty acids) that bind to albumin with high affinity, with the aim to elucidate whether conformational changes of BSA, induced by binding of these compounds, could be detected by 3-MP. The spectra were recorded using Bruker ELEXSYS II EPR spectrometer and spectral parameters, which reflect conformational changes determined by probe mobility, were measured.

**Results and discussion.** Preliminary results show that BSA-bound 3-MP clearly reflects the pH and temperature dependent changes in protein structure showing the existence of four forms of albumin at different acidities. Binding of fatty acids to BSA does not significantly alter the mobility of 3-MP and, even at high fatty acid to BSA ratios, only slight changes occur. Binding of bromazepam and ibuprofen to BSA both induced observable changes in the mobility of 3-MP, however the effect was more pronounced for ibuprofen. All these findings indicate that conformational changes of BSA could reliably be detected using spin label 3-MP. Hence, here we propose this probe to be a potentially good candidate for detection of conformational changes of albumin during the malignant and/or pathological processes.

References:

[1] A. Gurachevsky, S.C. Kazmierczak, A. Jörres, V. Muravsky, Application of spin label electron paramagnetic resonance in the diagnosis and prognosis of cancer and sepsis, Clin. Chem. Lab. Med. 46 (2008). doi:10.1515/CCLM.2008.260.

## **P10 Dynamics of AHL mediated quorum sensing in *Pseudomonas aeruginosa***

K. Nagy, V. Zsiros, O. Hodula, Á. Kerényi, O. Sipos, P. Galajda

Institute of Biophysics, Biological Research Centre of the Hungarian Academy of Sciences, Szeged, Hungary

e-mail: nagy.krisztina@brc.mta.hu

Quorum sensing (QS) is a fundamental phenomenon of bacterial communication that allows microbial populations to collectively control gene expression according to the population density. This synchronised group behaviour, which happens through simultaneous production and detection of signal molecules, offers several advantages to microbial communities such as production of virulence factors and antibiotics, biofilm formation or collective motion. *Pseudomonas aeruginosa* has a hierarchic QS system, specialized for specific homoserine lactone (HSL) molecules.

In our laboratory we investigate the dynamics of onset of the quorum state in *P. aeruginosa* under various conditions. For this purpose, we designed a microfluidic setup in which surface adhered bacteria can be studied for long period. Using mutants containing fluorescence reporter plasmid (pKRC12), we can follow with fluorescence microscopy how QS “turns on” at cellular level upon adding exogenous HSL. To reveal if there is any concentration dependent effect of HSLs on the onset of the quorum, bacteria were put into microfluidic gradient generator devices as well. Experiments were performed under flow and non-flow conditions. We found that the fluorescence intensity of the cells reaches a maximum value within 1-2 hours, and it remains for many hours (sometimes even for 12 hours) after washing the sample with pure HSL-free media. A cell-to-cell variability in the fluorescence intensities (indicating the QS state) was also noticed.

The work is supported by the Hungarian Scientific Research Fund (OTKA PD 112509).

## **P11 Fluorescence kinetics reveals Hofmeister effect on coenzyme FAD**

F. Sarlós, R. Nagypál, Á. Sipos, A. Dér, G. I. Groma

Institute of Biophysics, Biological Research Centre, Hungarian Academy of Sciences Szeged,  
Szeged, Hungary

e-mail: sarlos.ferenc@brc.mta.hu

The Hofmeister effect is a phenomenon of ion specificity in governing the solubility and aggregation state of proteins and other colloids[1]. Closed (aggregating) conformations are facilitated by a group of anions called kosmotropic ( $\text{SO}_4^{2-}$ , F), while open (highly soluble) structures are more probable in the presence of chaotropic anions ( $\text{ClO}_4^-$ ,  $\text{SCN}^-$ ). The experimental studies of this hardly understood phenomenon has been carried out mainly on macromolecules, being too complex for model calculation based on quantum mechanical/molecular dynamical methods.

Here we show that the effect takes place also on coenzyme FAD. This molecule consists of only two groups, and its characteristic conformational states can be categorized into open and closed forms. The populations of the open and closed conformers of the FAD molecule in aqueous solution were monitored by fluorescence kinetics in the 100 fs – 10 ns range, using the methods of time correlated single photon counting and fluorescence upconversion. The excited-state lifetime of the flavin chromophore of FAD is very different in open and closed conformations, according to its distance from the adenine group. The kinetics were analyzed by the basis pursuit denoising (BPDN) method optimized for multicomponent exponential decay[2], enabling to sensitively monitor the population of the different conformational states. The analysis identified a planar conformation with  $\tau_1 = 2.5$  ns and three closed ones, corresponding to  $\tau_2 = 80$  ps,  $\tau_3 = 10$  ps and  $\tau_4 = 2$  ps. The presence of kosmotropic and chaotropic anions did not change the fluorescence lifetimes but extensively controlled their relative amplitudes, exactly according to the Hofmeister effect.

[1]P. Lo Nostro and B. W. Ninham, Chem. Rev., 112 (2012) 2286-2322.

[2]G. I. Groma, Z. Heiner, A. Makai and F. Sarlós, RSC Adv., 2 (2012) 11481-11490.

## P12 Thermodynamic analysis of thermal unfolding of human serum albumin

M. Nemergut<sup>1</sup>, E. Sedlák<sup>2</sup>, D. Sedláková<sup>3</sup>, D. Belej<sup>1</sup> and D. Jancura<sup>1</sup>

<sup>1</sup> Department of Biophysics, P. J. Šafárik University, Jesenná 5, 041 54 Košice, Slovakia.

<sup>2</sup> Center for Interdisciplinary Biosciences, P. J. Šafárik University, Jesenná 5, 041 54 Košice, Slovakia.

<sup>3</sup> Department of Biophysics, Institute of Experimental Physics Slovak Academy of Sciences, Watsonova 47, 04001 Košice, Slovakia.

e-mail: Michal.Nemergut@gmail.com

Human serum albumin (HSA) is one of the most abundant proteins in the blood where it is present at a high concentration ( $\approx 600 \mu\text{M}$ ). HSA plays a special role in the transport of fatty acids, metabolites and drugs throughout the vascular system and also in maintaining the pH and osmotic pressure of plasma. For many drugs, reversible binding to serum albumin is a critical determinant of their distribution and pharmacokinetics. HSA is a single chain protein with 585 amino acids, with a molecular weight of  $\sim 66.5$  kDa. The structure of this molecule is composed from three homologous domains (I, II, and III) which are further divided into a pair of subdomains termed "A" and "B". According to the conventional view based on Sudlow's classification, drug ligands of HSA are accommodated at two main binding sites located in subdomain IIA (site IIA) and IIIA (site IIIA), respectively [1-3]. HSA is known to undergo different pH dependent conformational transitions, the N $\leftrightarrow$ F transition between pH 5.0 and 3.5, the F $\leftrightarrow$ E transition (acid expansion) below pH 3.5, and the N $\leftrightarrow$ B transition between pH 7.0 and 9.0 [4]. In this work, we performed detailed analyses of thermal unfolding of HSA. Our results indicate that thermal denaturation of albumin is an apparent two-step process described by different thermodynamic parameters and depends on scan rate, protein concentration and pH value of solvent. Moreover, thermodynamic properties of HSA are also significantly affected by the presence of ligands such as fatty acids. Detailed knowledge of thermodynamic properties of HSA as well as its ability to bind different ligands on pH value of solvent has a strong implication for its utilization as a part of drug delivery vehicles.

**Acknowledgment:** This work was supported by a project CELIM (316310) funded by 7FP EU Programs REGPOT and grant of Slovak grant agency VEGA 1/0423/16.

### References

- [1] N. A. Kratochwil, W. Huber, F. Muller, *Biochem. Pharmacol.* 64 (2002), 1355-1374.
- [2] S. Curry, *Drug Metab. Pharmacokinet.* 24 (2009), 342-357.
- [3] D. C. Carter, Ho, J. X. *Adv. Protein Chem.* 45 (1994), 153-203.
- [4] T. Peters, *All About Albumin: Biochemistry, Genetics, and Medical Applications*, Academic Press, 1995.

### **P13 Anthracene-9-carboxylic and niflumic acid inhibit growth and respiration of fungus *Phycomyces blakesleeanus***

T. Pajić<sup>1</sup>, M. Jovanović<sup>1</sup>, S. Križak<sup>1</sup>, T. Cvetić Antić<sup>2</sup>, M. Živić<sup>2</sup> and M. Stanić<sup>1</sup>

<sup>1</sup>Institute for Multidisciplinary Research, University of Belgrade, Kneza Višeslava 1, 11030 Belgrade, Serbia

<sup>2</sup>University of Belgrade – Faculty of Biology, Studentski trg 16, 11000 Belgrade, Serbia  
e-mail: tanja.pajic@pupin.rs

Anthracene-9-carboxylic (A9C) and niflumic acid (NFA) are frequently used substances for characterization of anion channels in electrophysiological measurements. However, their specificity is debatable, as it is known that these blockers interfere with auxin mediated growth in plants [1, 2] and also inhibit growth of some fungi, such as *Candida albicans* [3] and *Neurospora crassa* [4]. NFA is suggested as potential topical fungicide, and it is also used as non-steroidal anti-inflammatory drug [3]. Mechanisms of action of these substances are poorly understood, but many fungicides are known to achieve their effects through inhibition of respiratory chain components. In this study, we tested the effects of NFA on growth and respiration of *P. blakesleeanus* mycelium, as well as their effect on isolated mitochondria.

The effects of various concentrations of A9C (50 µM to 2 mM) and NFA (1 to 200 µM) on yield gain and growth inhibition were tested on *P. blakesleeanus* mycelium. Maximal growth inhibition compared to control for A9C of 89.7±3.7% was reached at 500 µM, while growth inhibition of 100% was reached with 100 µM NFA. Results were normalized to range from 0 to 100%, and as such fitted with a sigmoid curve to calculate half maximal inhibitory concentrations IC<sub>50</sub>. Obtained IC<sub>50</sub> for A9C was 129.84 µM, 5.6 times higher than for NFA, IC<sub>50</sub>=23.33 µM.

Concentrations from 5 to 800 µM A9C and 0.1 to 500 µM NFA were then applied to *P. blakesleeanus* mycelium while its respiration was measured. Again, NFA was more potent respiratory inhibitor than A9C, with 2.8 times lower IC<sub>50</sub> (49.85 µM compared to 141.51 µM). These experiments, however, do not indicate the site of action for A9C and NFA, i.e., if they are directly affecting some components of the respiratory chain. In the next step, effects of these compounds were tested on isolated mitochondria. Inhibition of oxygen consumption rate was 8.92±2.29, 8.42±2.28 and 6.31±1.78% for 200, 500 and 800 µM A9C, respectively, and 46.72±11.78% for 500 µM NFA. Far smaller effect of NFA and a very poor effect of A9C on mitochondrial respiratory rate indicate that the observed decrease in mycelial respiratory rate is a result of indirect inhibitory activity of tested compounds on respiration of the mycelium.

Among the effects of tested anion channel blockers is intracellular acidification [5]. Intracellular acidification inhibits phosphofructokinase, a pH sensitive, rate limiting step of glycolysis [6], thereby reducing substrate supply for mitochondrial electron-transport chain, and ultimately, ATP synthesis. These events could, at least in part, explain the effect of A9C and NFA on some anion channels whose activation requires non-hydrolytic ATP binding.

1. Burdach Z, Kurtyka R, Siemieniuk A, Karcz W (2014) Role of chloride ions in promotion of auxin-induced growth of maize coleoptile segments. *Annals of Botany* 114: 1023-1034
2. Thomine S, Lelievre F, Boufflet M, Guern J, Barbier-Brygoo H (1997) Anion-channel blockers interfere with auxin responses in dark-grown *Arabidopsis* hypocotyls. *Plant Physiology* 61: 204-208
3. Baker A, Northrop FD, Miedema H, Devine GR, Davies JM (2001) The non-steroidal anti-inflammatory drug niflumic acid inhibits *Candida albicans* growth. *Mycopathologia* 153: 25-28
4. Hanke GT, Northrop FD, Devine GR, Bothwell JHF, Davies JM (2001) Chloride channel antagonists perturb growth and morphology of *Neurospora crassa*. *FEMS Microbiology Letters* 201: 243-247
5. Brown CDA and Dudley AJ (1996) Chloride channel blockers decrease intracellular pH in cultured renal epithelial LLC-PK1 cells. *British Journal of Pharmacology*. 118: 443-444
6. François J, Van Schaftingen E, Hers HG (1986) Effect of benzoate on the metabolism of fructose 2,6-bisphosphate in yeast. *Eur. J. Biochem.* 154: 141-145

## **P14 Functional dynamics of H44 AppA mutants revealed by ultrafast spectroscopy**

**K. Pirisi<sup>1</sup>, A. Zieba<sup>2</sup>, R. Kapronczai<sup>1</sup>, G. Greetham<sup>3</sup>, P.J. Tonge<sup>2</sup>, S.R. Meech<sup>4</sup>, A. Lukacs<sup>1</sup>**

<sup>1</sup> Department of Biophysics, Medical School, Szigeti Str. 12, H-7624 Pécs, Hungary

<sup>2</sup> Department of Chemistry, and Department of Biochemistry & Cell Biology, Stony Brook University, Stony Brook, New York

<sup>3</sup> Central Laser Facility, Harwell Science and Innovation Campus, Didcot, Oxon OX11 0QX, United Kingdom

<sup>4</sup> School of Chemistry, University of East Anglia, Norwich Research Park, Norwich NR4 7TJ, United Kingdom

e-mail: katalin.pirisi@aok.pte.hu

BLUF domain family is an important class of photoactive flavoproteins which are involved in the photophobic response and in light controlled gene expression in bacteria. The mechanism of photoactivity in the BLUF domain has not yet been definitively established. Detailed studies of the gene-regulating AppA protein, which contains one of the best characterized BLUF domains reveal a kinetically complex photocycle with a number of steps occurring on the picosecond-microsecond time scale.

At low light and low oxygen conditions AppA binds to the transcription factor PpsR enabling transcription of photosystem biosynthesis genes. When AppA is irradiated by intense light or exposed to high oxygen conditions it will release PpsR which then binds to DNA shutting off production of photosystem biosynthesis genes.

Our earlier studies showed that the function of the protein after light absorption is triggered by the reorganization of the hydrogen bonding network surrounding the flavin. In this work we studied different mutants where we exchanged the histidine at the position 44 close to the C2 atom of the flavin. As this amino acid is hydrogen bonded to the flavin the mutations altered the hydrogen bonding network of the flavin. In order to characterize the photocycle we performed visible and infrared transient absorption measurements on these mutants.

## P15 Single Molecule Tracking questions the Exclusivity of $\zeta$ -Chain Interactions with the T-Cell Receptor

B.K. Rossboth, F. Baumgart, A. Reismann, G. Schütz, M. Brameshuber

Institute of Applied Physics, TU Wien, Wiedner Hauptstraße 8-10, 1040 Vienna, Austria

e-mail: rossboth@iap.tuwien.ac.at

The immune system protects an organism in a multitude of different ways. The T lymphocytes, with their respective  $\alpha\beta$ -T Cell Receptor (TCR), bear a grave role by binding foreign antigens and initiating the adaptive immune response. Even though the  $\alpha\beta$ TCR and its associated CD3 protein complex, assembled by  $\gamma\epsilon$ ,  $\delta\epsilon$ , and  $\zeta\zeta$  dimers, are long known to execute this vital task, much remains to be elucidated. The  $\zeta$ -chain represents an essential part of this receptor complex for assembly and membrane association, as well as for accurate signal initiation and was biochemically shown to be associated with the TCR as a homo-dimer. Most studies on the TCR/CD3 complex, however, were made by rather indirect methods, such as co-immunoprecipitation. With the recent progress made in light microscopy, more direct experiments are possible. In this work, single molecule tracking, as well as single particle tracking PALM [1] experiments were performed to get information on the diffusional behaviour of single chain – antibody labelled (scFv) TCR $\beta$  and  $\zeta$  linked to mEOS3.2.

Surprisingly, diffusional differences between the two proteins were found in transduced primary murine T cells, as a fraction of the  $\zeta$ -chain revealed two-fold faster diffusion than the TCR $\beta$ . The utilized algorithms for localization and tracking were evaluated before use ([2]) and found to be adequate for densities and SNRs determined in actual experiments and the results were confirmed by further algorithms. To exclude influences of a possible bias by endogenous, unlabelled  $\zeta$ -chain,  $\zeta$  was reconstituted in the  $\zeta$ -deficient murine T cell hybridoma MA5.8 [3]. Results reflected the same diffusion behaviour as observed in the primary cells.

This diffusional difference between  $\zeta$  and TCR $\beta$  indicate less stable interactions within the TCR/CD3 complex, than identified by biochemical methods and which are widely accepted in recent literature. Whereas TCR complex independent  $\zeta$  was shown to possibly be stabilized by H<sub>2</sub>O molecules within the membrane by molecular dynamics simulations [4], its physiological role is still to be elucidated, and the behaviour of  $\zeta$  within other receptor complexes, e.g. CD16 or NKp30 on Natural Killer cells would be of interest.

Currently, more direct experiments for probing the interactions of TCR $\beta$  and  $\zeta$  are performed by utilizing the analysis of co-diffusion using two-color TOCCSL [5] and micro-patterning combined with FRAP [6].

1. Manley, S., et al., High-density mapping of single-molecule trajectories with photoactivated localization microscopy. *Nat Methods*, 2008. 5(2): p. 155-7.
2. Chenouard, N., et al., Objective comparison of particle tracking methods. *Nat Methods*, 2014. 11(3): p. 281-9.
3. Sussman, J.J., et al., Failure to Synthesize the T Cell CD3 $\zeta$  Chain: Structure and Function of a Partial T Cell Receptor Complex. *Cell*, 1988. 52: p. 85-95.
4. Petruk, A.A., et al., The structure of the CD3  $\zeta\zeta$  transmembrane dimer in POPC and raft-like lipid bilayer: a molecular dynamics study. *Biochim Biophys Acta*, 2013. 1828(11): p. 2637-45.
5. Ruprecht, V., M. Brameshuber, and G.J. Schütz, Two-color single molecule tracking combined with photobleaching for the detection of rare molecular interactions in fluid biomembranes. *Soft Matter*, 2010. 6(3): p. 568-581.
6. Schwarzenbacher, M., et al., Micropatterning for quantitative analysis of protein-protein interactions in living cells. *Nat Methods*, 2008. 5(12): p. 1053-60.

## **P16 Fluorescence kinetics reveals Hofmeister effect on coenzyme FAD**

F. Sarlós, R. Nagypál, Á. Sipos, A. Dér, G. I. Groma

Institute of Biophysics, Biological Research Centre, Hungarian Academy of Sciences Szeged, Szeged, Hungary

e-mail: sarlos.ferenc@brc.mta.hu

The Hofmeister effect is a phenomenon of ion specificity in governing the solubility and aggregation state of proteins and other colloids[1]. Closed (aggregating) conformations are facilitated by a group of anions called kosmotropic ( $\text{SO}_4^{2-}$ , F), while open (highly soluble) structures are more probable in the presence of chaotropic anions ( $\text{ClO}_4^-$ ,  $\text{SCN}^-$ ). The experimental studies of this hardly understood phenomenon has been carried out mainly on macromolecules, being too complex for model calculation based on quantum mechanical/molecular dynamical methods.

Here we show that the effect takes place also on coenzyme FAD. This molecule consists of only two groups, and its characteristic conformational states can be categorized into open and closed forms. The populations of the open and closed conformers of the FAD molecule in aqueous solution were monitored by fluorescence kinetics in the 100 fs – 10 ns range, using the methods of time correlated single photon counting and fluorescence upconversion. The excited-state lifetime of the flavin chromophore of FAD is very different in open and closed conformations, according to its distance from the adenine group. The kinetics were analyzed by the basis pursuit denoising (BPDN) method optimized for multicomponent exponential decay[2], enabling to sensitively monitor the population of the different conformational states. The analysis identified a planar conformation with  $\tau_1 = 2.5$  ns and three closed ones, corresponding to  $\tau_2 = 80$  ps,  $\tau_3 = 10$  ps and  $\tau_4 = 2$  ps. The presence of kosmotropic and chaotropic anions did not change the fluorescence lifetimes but extensively controlled their relative amplitudes, exactly according to the Hofmeister effect.

[1]P. Lo Nostro and B. W. Ninham, Chem. Rev., 112 (2012) 2286-2322.

[2]G. I. Groma, Z. Heiner, A. Makai and F. Sarlós, RSC Adv., 2 (2012) 11481-11490.

## **P17 Electron Paramagnetic Resonance studies of radical reactions of a NADH analogue**

K. Sebők-Nagy<sup>1</sup>, D. Rózsár<sup>2</sup>, Á. Balázs<sup>2</sup>, L.G. Puskás<sup>2</sup> and T. Páli<sup>1</sup>

<sup>1</sup>Institute of Biophysics, Biological Research Centre, Hungarian Academy of Sciences, H-6726 Szeged, Temesvári krt. 62, Hungary

<sup>2</sup>AVICOR Ltd., H-6726 Szeged, Alsó kikötő sor 11, Hungary  
e-mail: seboknagy.krisztina@brc.mta.hu

The class of 1,4-dihydropyridine calcium antagonist is closely related to NADH, a ubiquitous biological reductant. The heterocyclic dihydropyridine ring is the common feature for various pharmacological activities of NADH analogues, which can be readily produced by Hantzsch pyridine synthesis. Application of a lot of types of medicine with 1,4-dihydropyridine has advanced greatly in the treatment of cardiovascular- and other spastic smooth muscle diseases. To get a deeper insight into the operation of calcium antagonists, a kinetic study of the reaction of Diethyl 2,6-dimethyl-1,2-dihydropyridine-3,5-dicarboxylate and 2,4,6-Tris(4-methoxyphenyl)pyrilium cation was carried out by Electron Paramagnetic Resonance (EPR) spectroscopy. The reaction was mapped with 2,2,6,6-Tetramethylpiperidine-1-oxyl as a radical source. In order to reveal the details of the mechanism, the spin trap 5,5-Dimethyl-1-pyrroline *N*-oxide was applied. The ratio of the components of the reaction was affected by the addition of *N*-(Ethoxy(phenyl)methyl)acrylamide, commonly used in organic chemistry. Deconvolution of the EPR spectra were carried out by the Marquardt-Levenberg fitting method by using Lorentzian and Voigt lineshape functions. The fitting resulted in 5 markedly distinct species, whose concentration distribution differed in the presence of (Ethoxy(phenyl)methyl)acrylamide. The reaction rates were calculated from the concentration distribution fitted with two exponentials for each species. We propose a reaction mechanism based on the results.

## **P18 The intensity of nonsynaptic epileptiform activity of leech Retzius neurons under different ionic conditions**

M. Stanojević<sup>1</sup>, S. Lopicic<sup>1</sup>, S. Spasic<sup>1</sup>, J. Nesovic-Ostojic<sup>1</sup>, S. Kovacevic<sup>1</sup>, V. Nedeljkov<sup>1</sup>, M. Prostran<sup>2</sup>

<sup>1</sup>Institute for Pathological Physiology, School of Medicine, University of Belgrade, Belgrade, Serbia;

<sup>2</sup>Institute for Pharmacology, Clinical Pharmacology and Toxicology, School of Medicine, University of Belgrade, Belgrade, Serbia

e-mail: marijastanojevic2002@yahoo.com

**Background:** Nonsynaptic mechanisms have an important role in molecular and cellular basis of epileptogenesis. Among these, changes in ionic composition of extracellular fluid contribute significantly.

**Aim:** The object of this study was to examine the mechanism of Ni<sup>2+</sup> - induced bursting of Retzius neurons of the free segmental ganglia of the leech *Haemopsis sanguisuga*, as a model of nonsynaptic experimental epileptiform activity. Different ionic conditions were tested in separate sets of experiments and the effects evaluated as a change in the intensity of the induced epileptiform activity.

**Methods:** Classical intracellular electrophysiological recording was used. Superfusion with 3 mM Ni<sup>2+</sup> in Ringer (Ri) saline has induced epileptiform activity characterized by rhythmical generation of paroxysmal depolarization shifts (PDSs). Its intensity was calculated as a percentage of PDS duration within its belonging interPDS interval. Several modified salines were applied (0 Na<sup>+</sup> Ri, 1.8 mM K<sup>+</sup> Ri, 0 Ca<sup>2+</sup> Ri, 10 mM Mg<sup>2+</sup> Ri). Student's *t*-test was used for statistical comparisons.

**Results:** Mean epileptiform activity intensity in control Ni<sup>2+</sup> saline was 49.09±1.92 %. Omitting external Na<sup>+</sup> terminated the activity, thus reducing its intensity to zero level (n=4, p<0.001). Both Ca<sup>2+</sup> omission and reduction of external K<sup>+</sup> significantly reduced the epileptiform activity intensity. For Ni<sup>2+</sup> - 0 Ca<sup>2+</sup> Ri the decrease was from 47.84±1.34 % (control) to 30.41±1.81 % (n=5, p<0.001), whereas for Ni<sup>2+</sup> - low K<sup>+</sup> Ri it was from 53.74±1.26 % to 33.48±1.44 % (n=6, p<0.001). Finally, introducing high Mg<sup>2+</sup> into the superfusing Ni<sup>2+</sup> Ri saline highly significantly reduced epileptiform activity intensity from 51.93±0.68 % to 15.56±1.18 % (n=7, p<0.001).

**Conclusions:** The underlying ionic mechanism of this invertebrate model of nonsynaptic epileptogenesis experimentally induced by Ca<sup>2+</sup> channel blockade with Ni<sup>2+</sup> in leech Retzius neurons was found to be Na<sup>+</sup> - dependent, Ca<sup>2+</sup> - and K<sup>+</sup> - modulated and Mg<sup>2+</sup> - suppressed. Sodium influx is mandatory for its generation, Ca<sup>2+</sup> - dependent currents also seem to be involved, and the activity of the Na<sup>+</sup>/K<sup>+</sup> pump relevant for the termination of the activity. Magnesium shows a significant suppressive effect on this Na<sup>+</sup> - dependent Ni<sup>2+</sup> - induced epileptiform activity.

**Acknowledgement** This work was supported by the Ministry of Education, Science and Technological Development of Republic of Serbia, grant number 175023.

**Keywords:** nonsynaptic epileptiform activity, leech Retzius neuron, ionic conditions

### **P19 Carbon-based biohybrides for optoelectronics**

T. Szabó<sup>1</sup>, T. Tomashević<sup>2</sup>, R. Panajotović<sup>2</sup>, Gy. Váró<sup>3</sup>, G. Garab<sup>4</sup>, K. Hajdu<sup>1</sup>, K. Hernadi<sup>5</sup>, L. Nagy<sup>1</sup>

<sup>1</sup>Institute of Medical Physics and Informatics, University of Szeged, Szeged, Hungary

<sup>2</sup>Institute of Physics, University of Belgrade, Belgrade, Serbia

<sup>3</sup>Institute of Biophysics, HAS Biological Research Center, Szeged, Hungary

<sup>4</sup>Institute of Plant Biology, HAS Biological Research Center, Szeged, Hungary

<sup>5</sup>Department of Applied and Environmental Chemistry, University of Szeged, Szeged, Hungary

e-mail: tiberatosz@gmail.com

Functional bio-hybrid nanocomposite materials are created from photosynthetic reaction center proteins (RC) purified from purple bacteria and from carbon-based materials (carbon nanotubes, carbon nanowires and graphene) and the optical and electric properties of the composites are characterized. RCs were successfully bound to the inorganic carbon materials with different procedures and the light induced change in the absorption and electric conductivity was measured. Spectroscopy measurements showed that RC kept its photo-activity after the binding. The current-voltage ( $I/U$ ) characteristics of the composites in the dark and under illumination indicated that there is an electrostatic/electronic interaction between the photo-active biological and the inorganic carrier samples. Our results indicated that the photo-induced conductance change was probably affected by the energy absorbed by the carbon carrier material directly, or through the heat dissipated by the RC after electronic excitation. The determination of the contribution of the heat dissipation to the conductivity change is in progress. The results will help us to design new generations of optoelectronic devices, e.g. sensors for highly specific biosensor applications, light-activated switches, photoelectric energy converter systems and microimaging devices.

## **P20 Direct mapping intercellular interactions: first steps towards brain metastasis formation**

A.G. Végh<sup>1</sup>, B. Varga<sup>1</sup>, R. Domokos<sup>2</sup>, C. Fazakas<sup>1</sup>, J. Molnár<sup>1</sup>, I. Wilhelm<sup>1</sup>, Z. Szegletes<sup>1</sup>, I.A. Krizbai<sup>1</sup> and G. Váró<sup>1</sup>

<sup>1</sup>BRC BF – Biological Research Centre of the Hungarian Academy of Sciences, Institute of Biophysics, Szeged, Hungary

<sup>2</sup>BBU – Babes-Bolyai University, Faculty of Physics, Cluj-Napoca, Romania

e-mail: vegh.attilagery@brc.mta.hu

The most life-threatening aspect of cancer is metastasis. The reasons behind why some primary tumors metastasize, thus have a worse outcome, compared to others that do not metastasize is still under debate. Dissemination of cancer cells predominantly involves lymphogenous or hematogenous routes. Among all metastatic foci, presence of brain metastasis is of very poor prognosis; the median survival time can be counted in months. Therefore, prevention or lowering their incidence would be highly desired both by patients and physicians. Since the central nervous system (CNS) lacks lymphatic circulation, metastatic cells invading the CNS must breach the interface between circulation and cerebral tissue: the blood-brain barrier. The establishment of firm adhesion between the cancer cell and the cerebral endothelial layer has a key role in this process.

Using the atomic force microscope, as a high resolution force-spectrograph, our aim is to explore the connections among the cell morphology, cellular mechanics and biological function in the process of transendothelial migration of metastatic cancer cells. Our model relies on direct measurement of intercellular interactions between a living cancer cell and a confluent endothelial layer as substrate. By immobilization of a living cancer cell to an atomic force microscope's cantilever, intercellular adhesion is directly measured at quasi-physiological conditions. Hereby we present our latest results using this cell decorated probe, to test directly the linkage establishment to a confluent layer of brain endothelial cells in the presence and absence of membrane fluidizing agent, with distinguished attention to membrane tether formation and dynamics. Moreover, spatial distribution of detachment strength is investigated for cancer cells of different origin. Pseudo colored three dimensional maps reveal highly valuable data on several nanomechanical parameters which play crucial role in intercellular interactions.

These results highlight the importance of cellular mechanics in brain metastasis formation and emphasize the enormous potential towards exploration of intercellular dynamics related processes. Nevertheless, underlines the power and potential of the Atomic Force Microscope as a highly accurate nano-force tool in cellular biomechanics and life sciences.

## **P21 Voltammetric detection G-quadruplex-based structural transitions in oligonucleotides**

P. Vidláková<sup>1</sup>, H. Pivonkova<sup>1</sup>, I. Kejnovska<sup>1,3</sup>, L. Trnkova<sup>2,4</sup>, M. Vorlíčková<sup>1,3</sup>, M. Fojta<sup>1,3</sup> and L. Havran<sup>1</sup>

<sup>1</sup>Institute of Biophysics of the Academy of Sciences of the Czech Republic v.v.i., Kralovopolska 135, CZ-61265 Brno, Czech Republic

<sup>2</sup>Department of Chemistry, Faculty of Science, Masaryk University, Kamenice 5, CZ-62500 Brno, Czech Republic

<sup>3</sup>CEITEC-Central European Institute of Technology, Masaryk University, Kamenice 5, CZ-62500, Brno, Czech Republic

<sup>4</sup>CEITEC, Brno University of Technology, Technická 3058/10, CZ-61600, Brno, Czech Republic  
e-mail: pavlinavidlakova@seznam.cz

Current intensive development in the electrochemical DNA sensors area is stimulating efforts of researchers towards studies of the behavior of synthetic oligonucleotides and their analogues at electrically charged surfaces. These studies are related to application of the oligonucleotides as, for example, capture probes in hybridization sensors.

Electrochemical methods, particularly when applied in connection with mercury-containing electrodes, are excellent tools for studying nucleic acids structure and monitoring structural transitions. We studied influence of the length of central (dG)<sub>n</sub> stretch (varying from 0 to 15 guanine residues) in 15-mer ODN (G0 to G15) on their electrochemical and interfacial behavior at the mercury and carbon electrodes. Dependence of peak G heights measured by AdTS CV at HMDE on number of G residues in ODN molecule results strong influence of electrochemical behavior of studied ODN on length of oligo-G stretch. Intensity of the signal increased with number of guanines up to G5 and decreased sharply with further elongation of the (dG)<sub>n</sub> stretch.

On the other hand, the intensity of guanine oxidation signal measured by AdTS SWV at PGE (peak G<sup>ox</sup>) was observed to increase continuously with number of guanines between 0 and 15. These results can be explained by forming of G-quadruplex in ODN molecules containing larger number of G residues. These results were confirmed by polyacrylamide gel electrophoresis and CD spectroscopy. CD spectra showed forming of antiparallel G-quadruplex in the case of ODN containing G stretch longer than 5 nucleobases.

This study has brought the first insight into behavior of oligonucleotides with segmental structure, composed of G-quadruplex forming and inherently single-stranded parts, at different electrically charged surfaces.

### **Acknowledgments**

This work was supported by grants of the Czech Science Foundation (15-08434S, P206/12/G151)

## **P22 Expression and spectral analysis of recombinant cytochrome-*b*<sub>561</sub> proteins**

Z. Márton<sup>1</sup>, K. Laskay<sup>1</sup>, A. Bérczi<sup>1</sup>, A. Tóth<sup>1,2</sup>, G. Rákhely<sup>1,2</sup> and L. Zimányi<sup>1</sup>

<sup>1</sup>Institute of Biophysics, Biological Research Centre of the Hungarian Academy of Sciences, Temesvári krt. 62, Szeged, H-6726, Hungary

<sup>2</sup>Department of Biotechnology, University of Szeged, Közép fasor 52, Szeged, H-6726, Hungary  
e-mail: zimanyi.laszlo@brc.mta.hu

Cytochrome-*b*<sub>561</sub> (CYB561) proteins are ubiquitous, ascorbate reducible, electron-transporting proteins with 6 trans-membrane helices. Their different versions participate in plant apoplastic defense, iron uptake, regeneration of ascorbate in neuroendocrine tissues and suppression of tumor growth. They contain two heme-*b* centers, one on each side of the membrane, liganded by the 4 consecutive core helices 2-5 via two pairs of conserved histidine residues. Although CYB561s are found in a number of animal and plant tissues and even more based on genome screening, with unknown localization, their low abundance allows their detailed study only when the protein under study is tag-labeled, heterologously-expressed and affinity-purified.

We have expressed several wild type and double mutant CYB561 proteins – with the two cytoplasmic-side His heme ligands replaced by Ala – in *Saccharomyces cerevisiae* YTHCBMS1 strain using both the native and the yeast strain optimized codon, with or without Strep-II or His tags on the C terminal or in non-cytoplasmic interhelical loops. Spectroscopic analysis of the purified proteins allowed the determination of the „apparent binding constants” for the low and high affinity „ascorbate binding sites”. Chemometric analysis of the spectra revealed slight differences reflecting different interactions in the heme pockets of various CYB561 proteins. The *Mus musculus* CYB561 D1 protein of unknown function has been purified for the first time, and its spectral properties – resembling more the plant vacuolar (tonoplast) and the animal chromaffin granule localized CYB561s than the mouse tumor suppressor (CYB561 D2) protein – will be discussed.

This work was supported by the Hungarian Scientific Research Fund, grant No. K-108697.

### **P23 Quantitative analysis of the spatial relationship of IL-9 and IL-2 receptors at the surface of human T lymphoma cells**

E. Nizsalóczki, P. Nagy, I. Csomós, G. Vámosi, L. Mátyus, A. Bodnár

Department of Biophysics and Cell Biology, Research Center for Molecular Medicine, Faculty of Medicine, University of Debrecen, H-4032 Debrecen, Egyetem tér 1. Hungary

IL-9 is a multifunctional cytokine with pleiotropic effects on T cells. The heterodimeric IL-9 receptor consists of the cytokine-specific  $\alpha$  subunit and the common  $\gamma_c$  chain. Expression of IL-9R $\alpha$  is mainly restricted to T cell subsets also expressing the heterotrimeric IL-2R, other member of the  $\gamma_c$  cytokine receptor family, in which IL-2 has a crucial regulatory role. Considering that IL-9 shares the signaling  $\gamma_c$  receptor subunit with IL-2, it is an intriguing question whether there is any correlation between cell surface localization of IL-9 and IL-2 receptors. Our recent confocal microscopy co-localization and FRET experiments demonstrated the bipartite spatial relationship of IL-9R with IL-2R at the surface of human T lymphoma cells: in addition to the co-expression of the two receptor kinds in common membrane domains, a considerable fraction of IL-9R and IL-2R could also be detected in spatially segregated membrane areas. Here we elucidate further the details and regulation of IL-9R distribution between these distinct membrane areas. Pair-wise co-localization of the two receptor kinds is characterized by quantitative analysis of confocal microscopy images, using two kinds of metrics (Pearson's correlation and Mander's co-localization coefficients). Numerical values of the metrics are compared to measurement-dependent confidence intervals created by scrambling the images for a given cell representing chance distribution of the two receptor kinds.

## **P24 Metabolism of EPR spin-probes in cell suspensions: assessment of cell permeability and intracellular reduction**

A. Pavićević<sup>1</sup>, S. Stamenković<sup>2</sup>, G. Bačić<sup>1</sup>

<sup>1</sup>University of Belgrade – Faculty of Physical Chemistry, EPR Laboratory, Studentski trg 12-16, 11158 Belgrade, Serbia

<sup>2</sup>University of Belgrade – Faculty of Biology, Center for Laser Microscopy, Studentski trg 3, 11158 Belgrade, Serbia

e-mail: ggbacic@ffh.bg.ac.rs

**Introduction and Aim.** A thorough understanding of the interaction between nitroxide spin-probes and cells is a prerequisite for their productive use in viable biological systems, including live animals. Here we studied three typical nitroxides having different cell permeability and reducing susceptibility, attempting to understand their interaction at the cellular level, with an ultimate goal to use these data in explaining results obtained for reduction in intact animals.

**Experimental.** Experiments were performed in solutions of ascorbate, samples of the whole blood, isolated erythrocytes and isolated astrocytes. Reduction of spin probes Tempol, 3CP (3-carbamoyl proxyl), and 3CxP (3-carboxy proxyl) was studied in the gas permeable Teflon tubes using EPR spectrometer operating at the X-band.

**Results and Discussion.** The rates of reduction of nitroxides in all samples were in the order Tempol >> 3CP > 3CxP reflecting the well known facts that piperidine rings are more susceptible to reduction than pyrrolidine rings and that the presence of charged groups has an influence on reduction. The reduction in the whole blood was faster than in suspension of isolated erythrocytes indicating that both intracellular and extracellular (most likely ascorbate) agents reduce nitroxides in the whole blood. All investigated nitroxides, including 3CxP, readily cross the erythrocytes membranes which is not surprising having in mind the specific structure of the membrane. However, depending on the type, reduction of nitroxides in suspension of astrocytes was 2-5 times faster than in suspension of erythrocytes. Since no reduction can occur in the extracellular medium, this points to the fact that apparently all nitroxides readily cross astrocyte's cell membrane as well as that astrocytes contain some very potent reducing species. This finding is somewhat surprising considering published data, especially for 3CxP (hydrophilic and negatively charged compound) being widely considered as an almost cell impermeable spin-probe.

**In conclusion,** *in vitro* experiments on isolated cells are important for modeling of the overall pharmacokinetic of these nitroxides *in vivo*.

## **P25 GTP-activated inactivating anionic current in Ph.bl**

S. Križak, N. Todorovic, T. Pajić, M. Živić

Institute for Multidisciplinary Studies, University of Belgrade  
Institute for Biological Research "Sinisa Stankovic", University of Belgrade  
School of Biology, University of Belgrade

We have recently described ORIC, osmotically activated current in *Phycomyces blakesleeanus* cytoplasmic droplet membrane (Križak S, Nikolić L, Stanić M, Žižić M, Zakrzewska J, Živić M, Todorović N. Osmotic swelling activates a novel anionic current with VRAC-like properties in a cytoplasmic droplet membrane from *Phycomyces blakesleeanus* sporangiophores Res Microbiol. 2015 166(3):162-73). Here, we demonstrate in the same model system, that GTP $\gamma$ -S applied from intracellular side activates a current in the absence of osmotic stimulation, that bears similarity to ORIC. Namely, GTP $\gamma$ -S activated current shows prominent inactivation at depolarised potentials, it is outwardly rectified and carried by anions. GTP $\gamma$ -S activated current is subjected to slow run-down during the experiment, as ORIC is. More detailed biophysical characterisation of GTP $\gamma$ -S activated current revealed that its rectification properties are  $V_{0.5} = 69 \pm 6$ ,  $Z_g = 0.87 \pm 0.09$ . The time constant of current inactivation at depolarised potential has voltage dependency similar to ORIC ( $\tau$  (10mV) =  $150 \pm 13$  ms and  $\tau$  (70mV) =  $51 \pm 7$  ms at ). Steady-state inactivation had  $V_{0.5} = -50 \pm 3$  mV. GTP $\gamma$ -S activated current could be mediated by the same channel complex as ORIC. Activation by GTP-dependent mechanism, along with the biophysical properties of ORIC current suggest that ORIC is a VRAC-like current. It is the only known example of the current with properties of VRAC (volume regulated anionic current) outside the Animal Kingdom.

## **P26 Design of PGLa-H tandem-repeat peptides with activity and selectivity testing against clinical bacterial isolates**

T. Rončević<sup>1</sup>, G. Gajski<sup>2</sup>, N. Ilić<sup>1</sup>, I. Goić-Barišić<sup>3</sup>, M. Tonkić<sup>3</sup>, L. Zoranić<sup>1</sup>, J. Simunić<sup>4</sup>, M. Benincasa<sup>5</sup>, M. Mijaković<sup>1</sup>, A. Tossi<sup>5</sup>, D. Juretić<sup>1,6</sup>

<sup>1</sup>Department of Physics, Faculty of Science, University of Split, Croatia; <sup>2</sup> Mutagenesis Unit, Institute for Medical Research and Occupational Health, Zagreb, Croatia; <sup>3</sup>Department of Clinical Microbiology, University Hospital Centre Split and University of Split School of Medicine, Split; <sup>4</sup>Laboratory of Cell Biophysics, Division of Molecular Biology, Rudjer Boskovic Institute, Zagreb, Croatia.; <sup>5</sup>Department of Life Sciences, University of Trieste, Trieste, Italy; <sup>6</sup>Mediterranean Institute for Life Sciences, Split, Croatia. larisaz@pmfst.hr

Antimicrobial peptides (AMPs) are promising candidates for new classes of antibiotics but tend to display an unacceptable toxicity to human cells. A naturally produced C-terminal fragment of PGLa, named PGLa-H, was reported to have a very low haemolytic activity with a moderate antibacterial activity. We designed a sequential tandem repeat of PGLa-H and its analogue with glycine substitution at key position. *Di*PGLa-H and its analogue showed markedly improved *in vitro* bacteriostatic and bactericidal activity against laboratory strains and multidrug resistant clinical isolates of both Gram-negative and Gram-positive pathogens. At the same time they were non-toxic for circulating human blood cells as assessed by haemolysis and cyto/genotoxicity assays. An analogue with a single glycine substitution showed a slightly better antibacterial activity and somewhat reduced cytotoxicity.

The detail structural analysis of *Di*PGLa-H and its analogue both in water and TFE water solutions was performed using the molecular dynamic simulations. MD simulations suggest a high content of helical conformation in TFE water solutions for both peptides, somewhat higher for *Di*PGLa-H that also preserves a small amount of  $\alpha$ -helical structuring in pure water, while the analog loses it completely. In the case of analog, the conformation in TFE water solutions seems to interchange between an  $\alpha$ -helix and a  $\pi$ -helix. These results are in substantial agreement with CD measurements. In the future these peptides may serve as useful lead compounds for developing non-toxic anti-infective agents against multi-resistant pathogens, especially for topical uses.

**Acknowledgements:** Authors acknowledge funding from Croatian Science Foundation project 8481 BioAmpMode and 4514 MS-FormDes.

**P27 Effects of gold nanoparticles, protected by self-assembling mixtures of ligands, on eukaryotic cells and model membranes.**

F. Guida<sup>1</sup>, V. Iacuzzi<sup>1</sup>, M. Şologan<sup>2</sup>, D. Marson<sup>3</sup>, S. Boccardo<sup>3, c</sup>, P. Pengo, L. Pasquato<sup>2</sup>, A. Tossi<sup>1</sup>, P. Posocco<sup>3\*</sup> and S. Pacor<sup>1\*</sup>

<sup>1</sup>Department of Life Sciences, University of Trieste, 34127, Trieste, Italy

<sup>2</sup>Department of Chemical and Pharmaceutical Sciences, University of Trieste, 34127 Trieste, Italy

<sup>3</sup>Molecular Simulation Engineering Laboratory (MOSE), Department of Engineering and Architecture, University of Trieste, 34127 Trieste, Italy

e-mail: \*pacorsab@units.it; paola.posocco@dia.units.it

Self-assembled monolayers (SAM) on NPs stabilize the gold core and improve NP functionality, thus becoming useful for applications in nanotechnology, biology, chemistry and medicine. Accordingly, studying how these nano-sized materials interact with model membranes and eukaryotic cells opens a wide range of applications from diagnostics to therapeutic agents. In this contribution we investigated the role of surface ligand arrangement and composition on the interaction with lipid bilayers and on cellular toxicity for two SAM-protected gold NPs featuring 'Striped' or 'Janus' morphology, respectively. Cellular effects were probed using colorimetric and flow cytometric assays, with reference cell lines such as human B-chronic leukaemia, and lung-derived lymphoblast or carcinoma cells, exposing them at increasing NP concentrations and times. Apoptotic and necrotic effects on cell lines were analysed using fluorescent probes emitting at different  $\lambda_{EM}$ , reporting on cell membrane integrity, as well as mitochondrial activity and membrane polarization. Results were supported by differential interference contrast (DIC) and confocal microscopy.

Furthermore, the binding capacity between NPs and model membranes was investigated using Surface Plasmon Resonance (SPR) technique, by first immobilizing liposomes (composed of DOPC or DPPC) on the sensor chip and then flowing increasing NP concentrations. The results confirmed that both NPs are able to bind the liposomes considered; in addition, it was possible to differentiate the behavior of the two NP systems, as a result of the different organization of ligands on the shell.

This work was supported by the "SINFONIA - Structure and FunctiOn at the Nanoparticle bioInterfAce" project (grant RBS114PBC6) within the Scientific Independence of Young Researchers (SIR) program funded by the Italian Ministry of University Research (MIUR) .



## Author Index

### A

Abbruzzetti S., 18  
Abo-Neima S.E., 51, 57  
Ambrosetti E., 44  
Andjus P.R., 40  
Arsov Z., 20, 31, 47, 49

### B

Babelova L., 4  
Bačić G., 39, 74  
Balázs Á., 67  
Batta G., 35  
Baumgart F., 65  
Bazzi S., 29  
Belej D., 62  
Beltrami A.P., 44  
Benincasa M., 76  
Bérczi A., 72  
Bernhart E., 45  
Bernstorff S., 24  
Bevc S., 43  
Bianchini P., 18  
Bischof H., 45  
Bizik J., 4  
Blass S., 45  
Boccardo S., 13, 77  
Bodnár A., 73  
Borgogna M., 21  
Božič B., 28  
Brameshuber M., 11, 36, 65  
Brettel K., 46  
Brumen M., 32  
Bruno S., 18  
Bugarski B., 23  
Bui V-C., 38  
Bukara K., 23  
Bulone D., 5  
Burikova M., 4

### C

Caponi S., 56  
Carrotta R., 5  
Casalis L., 44  
Cesselli D., 44  
Charoensin S., 45  
Cocuzza M., 42  
Csomós I., 73  
Cvetić Antić T., 63

### D

D. Antic S., 14  
Delač Marion I., 24  
Delcanale P., 18  
Delcea M., 38  
Depaoli M.R., 52  
Dér A., 61, 66  
Di Giuro C.M.L., 12  
Diaspro A., 17, 18  
DiLeonardo R., 50  
Dobovišek A., 32  
Dolanski Babić S., 33  
Domokos R., 70  
Donati I., 21  
Drvenica I., 23  
Dučić T., 40

### E

Ebner A., 4  
Eggeling C., 10  
Elhoseiny A., 57  
Emeršič T., 30  
Eroglu E., 45

### F

Fajmut A., 8, 32  
Fameli N., 12  
Fazakas C., 53, 70  
Foggi P., 18  
Fojta M., 55, 71

Frečer V., 27  
Fülöp G., 11

### G

Gaal Sz.M., 2  
Gajski G., 76  
Galajda P., 50, 60  
Garab G., 69  
Garvas M., 20  
Gilbert R., 25  
Giorgio C., 18  
Goić-Barišić I., 76  
Gomišček G., 28  
Gottschalk B., 45  
Gózdž W., 26  
Graier W.F., 45, 52  
Grama L., 46  
Greetham G., 64  
Greinacher A., 38  
Grgičin D., 24  
Groma G.I., 61, 66  
Groschner K., 12  
Gualdani R., 16  
Guida F., 77  
Guida M., 13

### H

Hajdu K., 54, 69  
Hallström S., 45, 52  
Haskó J., 53  
Havran L., 55, 71  
Hernadi K., 69  
Hianik T., 4  
Hodula O., 60  
Horváth R., 19  
Hořka M., 58

### I

Iacuzzi V., 77  
Iglič A., 26  
Ilić N., 76  
Ilić V., 23

Imamura H., 52

## J

Jancura D., 62

Jelenković B.M., 23

Jimenez-Garduño A.M., 56

Jovanić S., 23

Jovanović M., 39, 63

Juretić D., 76

## K

Kapronczai R., 46, 64

Kejnovska I., 71

Kerényi Á., 60

Khedr Y.I., 57

Kinka A., 54

Koffler A., 11

Koklič T., 20, 31, 47

Kokot B., 20

Kollár J., 27

Kotb M.M., 57

Kovacevic S., 68

Kovačić D., 1

Kovács T., 35

Kozelka J., 29

Kralj S., 26

Kralj-Iglič V., 26

Kristanc L., 28

Križak S., 63, 75

Krizbai I.A., 53, 70

Krmpot A.J., 23

## L

Laskay K., 72

Leitner M., 4

Librizzi F., 5

Liguori L., 56

Lopicic S., 68

Lukacs A., 46, 64

Lunelli L., 42

## M

Macková K., 58

Madarasz T., 48

Madreiter-Sokolowski C.T.,  
45, 52

Malinski T., 45

Malli R., 12, 45, 52

Mangione M.R., 5

Marek R., 29

Marsich E., 21

Marson D., 13, 77

Márton Z., 72

Matko J., 48

Mátyus L., 73

Medvedev N., 38

Meech S.R., 64

Mesarec L., 26

Miertus S., 27

Mijaković M., 76

Milošević N.T., 15

Miyazaki K., 14

Mojović M., 59

Molnár J., 53, 70

Montali C., 18

Motaweh H.A., 51, 57

Müller P., 46

Musio C., 56

## N

Nagy K., 50, 60

Nagy L., 54, 69

Nagy P., 35, 73

Nagypál R., 61, 66

Nedeljkov V., 68

Nemergut M., 62

Nesovic-Ostojic J., 68

Nguyen T-h., 38

Nizsalóczki E., 73

Novotný J., 29

Nyitrai M., 48

Nyúl-Tóth Á., 53

## O

Oneto M., 18

Ormos P., 22

Osteikoetxea-Molnar A.,  
48

## P

Pacor S., 13, 77

Pajić T., 63, 75

Palankar R., 38

Páli T., 67

Panajotović R., 69

Pantelić D.V., 23

Panyi G., 2

Paoletti S., 21

Parisse P., 44

Pasquardini L., 42

Pasquato L., 13, 77

Pavičević A., 39, 59, 74

Pederzoli C., 42

Pelzmann B., 45

Pennacchietti F., 18

Pirisi K., 64

Pirri C.F., 42

Pivonkova H., 71

Podgornik R., 7, 33

Podlipec R., 20, 31

Polonec P., 27

Popović-Bijelić A., 59

Posocco P., 13, 77

Potrich C., 42

Poturnayova A., 4

Praprotnik M., 43

Pricl S., 13

Prostran M., 68

Puskás L.G., 67

## R

Rabasović M.D., 23

Ragab M.F., 51

Rákhely G., 72

Rehman A.u., 54

Reismann A., 65

Rončević T., 76

Ross W.N., 14

Rosboth B.K., 65

Rossmann C., 52

Rost R., 45

Rózsár D., 67

**S**

Salamon K., 24  
San Biagio P.L., 5  
Santini G.C., 42  
Sarlós F., 61, 66  
Sattler W., 45  
Schütz G., 11, 65  
Sebők-Nagy K., 67  
Sedlák E., 6, 62  
Sedláková D., 62  
Serec K., 33  
Sevcsik E., 11  
Shrestha N., 12  
Simunić J., 76  
Sipos Á., 61, 66  
Sipos O., 50, 60  
Snejdarkova M., 4  
Sologan M., 13, 77  
Soltész L., 35  
Sonavane Y., 37  
Špaček J., 55  
Spasic S., 68  
Stamenković S., 39, 40, 74  
Stančić A., 23  
Stanić M., 63  
Stanojević M., 68  
Štrancar J., 20, 31, 47, 49  
Svetina S., 34  
Szabó T., 69

Szabo-Meleg E., 48  
Szanto T.G., 2  
Szegetes Z., 70

**T**

Tkalec U., 30  
Todorovic N., 75  
Tognolini M., 18  
Tomashevic T., 69  
Tomić S., 9, 33  
Tonge P.J., 64  
Tonkić M., 76  
Tossi A., 13, 76, 77  
Tóth A., 72  
Toth E.A., 48  
Tourk H., 51  
Travan A., 21  
Trnkova L., 71  
Tučeková Z., 27

**U**

Urbančić I., 20, 47, 49

**V**

Vaghi V., 42  
Vámosi G., 73  
van Breemen C., 12  
Varga B., 70

Varga Z., 2  
Váró G., 53, 70  
Váró Gy., 69  
Vass I., 54  
Végh A.G., 53, 70  
Viappiani C., 18  
Vidláková P., 55, 71  
Vilasi S., 5  
Vorlícková M., 71  
Vos M.H., 46  
Vuletić T., 24

**W**

Waldeck-Weiermair M.,  
45, 52  
Wilhelm I., 53, 70

**Z**

Zahradník I., 58  
Zahradníková A., 3, 58  
Zahradníková Jr. A., 58  
Zavadlav J., 43  
Zemljič Jokhadar Š., 28  
Žerovnik E., 41  
Zieba A., 64  
Zimányi L., 72  
Živić M., 63, 75  
Zoranić L., 37, 76  
Zsiros V., 60



## Notes

